UNIVERSITAT POLITÈCNICA DE CATALUNYA

Doctoral Programme

AUTOMATIC CONTROL, ROBOTICS AND COMPUTER VISION

Ph.D. Thesis

SOCIAL ROBOT NAVIGATION IN URBAN DYNAMIC ENVIRONMENTS

Gonzalo Ferrer Mínguez

Advisor: Alberto Sanfeliu Cortés

September 2015

Social robot navigation in urban dynamic environments

by Gonzalo Ferrer Mínguez

A thesis submitted to the Universitat Politècnica de Catalunya for the degree of Doctor of Philosophy

Doctoral Programme:
Automatic Control, Robotics and Computer Vision

This thesis has been completed at:
Institut de Robòtica i Informàtica Industrial, CSIC-UPC

Advisor:
Alberto Sanfeliu Cortés

Dissertation Committee:
Prof. Aníbal Ollero, Chairman
Prof. Rachid Alami
Prof. René Alquézar

The latest version of this document will be available at http://www.iri.upc.edu/people/gferrer.

SOCIAL ROBOT NAVIGATION IN URBAN DYNAMIC ENVIRONMENTS

Gonzalo Ferrer Mínguez

Abstract

Deploying mobile robots in social environments requires novel navigation algorithms which are capable of providing valid solutions in such challenging scenarios. The main objective of the present dissertation is to develop new robot navigation approaches able to solve in an intelligent way the navigation problem in urban settings while considering at the same time the interactions with pedestrians, similar to what people easily do with little attention.

Before studying in depth navigation algorithms, this thesis focuses on prediction algorithms to provide a more detailed model of the scene. Understanding human motion in outdoor and indoor scenarios is an appealing requirement to characterize correctly urban settings. Urban environments consist essentially of static obstacles and people, which are treated as dynamic and highly uncertain obstacles. Accordingly, it is mandatory to calculate people's intentions in order to successfully build a human prediction model that generates the corresponding human trajectories and considers their interactions with the environment, such as other pedestrians, static obstacles or even robots.

It is of great interest that service robots can navigate successfully in typical urban environments, which are dynamic and constrained. In addition, people's behavior should not be conditioned by the presence and the maneuvering of robots. To this end, the robot navigation should seek to minimize its impact on the environment, in our case, on people.

This thesis proposes new robot navigation methods that contemplate the social interactions taking place in the scene. In order to procure more intelligence to the navigation algorithm, we propose to integrate seamlessly the human motion prediction information into a new robot planning approach.

Real experimentation is essential for the validation of the navigation algorithms. As there are real people involved, we must validate the results in real settings since simulation environments have limitations. In this thesis, we have implemented all the prediction and navigation algorithms in our robotic platform and we have provided plenty of evaluations and testings of our algorithms in real settings.

Acknowledgements

I would like to thank my supervisor, Alberto Sanfeliu, for his unconditional support and his contagious enthusiasm. To Anaís Garrell and Iván Huerta for their valuable contribution to this work.

Thanks to the members of the dissertation committee for their dedication to the final revision of this thesis and for their valuable comments regarding the present work. The IRI's administrative and IT staff also deserve an acknowledgment for making my stay easier at the institute. I am also very indebted to the engineering team supporting the Tibi&Dabo robots: Fernando Herrero and Sergi Hernández.

Thanks to all my office colleges and the *iri-tupper* guys for sharing with me lots of good moments at the IRI. And finally, special thanks to my family and Elena for being at my side during all this time.

This work has been supported by the research projects:

- **CSD2007-018** MIPRCV-Consolider: Multimodal, Patter Recognition, and Computer Vision.
- **DPI2010-17112** RobTaskCoop: Cooperación robots humanos en áreas urbanas
- **FP7-ICT-2011-7-287617** ARCAS: Aerial Robotics Cooperative Assembly System.
- **DPI2013-42458-P** ROBOT-INT-COOP: Interacción, aprendizaje y cooperación robot-humano en áreas urbanas

Contents

Figures

Tables

1 Introduction

People usually take it for granted that mobility is a simple task: one simply decides to "move" from one place to another without major considerations. Inherently, multiple and complex processes are taking place on an *unconscious* level, but we do not even notice them. We can describe a simplified version of the navigation scheme as follows: we *perceive* the environment and integrate the gathered information into a given representation, a *map*, to *localize* ourselves on it. With this information we calculate the *plan* to follow and *execute* it accordingly. This simplified scheme gives a possible decomposition of the navigation topic in five different issues: perception, localization, mapping, planning and execution. In the present dissertation, we are interested in the perception, planning and execution, as well as how to combine them into a navigation scheme.

The scientific community has fulfilled to identify and isolate all these processes, while roboticists have achieved to implement solutions to these tasks into real robotic platforms. Intelligence is closely related to mobility and navigation. The envisage of an autonomous robot navigation has encouraged, and still encourages, fruitful research on Artificial Intelligence. During this pursuit of machine intelligence we have witnessed impressive results on the robotics field. Another important reason to develop navigation techniques is a social requirement. The start of the XXI c. has marked the beginning of a new era when crucial problems have already arisen in demography, ecology and in global management of resources. As a consequence, society has found itself in need of new and more efficient autonomous systems, as well as new transportation solutions, and thus, robots have become the ideal experimentation platforms to develop further sophisticated navigation paradigms.

For the last decades, many contributions have been made to the topic of robot navigation. Under certain conditions the navigation problem is considered entirely solved, although, *full autonomy* in robotics has not been reached yet. Robots are capable of solving the vast majority of navigation problems; however, there exist certain demanding situations when known methods are not capable of finding efficient and consistent solutions.

A few examples of limiting factors to current robot navigation are changing environments,

dynamic obstacles, imperfect perception, uncertainty on execution, etc. Individually, most of those problems have been solved, but, what happens when one of these factors is so hindering that the navigation solution generated is not correct? What happens when different combinations of these limiting parts take place? Definitely, we know that robot navigation can be improved: humans are able to perform well in incredibly challenging scenarios, such as the Shibuya crossing in Tokyo, the busiest in the world, the Dakar rally or the America's Cup of sailing yachts. The idea that the intelligence behind the robot navigation is on par with human intelligence may sound a little bold. Nevertheless, it constitutes a stimulating challenge for the robotics community in the long term.

Many researchers keep investigating the navigation issues to elaborate new approaches which will be able to solve major navigation problems. Robot navigation is a mature field of knowledge but, in general, people have expectations of a more intelligent robot navigation. Therefore, the objective of the present dissertation is to hopefully push a little the knowledge on the robot navigation field.

1.1 Motivation

From the very beginning of this work, the research direction is clear: we want to focus our efforts on the robot navigation topic, specifically stressing on the deployment of robotic platforms in urban environments. This research orientation has been motivated by the Tibi&Dabo robots, a unique mobile robotic platforms that constitute a very valuable research resource at the IRI[1] institute, that motivate us to take advantage of their navigation capabilities, as well as their interaction potential with people due to its pleasant appearance. In Sec. 2.1 we will explain the peculiarities of these robots in more detail and why they result so convenient for the development of the work of this thesis.

The former navigation approach developed at the institute [Corominas Murtra et al., 2010; Trulls et al., 2011] for the Tibi&Dabo robots, under the context of the URUS project [Sanfeliu et al., 2010], has been able to successfully navigate in urban environments. However, dynamic situations are not handled correctly, due to consider people in the environment as static obstacles. This fact perfectly exemplifies what we have discussed earlier, under certain conditions, navigation approaches are perfectly solved, nonetheless, when these conditions become more demanding, more considerations have to be taken to provide a valid solution. Thereby, the natural next step is to include people, treated as dynamic obstacles, into the navigation scheme. Many previous approaches have studied robot navigation in the presence of humans such as [Burgard et al., 1999; Thrun et al., 1999; Trahanias et al., 2005] in indoor museums, [Arras et al., 2003] with multiple robots in a exhibition pavilion, [Kanda et al., 2009; Satake et al.,

[1] Institut de Robòtica i Informàtica Industrial, CSIC-UPC

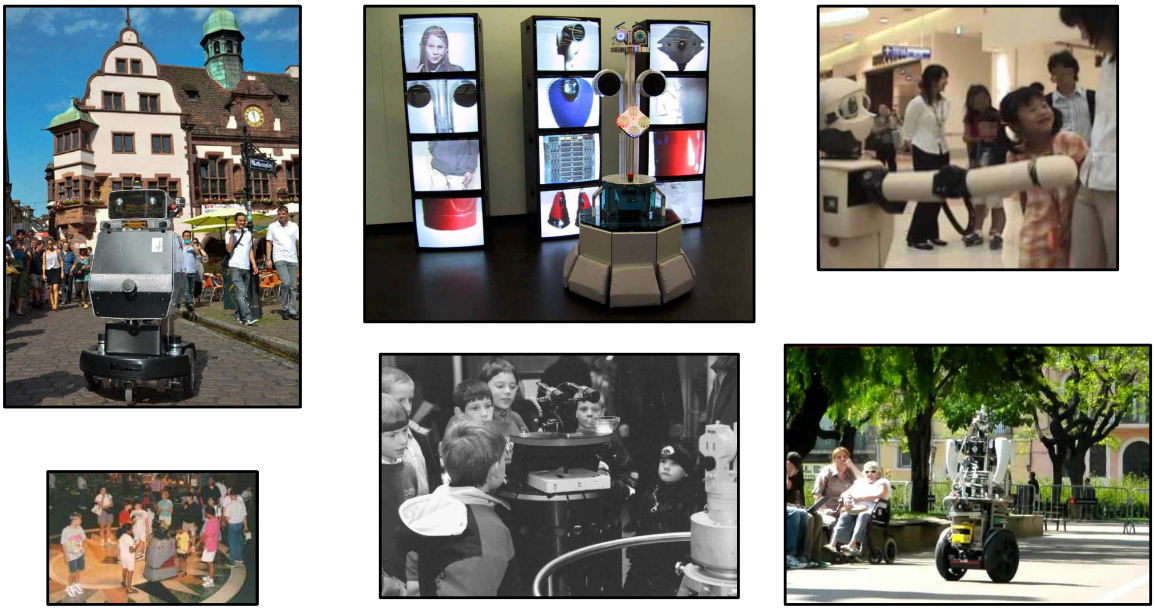

Figure 1.1: **Robot navigation works in the presence of people.** In the top-left image is depicted the Obelix robot [Kümmerle et al., 2014]. From left to right we find the RoboX [Arras et al., 2003], Robovie [Kanda et al., 2009]. In the bottom-left, MINERVA [Thrun et al., 1999], followed by RHINO [Burgard et al., 1999] and Tibi [Trulls et al., 2011].

2009] in a shopping mall or [Kümmerle et al., 2014] in the streets of a city. Some of these robots are depicted in Fig. 1.1.

In contrast to all those approaches, we decide to dedicate a considerable effort to study only the motion of people in urban or social environments. We believe that a deeper understanding of human motion may enhance the robot navigation. Besides, urban environments are highly dynamic, and thus, it makes sense to spend some time studying exclusively human motion aiming to predict human trajectories. Prediction, in a certain way, can be included into the *perception* subtask of the navigation topic, since we are forecasting or perceiving the position and velocity of moving obstacles in the future. The idea is to integrate this tool into a navigation scheme, with hope to improve the results.

In addition to satisfying all the constraints and calculating a valid navigation solution, we are highly motivated to introduce Human-Robot Interaction into the navigation system. If we want to deploy robots in urban environments, inevitably they must interact with people one way or another. Robots should share and coexist in the same environment as people do, and thus, it is desirable to adapt robots to the environment that belongs to humans. To do so, robots should minimize the impact to other pedestrians in the scene in a social manner. This Human-Robot Interaction can be considered to be passive, since the goal of the robot is to execute their navigation tasks without disturbing people. The overlapping of these two research fields, the navigation and interaction, originates opportunities to study new problems from a novel point

of view, in what we have denominated the *social mobile robotics*.

And finally, an important motivation is to develop low level robot abilities, *i.e.* the social robot navigation, in order to enrich ongoing robotic research lines carried out at the IRI institute, such as the social interaction with robots [Garrell, 2013; Villamizar et al., 2012], collaborative mapping [Retamino Carrión and Sanfeliu, 2014] or the hide and seek robot [Goldhoorn et al., 2014]. By providing a navigation scheme aware of people, we assert better conditions for the study of HRI or more complex tasks in future robotics projects at IRI.

1.2 Objectives and scope

The understanding of human motion in urban environments is of extreme importance in order to adapt service robots to typical human environments and not in the contrary. Our objective is to completely describe a urban scene: static obstacles, pedestrians and social motion interactions between people and robots. The first step is to obtain the structure of the environment, in terms of human intentionality and extract places of interest in the scene. Moreover, we want to model the generation of human trajectories, and thus, propose a prediction algorithm. In addition, we must consider how robot navigation influences human navigation and include it into the prediction model. These foreseen trajectories should consider pedestrians' goals as well as the interactions with other people, and more important, the interactions with robots.

Navigation algorithms are an essential part of this thesis. We need to study multiple navigation approaches before we can propose our own algorithm. Our aim is to obtain a robot navigation system that provides a valid navigation solution in urban settings. As explained before, our starting point is the work developed at the IRI institute [Trulls et al., 2011]. Since we have additional considerations, such as the robot impact towards the environment, it is mandatory to explore and implement new navigation algorithms that can provide a solution to our demands. At the same time, we need to understand the inherent principles in human navigation and incorporate them into the robot navigation scheme. Should robots behave as a person to be considered as equals by people? or, should robots take care of humans' trajectories on their own way? We will further develop these questions throughout the present thesis and hopefully answer them at the end of it.

Tackling the social navigation problem by only relying on a robust navigation is not enough, although this topic has grown enormously in the few past years. Aiming to obtain a navigation approach that is socially acceptable, we require a more intelligent approach that integrates navigation with prediction. This dual objective of finding a navigation solution and a solution that considers its impact towards the environment, will be a constant constraint over this work, and we will analyze it from different perspectives.

In order to validate our algorithms, we require tools where we can test our implementations

before deploying real robots with people. A simulated environment provides a good starting point and gives a first look at the behavior of the algorithm. In addition, it is very convenient to test the algorithms before deploying robots with real people. Robot navigation should be largely tested in real situations, since all the simulations have limitations. To this end, we have verified our algorithms in real environments with people. A great amount of time has been dedicated to the implementations of such algorithms and environments, mainly in `C++` under a ROS architecture.

In summary, the main goal of this thesis is to study robot navigation in urban environments and more concretely, we are interested in integrating them with human motion prediction algorithms. The necessary objectives can be listed as follows:

- Understand urban settings and human motion.
- Study of navigation algorithms.
- Integrate navigation and prediction.
- Consider the robot navigation impact towards the environment.
- Validate the model in simulations and real conditions.

We will discuss in Sec. 8.1 up to what degree these initial objectives have been fulfilled.

1.3 Thesis overview

The ordering of the chapters appearing in this work does not exactly correspond to the real development of those topics over time, as happens in many thesis. However, and for the sake of clarity, we have structured the thesis in three parts: two main parts where most of our contributions are introduced and the final Part III is dedicated to the closing remarks.

In Part I we build a complete prediction model of human motion in urban environments. This part is not exclusive to the robotics field, since it can be applied to other problems, such as surveillance or tracking. In this part, the robot is not an active agent of our algorithms, since no action is calculated, but it appears as a part of the environment since we want to model human responses to robots as well as to obstacles or other people.

Part II is dedicated to robot navigation. Our initial approach to robot navigation is a simple adaptation of well-known techniques to a social-aware solution. In the following chapters, we iteratively incorporate more elements to the navigation scheme, as an improvement to the navigation approach; at the end this block, we propose a navigation system completely integrated with prediction.

In the following list are briefly introduced the chapters of this thesis:

Chapter 1: Introduction. We have presented so far the motivations to carry out this thesis and the original objectives that we have established at the beginning of this research.

Chapter 2: Experimental setting We introduce the common validation methodology and the resources used through all our work, such as, the Tibi&Dabo robotic platform, the urban environments in which we plan to test our algorithms and the simulation tools. The limitations considered are also described, such as maximum robot velocity, environment, etc.

Chapter 3: Intentionality prediction. The first chapter of Part I is dedicated to define and estimate the *intention* of people when describing trajectories in social environments. At first sight, this chapter is not related to the main topic of this work, but as the thesis goes on, the contents presented here become essential for the development of future chapters. We propose a robotic task to exemplify the usefulness of the intentionality prediction.

Chapter 4: Human trajectory prediction. We introduce the Social Force Model (SFM) and present an extension of it that is the core part of our proposed prediction system. We introduce the estimation of additional features that we have identified to play an essential role on human prediction. At the end of the chapter we formulate a complete prediction framework to model urban scenarios, closing Part I.

Chapter 5: Social-aware reactive navigation. In our initial approach to robot navigation we propose a pure reactive navigation scheme that is socially-aware on its environment. We discuss some of the limitations of this approach as a motivation to go in depth in the study of robot navigation.

Chapter 6: Robot task: accompany people walking side-by-side. We propose a modification of Chapter 5 to achieve a concrete robotic task. To this end, we integrate the reactive navigation with intentionality prediction to enhance the performance of the robotic task. This chapter is a first step on the integration of navigation and prediction and we demonstrate the success of this approach, though it is not exempt of limitations.

Chapter 7: Anticipative kinodynamic planning. The last chapter of the Part II gathers all the contributions in a final navigation scheme that overcomes most of the presented limitations in robot navigation by introducing more restrictions and fully integrating prediction into the system. This chapter is the culmination of our thesis and condensates the contributions presented in previous chapters into a single navigation scheme.

Chapter 8: Closing remarks. At last, this chapter summarizes and discusses all our contributions. Future research lines that steam out from this work are also discussed.

Appendix A: People detection and tracking. Presents the perception system implemented in the robot. This topic is out of the scope of this thesis, however it becomes a very important

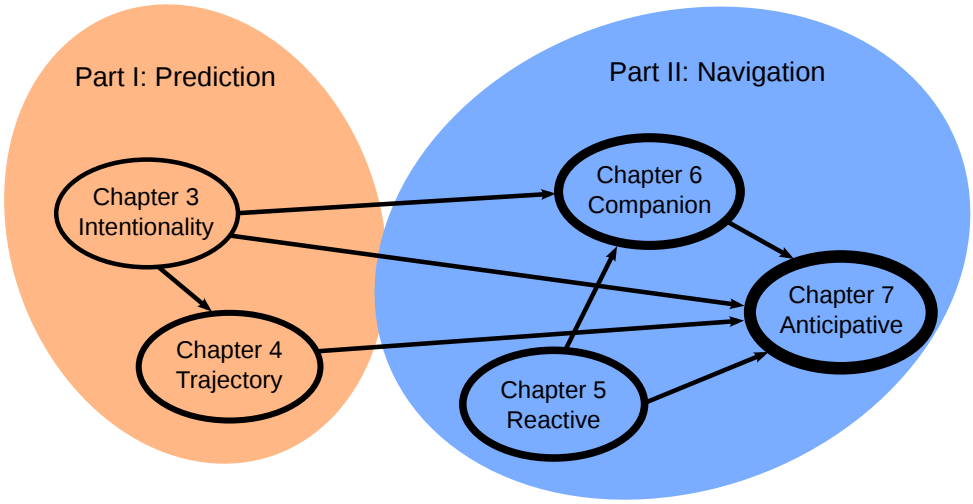

Figure 1.2: **Scheme of the thesis overview.** In the drawing is depicted the relations between the different chapters presented in this work.

problem to solve and we have dedicated some effort to this issue during the thesis.

In Fig. 1.2 is depicted the general scheme of the thesis and the relation between the different chapters that serves as a reference or a map for a more comprehensive reading. As it can be observed in Fig. 1.2, the first chapters presented are original approaches solving the required prediction problems, while the following chapters, regarding navigation, incorporate our prediction contributions into our approaches. This integration has been carried out gradually, from not considering prediction at all in Chapter 5, to finally integrate all our contributions into the same navigation scheme in Chapter 7.

We have organized the work in the following manner. Each chapter is independent and its content is self-explained in the same chapter or in a previous chapter (see dependencies in Fig. 1.2). To the authors' believe, we provide the necessary material to understand each chapter, and we have presented our contributions in a sequential manner. We start describing very simple motion features in Chapter 3 and we end integrating most of our contributions into a unified scheme in Chapter 7.

2

Experimental settings

In this chapter we describe the common resources that appear throughout this thesis as a recurrent point in all the experiments and validations carried out in upcoming chapters of this dissertation. We have decided to present these common resources in the beginning of this thesis since this brief presentation will hopefully help to understand part of the scope of this work.

The common resources include the Tibi&Dabo robotic platforms, the urban settings and the simulation tools. The robotic platform is an essential element for the study of robot navigation, since it is the active part executing our proposed algorithms. The environment consists of the physical setting, the obstacles and all the people walking and staying in the area. The idea of these testing environments is to experiment in a *controlled* location which faithfully includes all the elements present in typically urban scenes. At last, we present the simulation of the robot and the urban settings in order to test the algorithm and to grasp an initial idea of the proper functioning of the processes taking place. We can not afford to test it directly in a real environment with people, for safety reasons.

2.1 Robotic platform

In order to conduct all the experiments and to test the approaches presented, we have used two twin mobile service robots, developed for the URUS project, called Tibi&Dabo (Fig. 2.1), designed to work in urban pedestrian areas and interact with people. These robotic platforms are active research resources used in multiple projects at the IRI institute [1].

The Tibi&Dabo robots are built on a two-wheeled Segway RMP200 platform, which work as an inverted pendulum in constant balancing and they can be modeled as differential drive robots that can rotate on the spot very elegantly. Wheel encoders provide a very reliable odometry, since almost no wheel slipping occurs.

Besides the balancing mode, the robots can operate in the non-balancing mode by adding two caster wheels in a support structure, as it can be seen in Fig. 2.1. In this thesis we have used

[1] http://www.iri.upc.edu/research/mobile_robotics

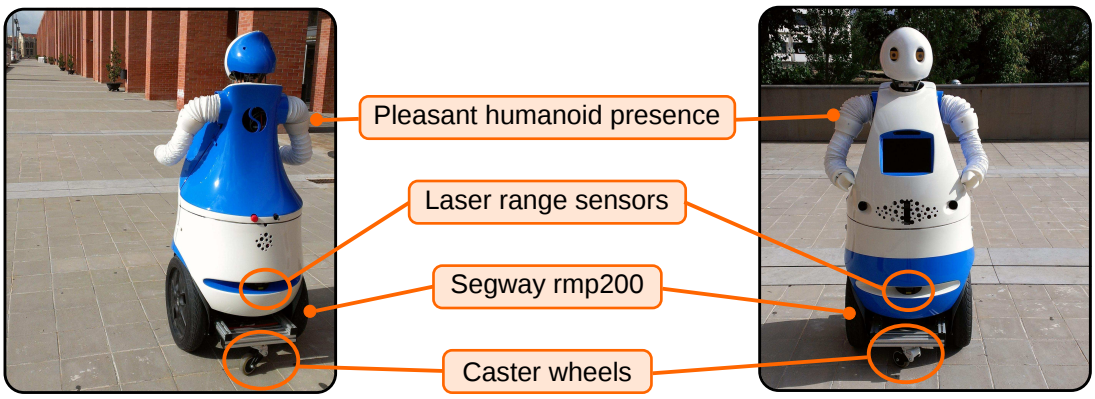

Figure 2.1: **The Dabo Robot.** Mobile robot platform used in most of this thesis experiments. The most relevant components of the robotic platform are indicated in the frontal and rear view.

both work modes, although we have observed that it is more desirable to use the 4-wheel configuration, since the balancing mode presents more problems, specially for the perception system, and the controllability of the platform, considering that the platform balancing controller is non-accessible to our control scheme.

The Segway RMP200 is meant to drive at speeds up to 16 km/h, or 4.4 m/s, which is by far more than required for our experiments, where our typical robot velocities are around 1 m/s. We have chosen to navigate at this velocity as a restriction imposed to the robot, since this value corresponds to typical pedestrians' velocities while walking in urban environments. We consider this platform to be very agile and elegant, as it is shown in the videos referenced in the next chapters.

To perceive the environment the robots are equipped with two Hokuyo UTM-30LX 2D laser range sensors used to detect obstacles and people. The laser scanners are located 40cm above the ground perceiving the horizontal plane from the front and rear of the robot. A stereo Bumblebee camera located in the eyes is used for computer vision purposes. In this thesis, the perception system is based purely on laser information and runs at approximately 20 Hz. A more precise information of the people detection and tracking is presented in Appendix A.

As social robots, Tibi&Dabo are designed to interact with people, thanks to their pleasant humanoid presence. They have several interaction elements to perform more friendly interactions, as a touchable screen, speaker, movable arms, head and LED illuminated face expressions. Power is supplied by two sets of batteries, one for the Segway platform and one for the computers and sensors, providing around 5h of full working autonomy.

Two on-board computers (Intel Core 2 Quad CPU @ 2.66 and 3.00 GHz) manage all the running processes and sensor signals and a laptop is used for external monitoring. The systems run Ubuntu-Linux and ROS [Quigley et al., 2009] as a middleware. Most of the algorithms presented in this thesis have been implemented in ROS and are available at their corresponding web-projects (see references in future chapters).

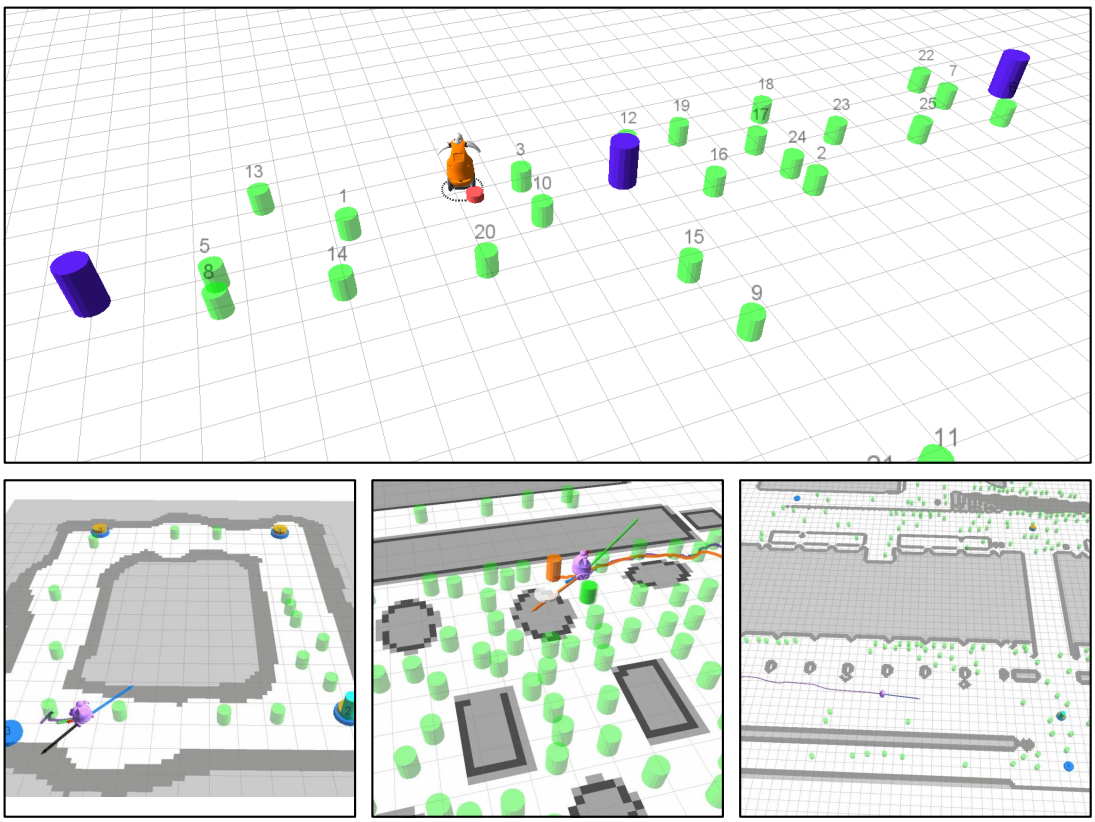

Figure 2.2: **Simulation environment.** Different captures of the simulation environment.

2.2 Simulation tools

Experimentation and testing of robot navigation algorithms are essential for research in mobile robotics. We propose to simulate a navigation environment, in order to obtain the basic mechanics of our algorithm. Simulation is a good starting point to grasp an initial idea of the active processes and their underlying behaviors; we follow this approach in most of the chapters of this thesis. However, simulation will always be a limited version of reality, although some simulations can be very realistic. Under the scope of this dissertation, we believe that, validation through simulations never substitutes real urban settings.

However, robot experimentation is a delicate matter particularly when there are people involved. For this reason, we believe that it is mandatory to start the validation of our robotic system in a simulated environment before any real interaction with people takes place, as we will detail in the following chapters.

We have developed three simulation tools: the robotic platform, a static environment consisting of obstacles and a dynamic environment in order to model moving people. In Fig. 2.2 we have selected some captures of our proposed simulation framework. The green numbered cylinders represent the simulated people, the robotic platform is drawn in more detail, in orange

or pink (previous version) and the lilac cylinders represent points of interest in the scene, as we will explain in Chapter 3. As it can be seen, we simulate a large number of pedestrians, although we are normally interested in a shorter amount of people to model the micro-interactions between the robot and its nearby surroundings.

The simulation framework used is a custom project built around ROS. Human motion is simulated using the work presented in Chapter 3 and 4, where we generate people tracks, that is, a sequence of positions over time with constant identifier *id*, which are modeled as random variables. The robotic platform is simulated according to a unicycle model that is controlled by the corresponding navigation algorithm. The simulation code can be found at the wiki page [2].

We have carried out all the simulations in a Intel Core2 Quad CPU Q9650 @ 3.00GHz and memory 3.8 GB, at an average rate of 5Hz. The hardware used for simulations is similar to the PC on-board the real robot.

2.3 Testing environments

For us roboticists, developing and implementing all those algorithms into systems and processes in a real environment represent a considerable effort, since we have spent a huge amount of time dedicated to this ungrateful task. In addition, unexpected problems often appear in real environments that were not considered in the simulated environment. Unfortunately, and according to the authors' beliefs, it is a mandatory step to validate our algorithms in a real environment, given the limitations of the simulation environment.

The biggest trouble that we have faced during this thesis is related to the development of the navigation algorithms and their corresponding validation. There is a clash between the need of a correct validation in a real environment and the assertion of a minimum degree of safety for the people.

So, we propose an intermediate step between a simulated environment and a real urban setting, that is a *controlled* urban-like environment. By doing so, we have left the lab, which is an important step, but still we can not completely enter the real world. If we follow the Technology Readiness Level (TRL) nomenclature, we have pushed our work into a higher degree of the TRL, by providing a model demonstration in a relevant environment. This testing environment, shown in Fig. 2.3, is located at the Universitat Politècnica de Catalunya (UPC), in the Facultat de Matemàtiques i Estadística, hereafter abbreviated as the FME.

The FME setting is depicted in Fig. 2.3 which consists of a rectangular area of more than $350m^2$ and free of obstacles. The area is bounded by two buildings at each side, the stairs delimiting with the university garden, on top of the FME and the street on the opposite side. In this controlled environment is where many of the initial experimentations of this thesis

[2] http://wiki.iri.upc.edu/index.php/Akp-navigation

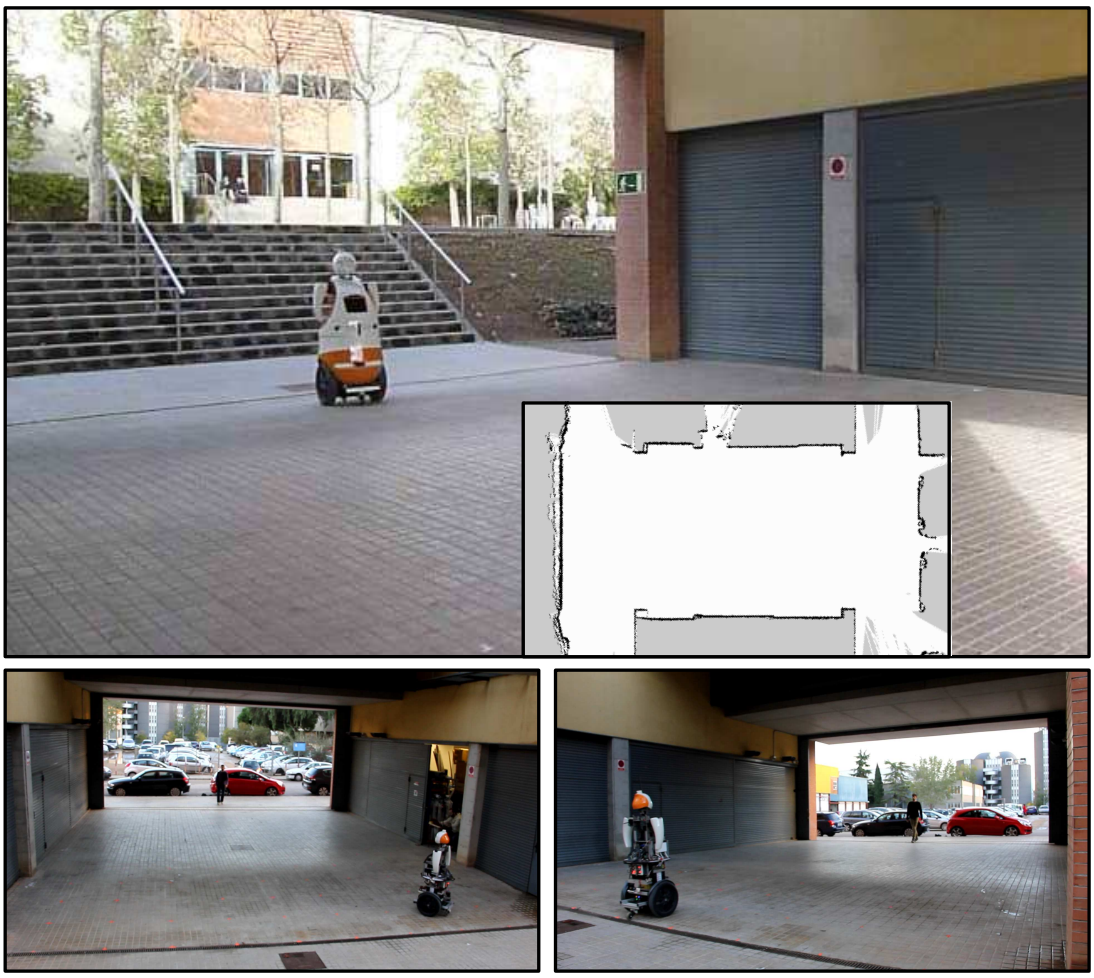

Figure 2.3: **Facultat de Matemàtiques i Estadística (FME).** The FME is located in the south campus of the UPC university.

have been carried out. With respect to the volunteers for doing the experiment, there have participated people with knowledge of robotics (mainly from the IRI institute) and people without knowledge of robotics that have been contacted to test the robotic system.

The FME environment has been extensively used throughout this thesis, primarily for parameters learning and initial testing. It has served as an excellent real environment to test the proposed algorithms, on an early stage of development, after simulations have been carried out.

The *controlled* environment approach has been typically followed by many other works when developing new robot technologies. Despite it is a very appropriate approach, we want to go one step further to test and experiment our algorithms in more realistic environments, since this *controlled* setting is a simplification of reality.

Regrettably, there is a big gap between the current legislation and cutting-edge research carried on mobile robotic platforms. In case of accident, it is unclear who is responsible. This slipping legal context discourages any further testing in urban settings. However, we desire

a more similar environment to an *uncontrolled* urban environment. To this end, the institute and the UPC university have prepared a special setting for further experimentation that aims to recreate the very similar conditions of a real urban setting, as shown in Fig. 2.4.

The experimental area, where some of the experiments of this thesis have been conducted, is denominated the Barcelona Robot Lab (BRL), located at the North Campus of the Universitat Politècnica de Catalunya (UPC).

The BRL, depicted in Fig. 2.4, is a large section of the campus covering over 10.000 m^2, including six buildings and a square, with multiple ramps, staircases and typical obstacles such as bulletin boards, bicycle stands, trashcans or flower pots. As it can be seen in Fig. 2.4, the BRL resembles a city, with students acting as normal people and the academic buildings as urban buildings. In the scope of this dissertation, we have used the BRL as the final testing environment of our algorithms providing the most realistic validation.

These two main environments, the FME and the BRL, appear recurrently in the next chapters, for navigation as well as for prediction issues. We have presented a three stage validation environments: a simulation, a controlled real environment and an almost urban environment in the university campus.

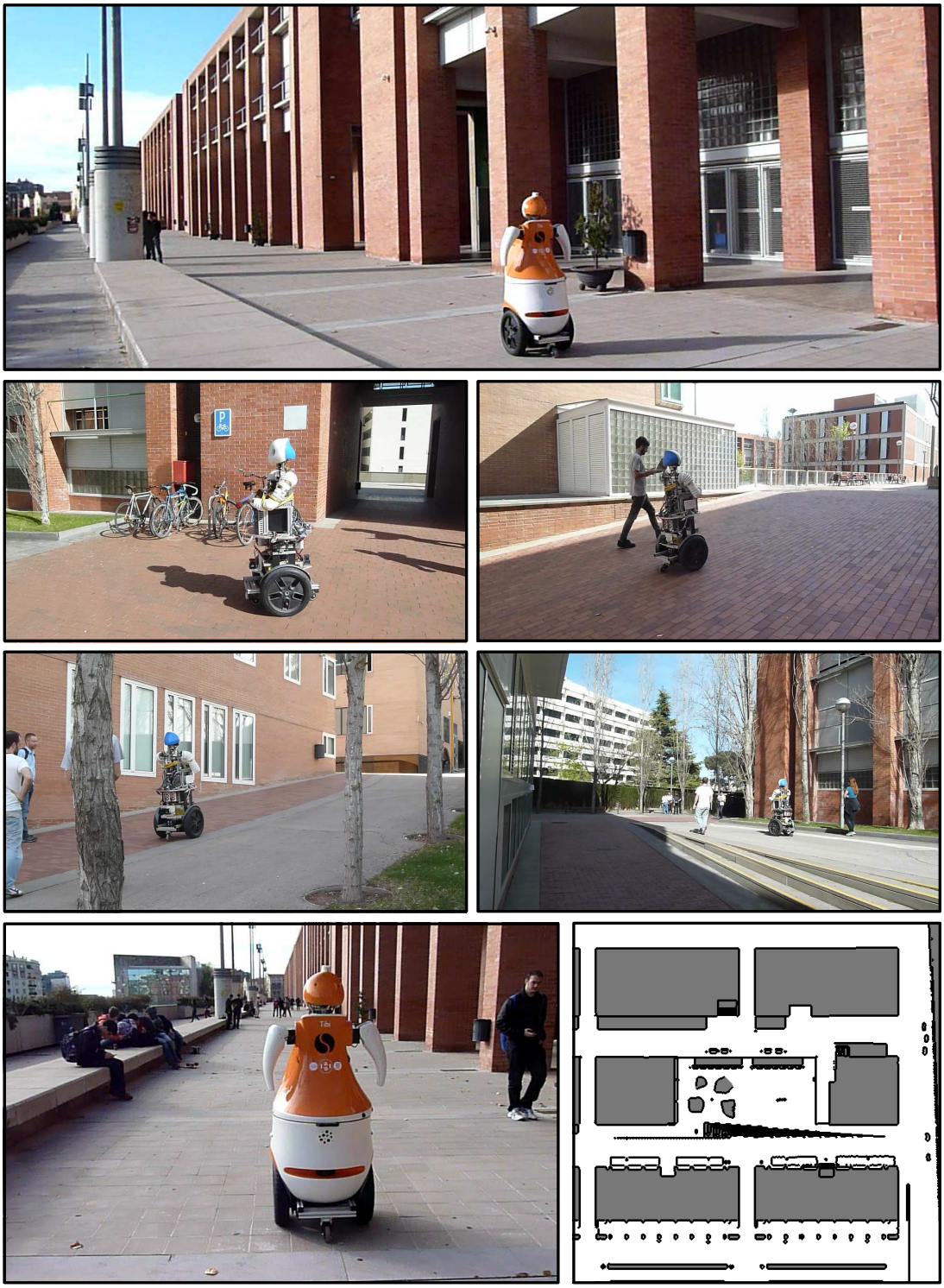

Figure 2.4: **Barcelona robot laboratory (BRL).** The BRL is located in the north campus of the UPC university. This environment is a huge area where many hundreds of students assist classes daily.

Part I

Prediction of human motion

3
Intentionality prediction

In this chapter we present the first contribution to our thesis, an essential starting step that has allowed us to build and develop our robotic algorithms. Before commanding the robot, we observe and understand the environment. A urban environment is plenty of static obstacles, such as buildings, corners, doors, etc. and people, which are treated as dynamic and highly uncertain obstacles. Accordingly, it is mandatory to formulate people's intentions successfully and build a model to calculate them.

Humans' intentions have been traditionally studied in other fields of knowledge such as Surveillance in Computer Vision and Action Recognition in Machine Learning. Nonetheless, we will present an approach that initially seems to be out of the scope of robotics. As long as the dissertantion progresses, this technique will be integrated into our other proposed algorithms, clearly enhancing them.

This chapter is based on our early work on trajectory evaluation published in the *International Conference on HRI* [Ferrer and Sanfeliu, 2011] and the journal publication in the *Pattern Recognition Letters* [Ferrer and Sanfeliu, 2014a].

3.1 Introduction

Human motion prediction in indoor and outdoor scenarios is a key issue towards human robot interaction and intelligent robot navigation in general. In the present chapter, we propose a new human motion intentionality indicator, denominated Bayesian Human Motion Intentionality Prediction (BHMIP), which is a geometric-based long-term predictor. In this context, we define the term *intentionality long-term prediction* as as a tool to forecast intentions or motivations that drive human behaviors. We specifically use this term whenever a person has the intention to walk towards a destination, that can be far away from his/her current position.

Two variants of the Bayesian approach are proposed, the Sliding Window BHMIP and the Time Decay BHMIP. The main advantages of the proposed methods are: a simple formulation, easily scalable, portability to unknown environments with small learning effort, low compu-

tational complexity, and they outperform other state of the art approaches. The system only requires training to obtain the set of destinations, which are salient positions that people normally walk to, such as doors, stairs or crossings. A comparison of the BHMIP is done with other well known methods for long-term prediction using the Edinburgh Informatics Forum pedestrian database [Majecka, 2009] and the Freiburg People Tracker ground-truth published in [Luber et al., 2011].

The development of social mobile robots that interact with humans and perform tasks together in everyday environments for navigating, guiding or accompanying tasks [Garrell and Sanfeliu, 2012; Fong et al., 2003] either in domestic or public spaces, requires the design of new navigation tools that take into account the human motion intentionality. Similarly, the development of more intelligent tracking and surveillance systems boils down to the development of new tools, for instance, a long-term prediction as proposed in the present thesis.

There is a large number of real world applications where motion intentionality can be applied. For example, human motion scene surveillance, where we can detect abnormal trajectories making use of prediction information, and thus identifying all those erratic trajectories; human tracking, to obtain a robust tracking of human motion; robot navigation in human environments, in order to adjust robot navigation to be aware of human motion; or social interaction, to improve the social interaction between robots and humans. All these issues require prediction information, preferably a long-term prediction.

In general, the analysis of future scenarios has been done in the literature using short-term prediction, which is a propagation of the current state into a certain time horizon, but it has several limitations, specially appreciable on more complex environments. In the present thesis we propose a new long-term human motion intentionality predictor based on geometry criteria, called Bayesian Human Motion Intentionality Predictor (BHMIP). The BHMIP has been validated in outdoor urban environments by using two well-known databases. Furthermore, the proposed method has been used in several real robot experiments, using the Tibi&Dabo robotic platforms (Sec. 2.1), while performing robot tasks. In Fig 3.1 is depicted an example of a robot companion experiment. In this particular robot experiment the use of prediction information has demonstrated to largely enhance the performance. We will show during the next chapters of the present thesis that forecasting tools such as the BHMIP greatly improve many robot applications, in our context, in urban or outdoor environments.

In addition, our method can be scaled into larger scenarios effortlessly and it is easily portable into unknown environments since destination points are easy to obtain. Both qualities are of great utility for real-world applications, for example, service robots that require to operate in an unusual urban environment.

In real-world applications, it is implicit that the destinations are obtained *a priori*, whether manually or using an automatic technique, as we will discuss later. However, it is important to note that the setting of destinations is essential for our approach. In this work, we assume

Figure 3.1: **Example of a destination in the environment.** In this controlled setting, the red pylon represents a scene destination that both the robot and the volunteer try to reach. We use the BHMIP to infer the most expectable destination of the person.

that we have a prior knowledge of the scene destinations, which have been obtained through an automatic procedure, for example by clustering the locations where people enter or leave the scene (we will later discuss this issue). Other techniques to construct automatically the set of destinations are presented in [Ikeda et al., 2012] or [Bruce and Gordon, 2004].

3.2 Related work

In general, it has been proved that intentions precede actions [Wolpert and Ghahramani, 2000], and thus, action recognition [Demiris and Khadhouri, 2006] becomes essential to understand many tasks and problems. Havlak and Campbell [2014] have anticipated intentions and take advance of it in vehicle crossings. Wang et al. [2013] have proposed an intention driven dynamic model for action recognition in table tennis and humanoids. In this work, we provide a more specific meaning to the intentions related to human motion, as an indicator useful for a posterior processing.

Concerning the wide variety of human motion predictors in the literature, two major human motion predictors (HMP) groups can be distinguished: a geometric-based group and a place dependent-based group. For the latter group, we have to learn the prediction model for each of the environments where the HMP is used. The geometric-based group does not always need to learn the human motion intentionality (HMI) for each specific environment, although training is also required in one way or another.

Bennewitz et al. [2002, 2005] have proposed a place-dependent method in which they analyze a collection of people's motion behaviors in an indoor environment by a clustering technique that uses the Expectation-Maximization algorithm. Once they have learnt the classes of motion trajectories, they have used these primitive trajectories as patterns for human motion trajectory association, and thus, inferring HMI. One of the main disadvantages of the place-dependent methods, as we will discuss later, is the lack of flexibility on abnormal observations, that is, all those erratic trajectories due to a person stopping or changing its destination. Our algorithm is able to quickly adapt to changes and perform successfully.

Vasquez [2007] and Vasquez et al. [2009] have clustered different motion patterns by a dissimilarity measure which allows the use of pairwise clustering algorithms in order to group observed trajectories into patterns. This approach has been extended by Pérez Hurtado et al. [2015] to partially observed trajectories and unknown destinations. Chen et al. [2011] have proposed a clustering method and three different prediction strategies based on the quality of the matching.

Using heuristics and geometric criteria, Foka and Trahanias [2007, 2010] have proposed a geometric-based method for human motion prediction that uses human motion intentionality in terms of goals. Prediction is done by identifying final destinations based on the instantaneous tangent angle in combination with a grid-based probability assignment to all final destinations. It has been used for on-line prediction for robot navigation in dynamic environments. Escobedo et al. [2014] have defined a social scene consisting of static destinations and the best points to join a social group and infer possible destinations when driving a robotic wheelchair using a Dynamic Bayesian Network. Our approach belongs to this group of HMI predictors, but it outperforms the Foka approach, as will be demonstrated in the results Sec. 3.5. Another geometrical approach, proposed by Ferrer and Sanfeliu [2011], has predicted future trajectories by minimizing the variance of curvature of the forecast paths.

A mixed approach, proposed by Ziebart et al. [2008, 2009], has used both place dependent and geometric criteria. They have used a reward function to generate the optimal paths towards a destination. This method can also be used as a modeling of route preferences as well as for inferring destinations. This method requires intensive place-dependent training, which is an important drawback for the generalization of its use as a predictor.

Dee and Hogg [2004] have proposed a vision-based prediction to infer intentionality, characterized as the combination of obstacles and free space pixels under the field of view of the person. Liu and Karimi [2006] have proposed a method for long term prediction using localization awareness. Other Computer Vision approaches like Pellegrini et al. [2009] have used intentionality to track people or the works of Khalid [2010]; Morris and Trivedi [2011] where intentionality has been used for activity recognition and abnormal detection, correspondingly. Panangadan et al. [2004] have classified people's activities and identified non-learned interactions in the scene.

3.3 Definition of intentionality features

In this section, we propose a definition of the basic intentionality features capable of quantifying the human motion intentionality (HMI) implicit on a trajectory with respect to the current position and orientation. This intentionality indicator should capture the probability that a human trajectory reaches a destination point D_m, among the set of destinations $\boldsymbol{D} = \{D_1, D_2, \ldots, D_M\}$ which describe the scene as a clear indicator for the inherent intentionality. To achieve this, we define the variable ϕ_{nm}, which is the angle between the current orientation of the target n and the vector to the destination point D_m, a relative measure of the orientation with respect to a destination (see Fig. 3.2 for clarification).

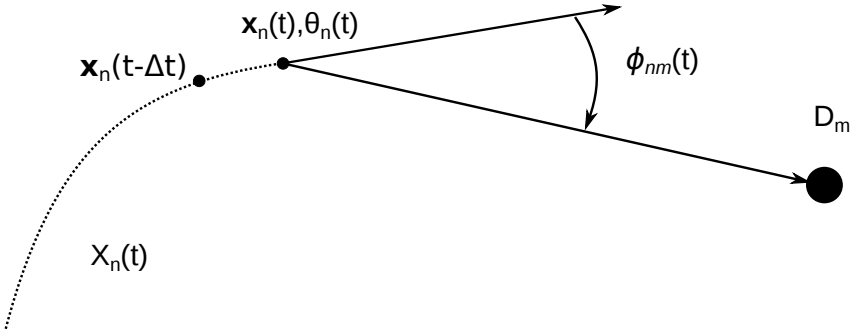

Figure 3.2: **The angle ϕ_{nm}.** It is defined as the angle described by the orientation vector of the target n at time t and the $\boldsymbol{x}_n(t) \rightarrow D_m$ vector.

In brief, we present a basic formulation necessary to analyze real trajectories. Let

$$\boldsymbol{X}_n(t) = \{\, \boldsymbol{x}_n(t_0),\ \boldsymbol{x}_n(t_0 + \Delta t), \ldots,\ \boldsymbol{x}_n(t - \Delta t),\ \boldsymbol{x}_n(t)\} \tag{3.1}$$

be a set of T positions (people's detections) from the initial time t_0 up to the current time t increasing in Δt time intervals. The point $\boldsymbol{x}_n(t) = [x(t), y(t)]_n$ is the position at time t, of the nth trajectory with respect to the world reference frame. Additionally, we define the orientation $\theta(t)_n$ as a function of the current position and the previous position, with respect to a global reference frame:

$$\theta(t) = \arctan\left(\frac{y(t) - y(t - \Delta t)}{x(t) - x(t - \Delta t)}\right). \tag{3.2}$$

Moreover, we define a set of destination positions $\boldsymbol{D} = \{D_1, D_2, \ldots, D_M\}$, that represents positions in a scene that people can go to. The existence of destinations is a requirement for most of the existing HMI methods. The set of destinations points must be known in advance and there are different methods to compute them. In our case we use the Expectation-Maximization method, as we will explain later. Other works, like [Luber et al., 2010] and [Ziebart et al., 2008,

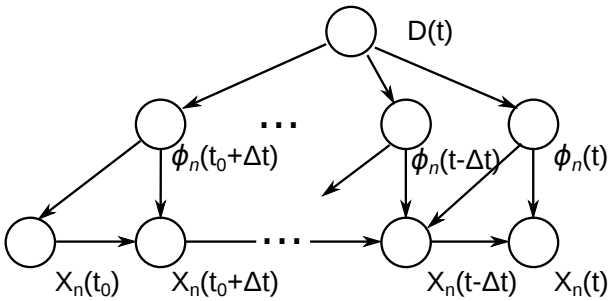

Figure 3.3: **Graphical model of the BHMIP.** Scheme of our classifier, the Bayesian Human Motion Intentionality Predictor.

2009], approximate these destinations as short-term propagations of the current state.

As it can be seen in Fig. 3.2, the angle $\phi_{nm}(t)$ is defined by the first derivative of the current trajectory and the $\boldsymbol{x}_n(t) \rightarrow D_m$ vector. By doing this, $\phi_{nm}(t)$ becomes a measure relative to a destination, while $\theta(t)$ is a global measure of the target's orientation. This difference will allow us to obtain a good characterization of the human motion intentionality.

Applying the kernel density estimation method [Silverman, 1986] to real HMI databases, we have verified that there exists a high similarity of the *pdf* of the ϕ angle and a Gaussian function, or a Von Mises distribution, if we would want to take into account the periodicity of the variable.

The scheme depicted in Fig. 3.3 corresponds to the graphical model that describes the basis of our algorithm. The relation of the destination D_m at time t is given by the relations of the nodes of this structure and determines the calculation of the probabilities used in the next section.

Although it is out of the scope of the present work, a real implementation requires some filtering of the detections in order to eliminate noise and outliers. We will simply consider that a previous filter exists, but for the understanding of the presentation of our approach it will not be discussed in this chapter.

3.4 The Bayesian Human Motion Intentionality Predictor

The problem of estimating the best destination is reduced to a sequential data classification, where the decision of choosing a destination is taken at each instant of time while the human is walking. There are many well known techniques solving the sequential data classification, such as the Naive Bayesian classifier, Hidden Markov Models or Conditional Random Fields. Our proposed technique is inspired in a Bayesian framework, in order to classify the motion intentionality. We will begin our analysis using an infinite window, that takes into account from the first observed position of the trajectory $\boldsymbol{x}_n(t_0)$ to the current observation $\boldsymbol{x}_n(t)$. We will

discuss later the importance of considering the complete sequence of observed positions of a trajectory, depending on its time elapsed since their observations. Intuitively, we are interested in the more recent observed positions of a trajectory since they are more significant to the destination classification than older ones. In the following subsections we will discuss this statement and formulate our classifier accordingly.

The method proposed in this chapter, denominated Bayesian Human Motion Intentionality Prediction (BHMIP), is a geometric-based method which uses a Bayesian classifier to compute the best prediction to a given destination position, for each position $\boldsymbol{x}_n(t)$ of the trajectory $\boldsymbol{X}_n(t) = \{\, \boldsymbol{x}_n(t_0),\ \boldsymbol{x}_n(t_0 + \Delta t), \ldots,\ \boldsymbol{x}_n(t - \Delta t),\ \boldsymbol{x}_n(t)\}$. We model the *pdf* function

$$P(\, \boldsymbol{x}_n(t) |\, \boldsymbol{x}_n(t{-}\Delta t), D_m) = \mathcal{N}(\phi; 0, \sigma_\phi^2) \tag{3.3}$$

conditioned by the previous position $\boldsymbol{x}_n(t - \Delta t)$ and the desired destination D_m as a Gaussian function. In Fig. 3.4 is depicted an example of this probability function to two destinations D_1 and D_2 centered at the position $\boldsymbol{x}_n(t)$, where we calculate their corresponding probabilities generated by the values ϕ_1 and ϕ_2.

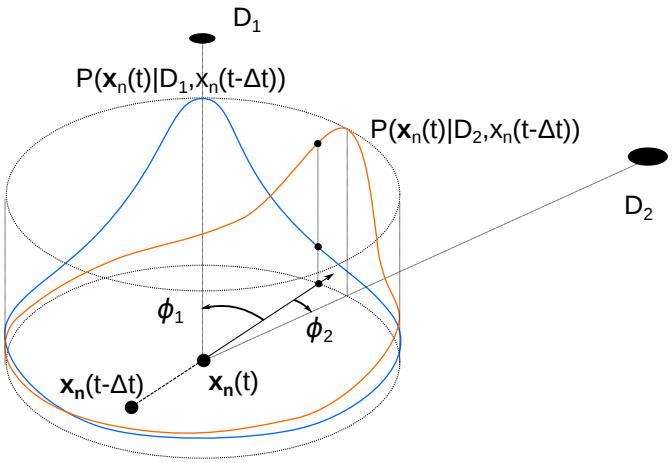

Figure 3.4: **Probability distributions.** Drawn of the different *pdf* functions depending on their corresponding destinations D_1 in blue and D_2 in orange. The probability of each of the destinations being the intentionality is also depicted, being more likely that the observations match to the intentionality to reach D_2.

3.4.1 Naive BHMIP

We have used the Naive Bayesian classifier for its simplicity and the requirement of minimal external parameters to tune. One of its requirements, as we will show later on, is the assumption of independence of their features. The method is simple, it only requires an initial learning of the positions deployed as destinations and it can be generalized to other geometric-based methods.

At each position $\boldsymbol{x}_n(t)$ of the trajectory $\boldsymbol{X}_n(t)$, we compute the probability to reach different

future destinations D_m, calculating the *a posteriori* probability function $P(D_m|\,\boldsymbol{x}_n(t),\,\boldsymbol{x}_n(t-\Delta t))$, taking into account the accumulated trajectory $\boldsymbol{X}_n(t)$.

The joint probability $P(\,\boldsymbol{X}_n(t)|D_m)$ can be obtained easily using the chain rule as follows:

$$\begin{aligned} P(\,\boldsymbol{X}_n(t)|D_m) &= P(\,\boldsymbol{x}_n(t_0),\,\boldsymbol{x}_n(t_0+\Delta t),\ldots,\,\boldsymbol{x}_n(t-\Delta t),\,\boldsymbol{x}_n(t)|D_m) \\ &= P(\,\boldsymbol{x}_n(t)|D_m,\,\boldsymbol{x}_n(t-\Delta t),\ldots,\,\boldsymbol{x}_n(t_0))\cdot \\ &\quad P(\,\boldsymbol{x}_n(t-\Delta t)|D_m,\,\boldsymbol{x}_n(t-2\Delta t),\ldots,\,\boldsymbol{x}_n(t_0))\cdot \\ &\quad \vdots \\ &\quad P(\,\boldsymbol{x}_n(t_0)|D_m). \end{aligned} \tag{3.4}$$

For each trajectory $\boldsymbol{X}_n(t)$ we have considered Markovian properties, where there are dependencies in positions only between consecutive positions $\boldsymbol{x}_n(t)$ and $\boldsymbol{x}_n(t-\Delta t)$. As it can be observed in Fig. 3.3, the $\phi_n(t)$ variable is function of two observed position at instants t and $t-\Delta t$ and this information relating the current orientation $\theta(t)_n$ and the destination D_m can be treated independently at each instant of time with respect to classifying the destination D_m. Consequently, we can rewrite (3.4) more compactly as:

$$P(\,\boldsymbol{X}_n(t)|D_m) = P(\,\boldsymbol{x}_n(t_0)|D_m)\prod_{\tau=t_0+\Delta t}^{t} P(\,\boldsymbol{x}_n(\tau)|D_m,\,\boldsymbol{x}_n(\tau-\Delta t)). \tag{3.5}$$

Using the Bayes theorem we can compute the *posterior* probability of the destination D_m, given the current and previous positions of the trajectory $X_n(t)$

$$P(D_m|\,\boldsymbol{X}_n(t)) = \frac{P(\,\boldsymbol{X}_n(t)|D_m)P(D_m)}{P(\,\boldsymbol{X}_n(t))}, \tag{3.6}$$

where the *prior* probability $P(D_m)$ to reach the destination D_m is calculated beforehand when obtaining the map of destinations $\boldsymbol{D}$, as we will show later.

Accordingly, we formulate the BHMIP in the following manner: if the *posterior* probability to a specific destination D_m is greater than the *posterior* probability to go to another destination D_j, that is

$$D^* = D_m \quad \text{if} \quad P(D_m|\,\boldsymbol{X}_n(t)) > P(D_j|\,\boldsymbol{X}_n(t)) \quad \forall m \neq j, \tag{3.7}$$

then D_m will be the best destination D^* describing the current human motion intention. The intention probability is thus defined by the maximum probability in (3.7) $P\big(\mathcal{D}_n(t)=D^*|\,\boldsymbol{X}_n(t)\big)$, where $\mathcal{D}_n(t)$ is the inner intention at time t for the nth person to reach the destination $D_m \in \boldsymbol{D}$.

By replacing (3.5) into (3.6) we obtain a compact formulation of the probability of the

intention of (3.7):

$$P\big(\mathcal{D}_n(t) = D_m |\, \boldsymbol{X}_n(t)\big) = \frac{P(D_m)}{P(\,\boldsymbol{X}_n(t))} P(\,\boldsymbol{x}_n(t_0)|D_m) \prod_{\tau=t_0+\Delta t}^{t} P(\,\boldsymbol{x}_n(\tau)|d_m,\, \boldsymbol{x}_n(\tau-\Delta t)). \tag{3.8}$$

This equation serves as the basic approach to formulate our classifier. In the following subsections, we propose variations of this formulation in order to overcome the problems generated by changes in intentionality, *i.e* the inner destination D^* has changed.

3.4.2 Sliding Window BHMIP

As stated before we want to provide a solution to the questions: what if a person changes her/his path? what if the intentionality of a person changes in the middle of a walk? As we are evaluating partial trajectories $\boldsymbol{X}_m(t)$ and not the full observed trajectory $\boldsymbol{X}_m$, we don't know the true final destination until we have reached it. So in addition to the uncertainty associated to the decision of the best destination, there is the possibility that past observed trajectories truly indicate a correct intentionality until this intentionality changes and its estimation becomes inconsistent with respect to the past observations.

Inspired by the Sliding Window method [Dietterich, 2002] for sequential classification, we define the length or the time interval of past positions $\boldsymbol{x}_n(t)$, discarding older person's positions and keeping the most recent observations. By doing this, we provide a robust solution to changes in intentionality without formulating a completely new approach that overcomes this issue. The resultant classifier is obtained by simply rewriting (3.5) into

$$P(\,\boldsymbol{X}_n(t)|D_m) = \prod_{\tau=t-w}^{t} P(\,\boldsymbol{x}_n(\tau)|D_m,\, \boldsymbol{x}_n(\tau-\Delta t)). \tag{3.9}$$

We have defined a new parameter w, the length of observation. This parameter is calculated on a training stage of the algorithm to optimize the results obtained by the BHMIP-SW. The improvement of this solution, although it is minor when applied on typical or normal trajectories, it has proved to work better specially in abnormal trajectories, where unexpected behaviors of people are observed. We will discuss in Sec. 3.5.3 more details on this.

3.4.3 Time Decay BHMIP

We have incorporated an additional feature into the BHMIP to weight in a different way the contributions of the past positions to our proposed method. Intuitively, we assume that new observed positions are more determinant than older ones.

If we take a step further the Sliding Window BHMIP, then we require a temporal dependency for the weights or contributions of past poses. Newer observations are more determinant to

the intentionality predictor, and thus, these observations should be weighted higher than older observations. In accordance to this idea and based on the Sliding Window BHMIP approach, we propose a variation that makes use of a non-constant window that degrades as a function of time:

$$P(\boldsymbol{X}_n(t)|D_m) = \prod_{\tau=t-w}^{t} P(\boldsymbol{x}_n(\tau)|D_m,\ \boldsymbol{x}_n(\tau-\Delta t))^{g(t-\tau)}. \tag{3.10}$$

The domain of the function $g(t-\tau)$ is the elapsed time since the observation $\boldsymbol{x}_n(\tau)$ took place and it is positive by definition. The output of the g function is in the interval $[1, 0]$, being 1 for the current position, the higher weighted probability and 0 for the most distant in time. For this reason, we propose to use the exponential function,

$$g(t) = e^{-\frac{t}{\sigma_w}} \tag{3.11}$$

that satisfies all the above mentioned requirements. Again, we have added an additional parameter that will be calculated in order to optimize the performance of the algorithm, as discused above for the BHMIP-SW. The performance of the Time Decay approach (BHMIP-D) will be discussed in the following section.

3.5 Experiments

We have used two different databases to validate the results presented in this chapter. The Edinburgh Informatics Forum Pedestrian database [Majecka, 2009] is a set of human trajectories at the Informatics Forum, the main building of the School of Informatics at the University of Edinburgh (see Fig. 3.5-*Left*). The data covers several months of observations which have resulted in about 1.000 observed trajectories each working day, and at present has more than 92.000 observed trajectories. The sample rate is 9 positions per second. A set of eight final destinations are identified.

The Freiburg People Tracker [Luber et al., 2011] ground truth consists of a set of 162 person tracks at the city center (see Fig. 3.5-*Right*), resulting in more than 10.000 manually labeled positions in order to validate their multi hypothesis people tracker. The sample rate is approximately 50 positions per second.

A total of 1.280 trajectories from the Edinburgh database were studied, each trajectory consisting of an average of 100 positions. The trajectories are divided into two sets, one set for training and the other for testing. As the Freiburg database has less people's tracks available, 30% of the trajectories were used for training purposes and 70% of the trajectories were used for testing, each trajectory consisting of an average of 500 positions.

3.5.1 BHMIP parameters learning

One of the main advantages of the geometrical or place-independent methods for prediction is that a set of primitive trajectories is not required. However, they are not excluded from training: the set of destinations requires to be defined somehow. One simple solution might be a manual setting of the trajectories into salient positions such as stairs, elevators, doors, etc.. The solution adopted in this work, although, has been a clusterization of positions into destinations.

A general view of the Edinburgh Informatics Forum is depicted in Fig. 3.5-*Left*. The scene is taken from a camera fixed at 23m above the floor. For the purpose of the present chapter, 8 final destinations D_m have been estimated using the Expectation-Maximization algorithm [Bishop et al., 2006] of the starting and ending positions of each trajectory. Some of these final destinations coincide with entry/exit points. The same procedure has been carried out for the Freiburg database (Fig. 3.5-*Right*), where all the initial and final points of each trajectory are depicted and the clusterization of the destinations is shown, as well as the covariances on those positions.

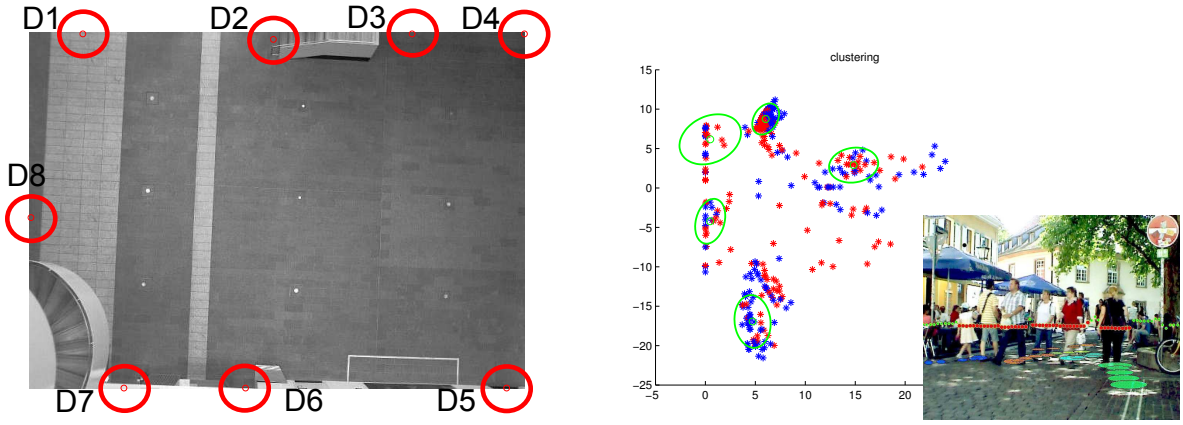

Figure 3.5: **Databases description.** On the *Left*, the map of the Edinburgh Informatics Forum, presented in [Majecka, 2009]. Eight different destinations are drawn as red circles. On the *Right*, the Freiburg database environment, where there are shown the clusters of the destinations, and on the bottom, a picture of the environment, thanks to Luber et al. [2011]. In both cases a EM algorithm has been used to estimate the set of destinations.

As discussed in Sec. 3.4, the two BHMIP methods proposed make use of past information. The width w and σ_w of the window are parameters of the system and the performance of the predictor depends on these values.

We have evaluated the accuracy of prediction by doing the following: we provide an observation of the trajectory corresponding to the interval $[0, t]$ from the beginning $t = 0$ to the current time t. We incrementally augment the current time t until it reaches the end of the trajectory $t = T$. For every observation provided of a given trajectory, we calculate the most likely destination according to each method and then check if the prediction is or not correct.

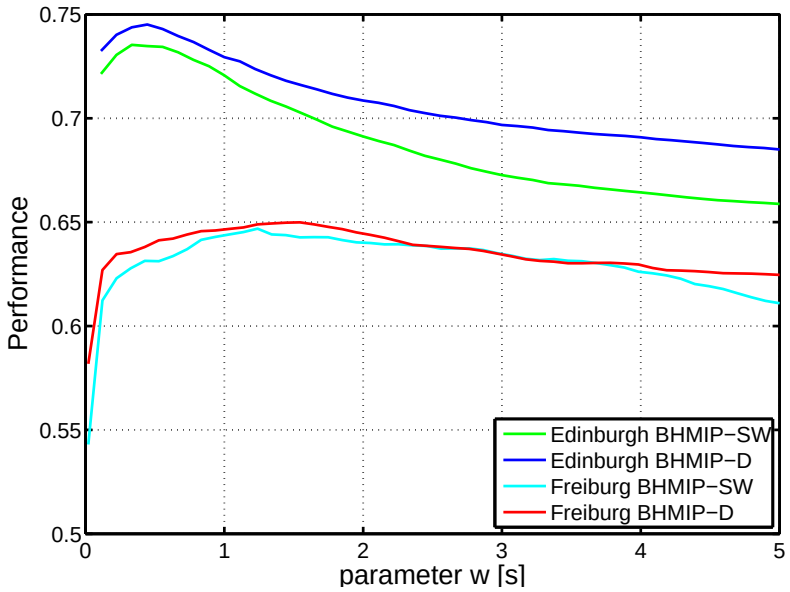

Figure 3.6: **Performance results.** Drawing of the performance results versus the parameter w and σ_w (in seconds), using the Edinburgh and the Freiburg database.

Fig. 3.6 draws the performance of each method depending on the value w and σ_w (the window width), which is measured in seconds.

For the Edinburgh database results, there is a clear optimum for the Sliding Window BHMIP at $w = 0.444s$ and for the Time Decay BHMIP at $\sigma_w = 0.5s$. The results for the Freiburg database are not clear, the best performance is for $w = 1.5s$, however the performance presents a flat behavior for $w > 2s$. For this reason, we have chosen a time width w and σ_w roughly around $0.5s$ for both databases, which corresponds to the reaction time of the system to make good predictions.

3.5.2 BHMIP testing

In this subsection, we analyze the proposed methods, the Sliding Window Bayesian Human Motion Intentionality Predictor (Sec. 3.4.2) and the Time Decay BHMIP (Sec. 3.4.3). The w and σ_w parameters have been obtained previously. In addition, a comparison with other methods is shown. We will stress on the advantages of our approach with respect to the state of the art methods.

A comparison with other approaches is difficult since no other methods use destination points as they have been defined in this chapter. The geometrical-based method, that we have implemented for comparison, is the approach proposed by Foka and Trahanias [2010]. Originally, this method treats all the cells on a grid map, corresponding to obstacles, as possible destinations and computes the best cell as the destination a person aims to. One limitation of the method appears when the destination is not an obstacle. For this reason, we have made

the following modifications in the method: the interesting cells of the map are translated into the same destination points defined in our approach, and by doing this, we are not constraining the position of the destinations to grid cells. The other implemented method is the approach proposed by Bennewitz et al. [2005] as one of the most representative prediction methods of the place-dependent group. A set of primitives is obtained for both databases applying the Expectation-Maximization algorithm. With the purpose of comparing with the BHMIP, we have assumed a correct prediction if the corresponding primitive associated to the current trajectory finishes at the desired destination. We have used a different sampling rate for the two databases, however the four methods use the same sampling rate when testing each database.

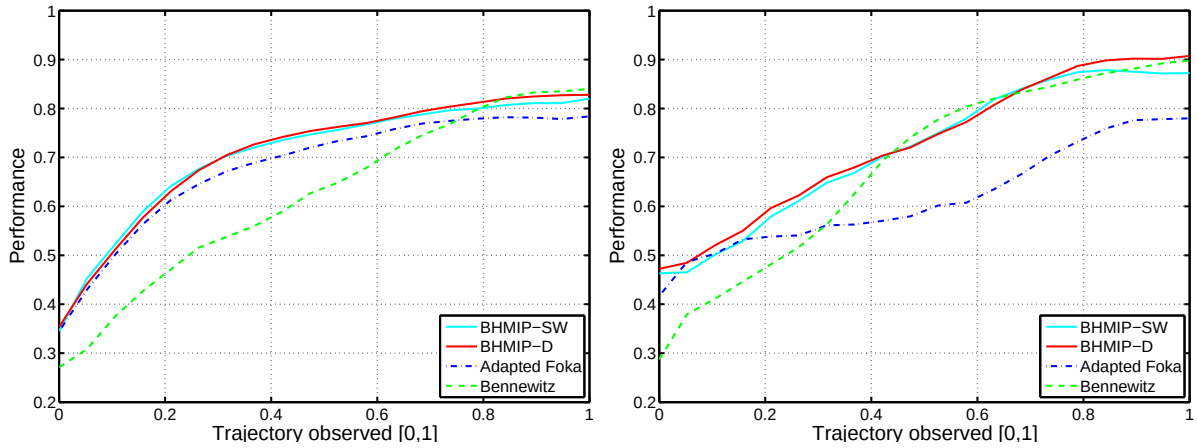

Figure 3.7: **Performance results.** On the *Left*, performance of the algorithm against other state of the art methods, using the Edinburgh database. On the *Right*, the performance on the Freiburg database. The horizontal axis is the percentage of time to complete the trajectories, where 1 is the total time to complete the trajectories.

A comparison of the results, for the four methods, is shown in Fig. 3.7. The figure on the left shows the performance in the Edinburgh database. The geometrical methods (BHMIP-SW, BHMIP-D and Adapted Foka) present a better performance at early stages of the evaluation than the place-dependent (Bennewitz), although for long observations it scores a 84% of success rate.

In Fig. 3.7-*Right* is depicted the performance using the Freiburg database. As it can be seen, the Bennewitz method could not obtain such a good performance after short observations (t small), but it improves the accuracy after considering longer observations. However, the performance of the place-dependent varied for each scenario. At the Freiburg city center (Fig. 3.7-*right*), where 5 destinations and 20 primitive trajectories are clearly defined, the method obtains almost 90% of accuracy when the complete trajectory is considered and a mean of 68.47% (See Table 3.1). On the other hand, the performance obtained for the complete trajectory at the Edinburgh scenario (which consists of 8 destinations and more than 50 primitive trajectories) is 84% but its average performance is under 62.07%. The reason for such a performance at the Edinburgh Forum is due to the fact that the trajectories are in an open area with less structural

constraints, therefore more unexpected trajectories might occur. Nevertheless, a fully observed trajectory can't be considered as a prediction problem but a classification problem.

Considering the previous reasoning, the BHMIP is a method well suited for real-time prediction. It can provide rapidly an accurate prediction of people's trajectories. Also, the geometrical-based methods are more indicated in open scenarios, where prediction is done in areas consisting of many destination points.

3.5.3 BHMIP on abnormal trajectories

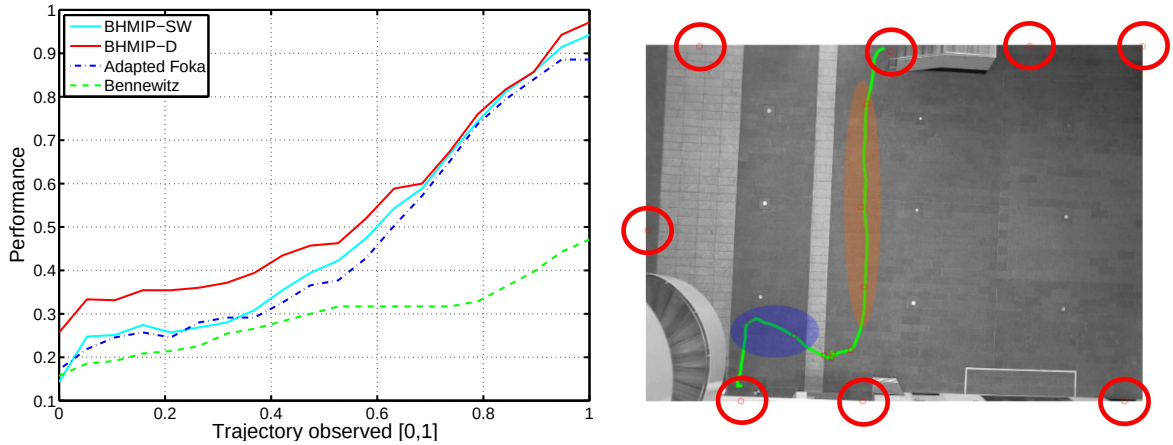

Figure 3.8: **Performance results.** On the *Left*, performance of the algorithm using a selected set of abnormal trajectories in the Edinburgh database. On the *Right*, an example of an abnormal trajectory, where a change in the destinations occurs in the middle of the path.

Observing the behavior of the human trajectories, we have seen that there are people that walk from an origin to a destination without stopping, maintaining a constant speed. Other people stop one or several times and change their velocity. There are also people that modify their trajectories several times and then stop in some places before reaching their destination. All these abnormal cases are specially interesting since they represent a challenge for any prediction method. That is the reason to select a set of specially challenging trajectories to classify. On many of these abnormal trajectories appear changes in intentionality. An example of an abnormal trajectory can be seen in Fig. 3.8-*Right*.

The results are shown in Fig. 3.8-*Left*. All the methods fail to determine initially the correct destination. It is not surprising since we have set the dataset to contain trajectories with changes in destinations and other abnormalities. Nonetheless, the geometrical approaches behave in general better at late stages of the intentionality prediction. They are capable of quickly recover from changes in destinations while the place-dependent approach presents more problems to adapt.

Table 3.1 shows a summary of the overall performances of the evaluated methods, each per-

Table 3.1: Overall performance of our intentionality prediction methods compared to state of the art algorithms in different databases.

	Edinburgh	Freiburg	"Abnormal"
BHMIP-SW	70.81%	71.59%	49.00%
BHMIP-D	71.10%	72.74%	54.29%
Adapted Foka	68.22%	61.93%	47.00%
Bennewitz	62.07%	68.47%	29.29%

centage is the mean of the performance of every experiment carried out before. Furthermore, we can observe that both BHMIP methods present a better performance in all situations, being the BHMIP-D slightly better and more adaptable to abnormal trajectories than the Sliding Window BHMIP.

3.5.4 Experiments in a robotic task

The main motivation to develop the BHMIP is, of course, a direct application to robotic tasks. More concretely, the presented work was developed as a key tool for a robot companion experiment [Ferrer et al., 2013c], as we will discuss more in depth in Chapter 6. These results only exemplify the usefulness of the BHMIP applied to robotic problems. In brief, the main task of the robot in this experiment is accompanying a person. The robot companion predicts the human target's destination and uses this information to predict where the human will be and positioning the robot in the best place. In addition, the companion task is carried out successfully under the presence of obstacles and moving people (see Fig. 3.9). Under the framework of the robot companion task, we observed that the consideration of human motion prediction enhances the performance of the method: a set of 45 real-life experiments with different volunteers have been carried out. Three different scores were examined: "Robot's Intelligence", "Human-Like Motion" and "Level of confidence". For each score examined, the average of the results showed an important increase, compared to not using the prediction information (the BHMIP), while accompanying the volunteer, as depicted in table 3.2.

Table 3.2: Increase of performance after using prediction information in a robotic task.

	Robot's Intelligence	Human-Like Motion	Level of confidence
% increase due to BHMIP	38.89%	52.78%	43.9%

Real trajectories are subject to disturbances, as a part of the real world settings. The BHMIP handled correctly most of the uncertainties and quickly adapted to changes in intentionality.

We have presented just a simple example where the human prediction enhances a certain

Figure 3.9: **Example of a real robot experiment.** The left image corresponds to the robot camera. On the center of the image Dabo is accompanying a person to her desired goal while navigating in a urban environment. The right image corresponds to the robot GUI, built on ROS architecture. Green cylinders correspond to persons' detections and the orange cylinder corresponds to the target to be accompanied.

utility, but the use of forecasting tools like the BHMIP may improve a countless number of robot applications, specially in urban or outdoor environments.

3.6 Summary

In the present chapter we have presented a novel and accurate human motion intentionality indicator, denominated Bayesian Human Motion Intentionality Prediction (BHMIP), which is a geometric-based long-term predictor. This novel contribution is essential for the development of future contributions, specially for navigation and accompany tasks, as explained later.

We have proposed two variants of the algorithm: the BHMIP-SW (sliding window) and the BHMIP-D (time decay). The performance of both are successful, but the BHMIP-D behaves better under challenging trajectories, as demonstrated in the abnormal database.

We have presented a simple formulation, a low computational complexity and it outperforms other state of the art approaches. The system requires minimal training, since it is place independent and only the set of the scene destinations must be obtained, although it might be obtained using geometrical or manual methods as well.

A comparison of the BHMIP is done with other well known methods for long-time prediction using the Edinburgh Informatics Forum pedestrian and the Freiburg People Tracker databases. Additionally, experiments in a real scenario are carried out including a set of volunteers walking in the presence of a two-wheeled mobile robot, to validate the overall performance of the BHMIP.

The next logical step, which is explained in the next chapter, is to obtain a propagation model of the predicted human motion in order to complete the forecast information that can be extracted from people's observations.

4

Human trajectory prediction

In the previous Chapter 3 we introduced the *intentionality prediction* concept that will be fully exploited in the present Chapter 4. The objective of this chapter is to introduce a complete prediction framework for human motion that closes the prediction Part I of the thesis.

We have based our prediction algorithm in the Social Force Model (SFM) by Helbing and Molnar [1995] to shape person-to-person and obstacle-to-person interactions. As a contribution of this chapter, we propose to expand the SFM by considering robot-to-person interactions as well, and thus, we can employ it to develop the theory described in the subsequent parts of the present thesis based on the "Extended Social Force Model" (ESFM).

Aiming to improve the human trajectory prediction, we propose a finer estimation of the parameters of the ESFM that are responsible for the generation of predictions. Accordingly, we have identified three different basic behaviors: *Aware*, *Balanced* and *Unaware*. In this chapter we will discuss how to integrate this estimation into the prediction of trajectories and we will show its results in real environments.

We have formulated the human trajectory prediction in an easily generalizable way, since this tool can be useful for many applications, not only robotics.

The prediction framework is mainly based on our publication in the *International Conference on Robotics and Automation* [Ferrer and Sanfeliu, 2014b]. The work presented in Sec. 4.3 describing the ESFM has been published in the *International Conference on Intelligent Robots and Systems* [Ferrer et al., 2013a] and appears in the thesis by Garrell [2013] as a result of our collaboration.

4.1 Introduction

As stated before, in this chapter we present a complete probabilistic framework for human motion prediction in urban or social environments. The aforementioned framework consists of the intentionality predictor (BHMIP) presented previously, the trajectory prediction algorithm and the behavior estimator. We analyze human trajectories under the influence of an heterogeneous

environment, where there are moving people, objects and robots, as well as static obstacles.

Our approach makes use of the Social Force Model (SFM) of Helbing and Molnar [1995] to build realistic human trajectories. We propose an extension to the SFM that takes into account the micro-interactions between pedestrians and robots and we obtain the robot-to-person interaction specifically suited for Tibi&Dabo robots.

Additionally, we formulate a powerful and useful tool: the human motion behavior estimator. We suggest to estimate the interaction parameters required in the SFM for every target to improve the prediction performance. Every person is different and behaves differently in identical situations, especially when robots appear. This serves as a motivation to obtain the estimation of human behavior for enhancing the human motion prediction. Three different basic behaviors have been detected: *Aware*, *Balanced* and *Unaware*. One of the main contributions of the present chapter is to make use of the behavior estimator to formulate a reliable prediction framework of people's trajectories under the influence of moving people, robots and in general any moving obstacle.

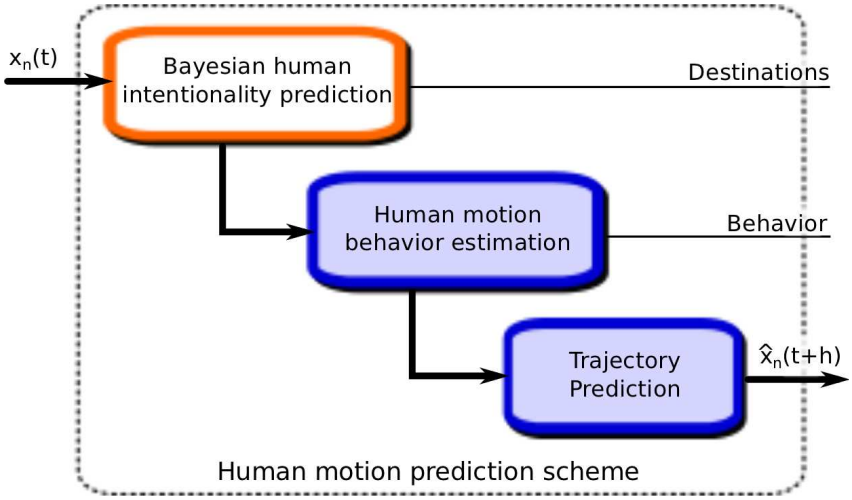

Figure 4.1: **Prediction scheme.** A basic scheme of the proposed prediction algorithm and required estimators for a complete framework for human motion prediction.

In Fig. 4.1 is depicted a scheme of the prediction framework. Firstly, we use the Intentionality Predictor (BHMIP) to estimate the best destination a person aims to. The information extracted by the BHMIP is used in the following module, the Behavior Estimator. At last, we combine the intentionality information plus the behavior information to provide an enhanced prediction of human trajectories, as depicted in Fig 4.2. The last two modules of the scheme are the main contributions of the present chapter.

We have demonstrated the good performance of our long-term prediction algorithm in real scenarios, comparing to other prediction methods. In addition, we have implemented the prediction framework into the robot software structure, aiming to use it in future chapters of

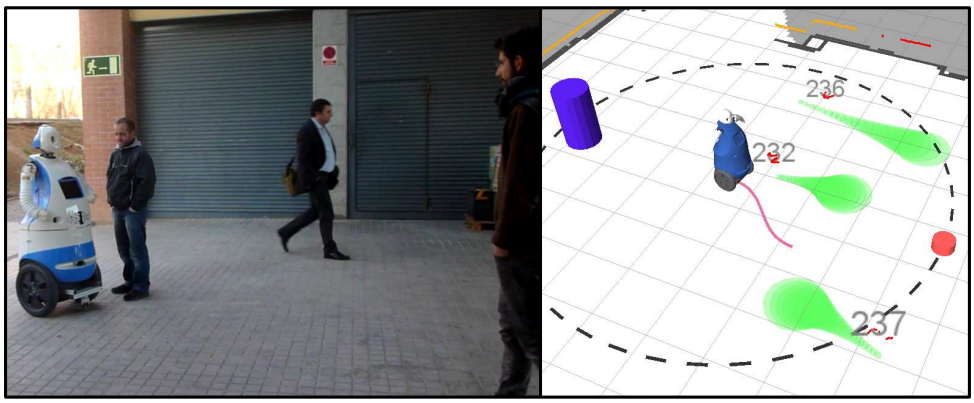

Figure 4.2: **Urban environment.** Scene corresponding to the FME, where part of the experiments were carried out. Prediction position covariances are drawn as green ellipses projected and superposed in the plane.

this thesis.

4.2 Related work

There exists a wide variety of approaches to predict human motion, such as social fields or forces, optimal control, geometry-based methods, inverse reinforcement learning, hidden Markov models, etc. We have based our work on the social field or forces methods. These methods present an important advantage over other approaches, they model the interactions between all the elements in the environment in a simple and easy way to calculate, while other approaches do not even consider interactions, providing a path in a static environment.

Human motion has been studied in terms of social fields or forces [Helbing and Molnar, 1995; Zanlungo et al., 2011; Huang et al., 2006] where changes in behavior can be explained by these virtual forces. The social-force model (SFM) described in [Helbing and Molnar, 1995] takes into account both the goal and the interactions by defining a summation of existing forces describing people's trajectories.

The work of Zanlungo et al. [2011] has treated the problem by considering a collision time which determines the magnitude of the interacting force. Nevertheless, this model is not able to explain why different people behave differently, under the same configuration of the scene. In [Garrell et al., 2009; Garrell and Sanfeliu, 2012] has been proposed a potential field based on the SFM to model groups of people and guide them. The study of human motion has motivated many studies directly applied to robot navigation. Huang et al. [2006] have proposed a robot vision-guided local navigation, where they characterize a model of human navigation. Similar to the virtual forces, Antonini et al. [2006] have modeled short term behavior of individuals as a response to the presence of other pedestrians.

Human trajectories can be also generated following control laws. In [Arechavaleta et al., 2006b,a, 2008], the human motion prediction has been obtained using control criteria in controlled environments. Papadopoulos et al. [2013] have used inverse optimal control to generate human trajectories and Shin et al. [1993] have generated paths using clothoids. Vieilledent et al. [2001] have related velocity and curvature to generate human trajectories. These methods generated very realistic paths under some conditions, superior to the SFM, however they do not model the simultaneous and subtle interactions that take place in a urban environments between people, and thus, these models are not accurate on realistic urban dynamic situations.

Human motion can also be explained in terms of geometric criteria. We already introduced some of these works on Chapter 3, such as [Foka and Trahanias, 2010]. Moussaïd et al. [2011] have proposed a method to adapt human walking speeds and directions based on behavioral heuristics. Bruce and Gordon [2004] infer destinations in a scene and plan accordingly for an intelligent trajectory estimation against occlusions for tracking applications.

Lately, learning techniques have become very popular to model human motion. Clustering methods, such as the work of Bennewitz et al. [2005] presented in the previous chapter, can be used to calculate the future position of a person's trajectory. They analyze a collection of people's trajectories in indoor environments and cluster those motion trajectories, by using the Expectation-Maximization algorithm into primitive trajectories. Similarly, Vasquez et al. [2009] and Sehestedt et al. [2009] have clustered and learned a Hidden Markov Model to classify and predict trajectories. Castro-González et al. [2010] have clustered typical crossing behaviors and predict people's trajectories as a result of those interactions.

Chung and Huang [2010] have studied spatial effects to build trajectories in a socially acceptable manner. In [van den Berg et al., 2008, 2011] it has been proposed the simulation of multiple agents interacting simultaneously moving in a common space, which has been used by Kim et al. [2015] to predict pedestrians' trajectories.

Inverse Reinforce Learning (IRL) has been followed by many works [Ziebart et al., 2009; Henry et al., 2010; Luber et al., 2012; Kuderer et al., 2012] as a tool to learn the parameters describing human motion and identifying the navigation features that could be useful for robot navigation, simulations or predictions. Vasquez et al. [2014] have proposed a comparison of many navigation features used in the IRL in different works.

The Social Force Model presents accuracy limitations when performing micro-prediction of human motion. The work of Kuderer et al. [2012] have proposed a learning-based motion prediction approach which compares to the SFM. Nonetheless, it is still unclear which approach works better since the calibration of models may be tricky and leads to contradictory conclusions. We will discuss more on this issue in the summary 4.7 of the chapter, after the experimentations have been carried out.

4.3 The Extended Social Force Model

We need a model in order to predict human trajectories, as estated before, we have chosen to base our work on the Social Force Model (SFM). This model suggests that the motion of pedestrians can be described as if they would be subject to "social forces". These forces are a measure for the internal motivations of the individuals to perform certain actions (movements), which model the micro-interactions between people in a manner that resembles the physical properties of gas. This theory is presented and further developed throughout this dissertation.

We encountered two main problems when trying to adapt the SFM to the prediction framework. The first problem is due to the SFM requiring information of attractors or goals in order to work. This problem is directly solved by the BHMIP, see Chapter 3, which provides an estimation of the most expectable destination that a person is aiming to. The second problem, the SFM does not consider the interaction between people and robots. In order to achieve a model capable of representing the interactions between pedestrians, obstacles and robots in typical social environments, we propose the Extended Social Force model (ESFM), based on [Helbing and Molnar, 1995], which is one of the main contributions of the present chapter.

In the following paragraphs, the internal forces for both robots and humans are described according to the original SFM, however we have discussed the variations provided by the ESFM when necessary. Moreover, people's internal forces are used to predict his/her motion as will be described in Sec. 4.5.

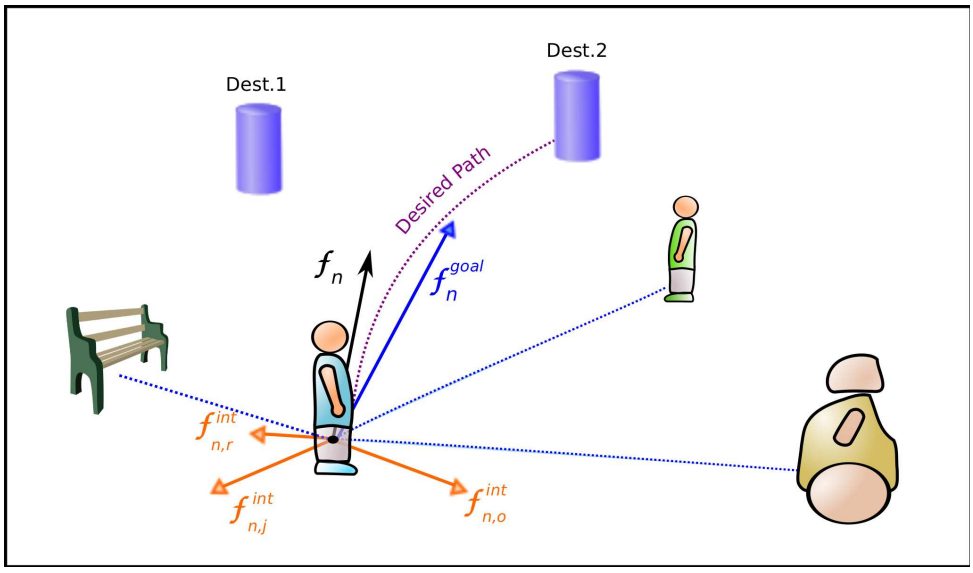

Figure 4.3: **Extended Social-Force Model.** Diagram of the social forces corresponding to the person p_n. The blue arrow represents the force aiming to a destination and the orange arrows represent each of the different kinds of interaction forces: person-to-person, object-to-person and robot-to-person. The summation of all the forces is represented as the black arrow $\boldsymbol{f}_n$.

Formally, the original SFM considers the pedestrian p_n with mass m_n as a particle abiding the laws of Newtonian mechanics and makes use of attractors and repulsors in the continuous space to characterize motion. Hence, the basic equation of motion for a pedestrian is given by the social force term

$$\boldsymbol{f}_n(t) = \frac{d\,\boldsymbol{v}_n(t)}{dt} m_n, \tag{4.1}$$

where the social force $\boldsymbol{f}_n(t)$ is related as the derivative of the velocity $\boldsymbol{v}_n(t)$, which describes the trajectory of the pedestrian p_n over time. For the sake of simplicity, we will value m_n as the unity for every person considered.

A person is attracted to a goal in the scene or a destination following the presentation of Chapter 3, as depicted in Fig. 4.3. Thus, the steering force is formulated as:

$$\boldsymbol{f}_n^{goal}(t, \mathcal{D}_n(t)) = k_n(\, \boldsymbol{v}_n^0(\mathcal{D}_n(t)) - \, \boldsymbol{v}_n(t)), \tag{4.2}$$

where the pedestrian p_n tries to move at a *desired speed* v_n^0 in a *desired direction* $\boldsymbol{e}_n$, such as $\boldsymbol{v}_n^0 = v_n^0\, \boldsymbol{e}_n$. The *desired velocity*'s direction is given by a vector pointing from the present position of the person to the next subgoal or destination. At this point we have introduced the concept of intentionality $\mathcal{D}_n(t)$, proposed in the previous Chapter 3 and estimated thanks to the BHMIP, and that is the reason why $\boldsymbol{v}_n^0$ appears as a function of the intentionality $\mathcal{D}_n(t)$ at time t. The original formulation of the SFM assumes a prior knowledge of this desired velocity. The *desired velocity* module is the one at which the person feels more comfortable to walk and is estimated by averaging observations. The relaxation time is the interval of time needed to reach the desired velocity and the desired direction, where $k_n = 1/\tau_n$ and τ_i is the time for a human to take a step, 0.5 seconds approximately.

Furthermore, repulsive effects from the influences of other people, obstacles and robot in the environment are described by the interaction forces. These forces prevent humans from walking along their intended direction, moreover, they are modeled as a summation of forces either introduced by other pedestrians p_j, $\boldsymbol{f}_{n,j}^{int}(t)$, by obstacles, $\boldsymbol{f}_{n,o}^{int}(t)$, and, in the present study we model the interaction due to robots $\boldsymbol{f}_{n,r}^{int}(t)$. A diagram of the social forces corresponding to the person p_n is plotted in Fig. 4.3. The resulting force $\boldsymbol{f}_n(t)$ governs the trajectory described by the target p_n at time t

$$\boldsymbol{f}_n(t) = \boldsymbol{f}_n^{goal}(t, \mathcal{D}_n(t)) + \sum_{j \in P \setminus n} \boldsymbol{f}_{n,j}^{int}(t) + \sum_{o \in O} \boldsymbol{f}_{n,o}^{int}(t) + \sum_{r \in R} \boldsymbol{f}_{n,r}^{int}(t), \tag{4.3}$$

being P the set of people moving in the environment where the human interacts, R is the set of robots and O is the set of obstacles. At this point, we are introducing a variation to the classical SFM. The SFM considers all interactions as a summation of equally interacting forces, however, the Extension of the SFM stresses on the fact that we can quantify different interactions

between different kinds of targets. In our case, we are interested in providing a valid model to generate trajectories in the presence of robots as well as obstacles and people, and thus, we have characterized these interactions differently for people, obstacles and robots. As we will detail later in Sec. 4.4, we can provide a more accurate version of the model by estimating additional features such as the human motion "behavior".

The repulsive interaction forces are approximated to exponentials, according to the SFM

$$\boldsymbol{f}_{n,z}^{int}(t) = a_z e^{(d_z - d_{n,z}(t))/b_z} \hat{\boldsymbol{d}}_{n,z}, \tag{4.4}$$

where z is either a person, a robot or a static object in the environment, as a peculiarity of the ESFM with respect to the SFM. a_z and b_z denote respectively the strength and range of interaction force, d_z is the sum of the radii of the pedestrian and its interacting entity. The distance $d_{n,z}(t)$ from the person n to the target z at time t and $\hat{\boldsymbol{d}}_{n,z}$ is the unity vector $z \rightarrow n$. In order to calculate the Euclidean distance between n and z, humans and objects are assumed to be of circular shape with radii r_n and r_z.

Given the limited field of view of humans, influences might not be isotropic. This is formally expressed by scaling the interaction forces with an anisotropic factor depending on $\varphi_{n,z}$ between $\boldsymbol{v}_n$ and $\boldsymbol{d}_{n,z}$

$$w(\varphi_{n,z}) = \left(\lambda_z + (1-\lambda_z)\frac{1+cos(\varphi_{n,z})}{2}\right), \tag{4.5}$$

where λ_z defines the strength of the anisotropic factor

$$cos(\varphi_{n,z}) = -\boldsymbol{n}_{n,z} \cdot \boldsymbol{e}_r. \tag{4.6}$$

The term $\boldsymbol{n}_{n,z}$ is the normalized vector pointing from the position of z to person p_n which describes the direction of the force. Fig. 4.4 presents the value of the presented forces and the anisotropic factor.

The parameters $\boldsymbol{\rho} = \{k, a_z, b_z, \lambda_z, d_z\}$ are defined depending on the nature of the object, for instance, there is a set of parameters for the person-to-person interaction and the obstacle-to-person interaction, as described in other works such as [Zanlungo et al., 2011; Luber et al., 2010]. In this section we obtain the parameters describing the robot-to-person interaction since, to the authors' knowledge, these parameters had not been obtained before. The parameters are obtained using real experimental trajectories and a genetic algorithm, see Sec. 4.6.1.

In the following sections we will introduce a complementary concept to the calculation of the ESFM parameters $\boldsymbol{\rho}$, not only depending on the nature of the object, but an estimation of the parameters depending on the observation of the trajectory. This method provides a more accurate trajectory prediction as we will discuss later.

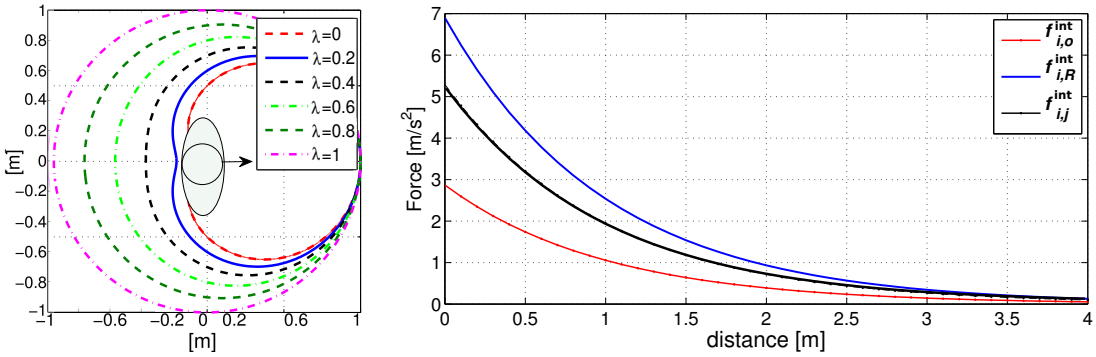

Figure 4.4: **Anisotropic parameter and forces modules.** *Left:* Representation of (4.5), defined as the given limited field of view of humans. *Right:* Forces magnitudes, the x-axis shows the distance from person p_n to an object, a person p_j or the robot r. The radius of p_n is $0.2m$ and the sum of the radii of p_n and p_k is 0.4m. For a robot, the considered radius is $1m$.

4.3.1 ESFM's parameters learning

We consider three kinds of interaction forces: person-to-person, obstacle-to-person and robot-to-person. The first and the second interactions have been studied in previous papers like [Helbing and Molnar, 1995; Zanlungo et al., 2011; Luber et al., 2010]. However, the robot-to-person interaction parameters were not directly obtained in any previous work, thereby, in this section we present a learning method to obtain the parameters $\boldsymbol{\rho} = \{k, a_{rp}, b_{rp}, \lambda_{rp}, d_{rp}\}$.

We decouple the training in two steps: firstly, we optimize the intrinsic parameters of the model forces k describing the expected human trajectories under no external constrains. By asserting no additional interaction, then we guarantee $\boldsymbol{\rho} = \{k, 0, 0, 0, 0\}$, which greatly simplifies the optimization of parameters to a single parameter. All optimizations used to learn the model forces parameters are carried out using genetic optimization algorithms [Goldberg, 1988] minimizing the following error function:

$$k^* = arg\min_k \left\{ \sum_{N'} \sum_{time} \| \boldsymbol{x}_o(t) - \boldsymbol{x}_e(t, \boldsymbol{\rho}) \| \right\}, \tag{4.7}$$

where $\boldsymbol{x}_o$ is the person's observed position and $\boldsymbol{x}_e(t, \boldsymbol{\rho})$ is the expected position after integrating the previous known position, according to (4.1) and calculating the corresponding steering forces as described in (4.2).

Secondly, we optimize the extrinsic parameters of the force interaction model $\{a, b, \lambda, d\}$ under the presence of a moving robot, making sure it is the only external force altering the outcome of the described trajectory. In this case, we have recorded N trajectories, different than

the trajectories N' of the first optimization step, in order to calculate the force parameters:

$$\{a, b, \lambda, d\}^* = arg \min_{\{a,b,\lambda,d\}} \left\{ \sum_N \sum_{time} \| \boldsymbol{x}_o(t) - \boldsymbol{x}_e(t, \boldsymbol{\rho}) \| \right\}, \tag{4.8}$$

where the observations $\boldsymbol{x}_o(t)$ correspond to the only person in the scene and the expected positions $\boldsymbol{x}_e(t, \boldsymbol{\rho})$ are calculated integrating the forces described in (4.3) and (4.2), now fixing the k parameter to $\boldsymbol{\rho} = \{k^*, a, b, \lambda, d\}$ as calculated in the first step of the optimization.

We have prepared a database in a real environment, as explained in Sec. 4.6.1, where we recorded more than 80 human trajectories using a laser sensor, and then, we manually labeled people's positions along the trajectory. A total of 20 volunteers participated in both parts of the experiment.

4.4 Behavior estimation

During experimentation in real scenarios [Ferrer et al., 2013a,b] we observed a high variability in human motion and it served as the motivation to develop the present work. Given the high variability of human behavior, it is difficult to accurately predict human motion using the same set of parameters $\boldsymbol{\rho} = \{k, a, b, \lambda, d\}$ for all people, since there is a clear disagreement between predictions and observations. As a result, our hypothesis is that each pair of interactions is characterized by an specific set of parameters $\boldsymbol{\rho}_l$. Therefore, the prediction problem becomes an estimation of those specific behaviors $\boldsymbol{\rho}_l$. We take into account additional considerations to estimate trajectories, similar to inferring motion intentions in a complex environment [Ferrer and Sanfeliu, 2014a], to alleviate the "high variability of trajectories" issue observed in real environments.

To this end, we define a set of possible behaviors $\boldsymbol{B} = \{B_1, B_2, \ldots, B_L\}$, each of them directly corresponds to a set of interaction parameters $\boldsymbol{\rho}_l = \{k_l, a_l, b_l, \lambda_l, d_l\}$, which define the interaction forces according to the ESFM. In addition, the inherent variable $\mathcal{B}_{n,q}$ is the estimated behavior between the target n and q, and it can be any behavior $\mathcal{B}_{n,q}(t) \in \boldsymbol{B}$. Accordingly, we propose a method to infer the latent state $\mathcal{B}_{n,q}(t) = B_l$ of a person that describes its force interaction with its nearby targets, and thus, its trajectory.

The behavior $\mathcal{B}_{n,q}(t)$ corresponds to the interaction between two people. For instance, a person may react very conservatively to an unexpected target while simultaneously behave passively with a companion. As depicted in Fig. 4.5, we can observe how different targets exert different forces which can only be explained if different behaviors are applied to each target.

The set of behaviors corresponding to one target is defined as $\mathcal{B}_n(t) = \{\mathcal{B}_{n,q}(t), \quad \forall q \neq n\}$ as

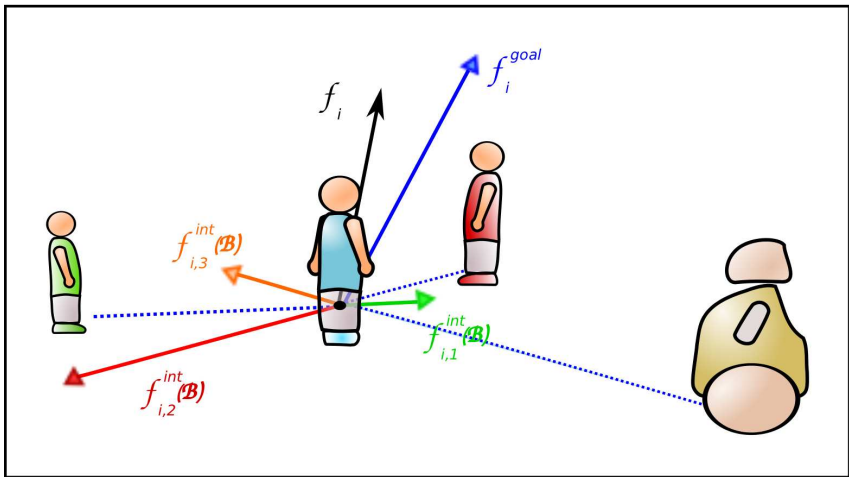

Figure 4.5: **Behavior ESFM.** Scheme of the social forces based on behavior estimations. As it can be seen, the behavior $\mathcal{B}_i$ determines the magnitude of the interacting forces, and hence, they are directly responsible of the described trajectories.

the set of parameters that describe the interactions of the nth target and its surrounding targets:

$$\boldsymbol{f}_n^{int}(t, \mathcal{B}_n(t)) = \sum_{q \in Q} \boldsymbol{f}_{n,q}^{int}(t, \mathcal{B}_{n,q}(t)). \tag{4.9}$$

We propose to use a Hidden Markov Model (HMM) to classify the sequential data information to infer the hidden behavior state:

$$\begin{aligned} P\big(\mathcal{B}_{n,q}(t) = B_l |\, \boldsymbol{X}(t)\big) = \eta \cdot P\big(\, \boldsymbol{X}(t) | \mathcal{B}_{n,q}(t)\big) \cdot \\ \sum_{\mathcal{B}_{n,q}(t-1)} P\big(\mathcal{B}_{n,q}(t) | \mathcal{B}_{n,q}(t-1)\big) P\big(\mathcal{B}_{n,q}(t-1) |\, \boldsymbol{X}(t-1)\big), \end{aligned} \tag{4.10}$$

where

$$P\big(\, \boldsymbol{X}(t) | \mathcal{B}_{nj}(t)\big) = \mathcal{N}\big(\| \hat{\boldsymbol{f}}_{obs}^{int}(t) - \boldsymbol{f}_n^{int}(t, \mathcal{B}_n(t))\|; \mu_{\boldsymbol{f}}, \Sigma_{\boldsymbol{f}}\big) \tag{4.11}$$

is a Gaussian distribution. The estimated interaction force is formulated as

$$\hat{\boldsymbol{f}}_{obs}^{int}(t) = \boldsymbol{f}_{obs}(t) - \boldsymbol{f}_n^{goal}(t, \mathcal{D}_n(t)), \tag{4.12}$$

where we can calculate the observed force $\boldsymbol{f}_{obs}(t)$ following (4.1) and the force $\boldsymbol{f}_n^{goal}(t, \mathcal{D}_n(t))$ to its goal by using (4.2), which is only possible after estimating the intentionality $\mathcal{D}_n(t)$ thanks to the BHMIP. The resulting subtraction is the estimated interaction force $\hat{\boldsymbol{f}}_{obs}^{int}(t)$. If it is well modeled, its value should be close to (4.9) which is the calculation of the interacting forces.

4.4.1 Behavior clustering

We need to obtain certain knowledge about the values of the basic classes $\boldsymbol{B}$ in order to use the proposed algorithm. Consequently, the clustering problem boils down to obtain a large set of $\boldsymbol{\rho}_{nq} = \{k, a_{nq}, b_{nq}, \lambda_{nq}, d_{nq}\}$ parameters, which are direct responsible for the motion behaviors as explained in this section.

We can obtain the estimated force of interaction $\hat{\boldsymbol{f}}_{obs}^{int}(t)$ as described in (4.12). However, we now require a function or method to calculate the values of $\boldsymbol{\rho}$, the social forces parameters, that fit better to the observation of the force $\hat{\boldsymbol{f}}_{obs}^{int}(t)$. We ensure, as explained in Sec. 4.6.2, that the training data acquired to calculate the parameter $\hat{\boldsymbol{\rho}}_{n,q}$ is generated only by the interaction of the target n with a single target q:

$$\hat{\boldsymbol{\rho}}_{n,q} = arg\min_{\boldsymbol{\rho}} \Big(\sum_{\tau=t-w}^{t} \| \hat{\boldsymbol{f}}_{obs}^{int}(\tau) - \boldsymbol{f}_{n,q}^{int}(\tau, \boldsymbol{\rho}) \|^2 \Big). \tag{4.13}$$

In general, any method to calculate this minimization solves the problem of finding the best $\hat{\boldsymbol{\rho}}_{n,q}$. We have chosen a sampling method, the Markov Chain Monte Carlo Metropolis-Hastings (MCMC-MH) [Andrieu et al., 2003]. The problem to be solved is treated as a stochastic optimization, since w is small, and hence, we provide a few number of observation forces to calculate the $\hat{\boldsymbol{\rho}}$. We make use of *a priori* information of values of typical $\boldsymbol{\rho}$ parameters calculated in other works [Zanlungo et al., 2011; Luber et al., 2010; Ferrer et al., 2013a] to constrain the search space.

Algorithm 1 MCMC-MH Learning

```
Initialize ρ^(0)
for i = 0 to N − 1 do
    Sample u ∼ U_[0,1]
    Sample ρ* ∼ q(ρ*|ρ^(i))
    if u < P(e(ρ*), e(ρ^i)) then
        ρ^(i+1) = ρ*
    else
        ρ^(i+1) = ρ^(i)
    end if
end for
```

In Alg. 1 is depicted the basic procedure. The function $e(\boldsymbol{\rho}) = \sum \| \hat{\boldsymbol{f}}_{obs}^{int}(\tau) - \boldsymbol{f}_{n,q}^{int}(\tau, \boldsymbol{\rho}) \|^2$ is the accumulated quadratic error and $q(\boldsymbol{\rho}^*|\boldsymbol{\rho}^{(i)})$ is a Gaussian distribution centered a $\boldsymbol{\rho}^{(i)}$. The joint probability $P(e(\boldsymbol{\rho}^*), e(\boldsymbol{\rho}^i))$ is modeled as a Gaussian distribution.

Once we have obtained a set of $\boldsymbol{\rho}_{n,q}$ parameters (for simplification referred hereafter as $\boldsymbol{\rho}_k$), we make use of the Expectation-Maximization algorithm to obtain the clusters of $\boldsymbol{\rho}_l$, and thus, the behavior primitive classes $B_l \in \boldsymbol{B}$.

A straightforward implementation of the EM algorithm solves the problem of finding a set of clusters, since all the required elements are known. The Expectation is calculated as:

$$\gamma(\boldsymbol{\rho}_k) = \frac{\pi_l \mathcal{N}(\boldsymbol{\rho}_k; \mu_l, \Sigma_l)}{\sum_j^L \pi_j \mathcal{N}(\boldsymbol{\rho}_k; \mu_j, \Sigma_j)} \tag{4.14}$$

and the Maximization:

$$\pi_l = \frac{\sum \gamma(\boldsymbol{\rho}_k)}{\sum \gamma(\boldsymbol{\rho})} \tag{4.15}$$

$$\mu_l = \frac{\sum \gamma(\boldsymbol{\rho}_k) \cdot \boldsymbol{\rho}_k}{\sum \gamma(\boldsymbol{\rho}_k)} \tag{4.16}$$

$$\Sigma_l = \frac{\sum \gamma(\boldsymbol{\rho}_k) \cdot (\boldsymbol{\rho}_k - \mu_l)(\boldsymbol{\rho}_k - \mu_l)^\top}{\sum \gamma(\boldsymbol{\rho}_k)} \tag{4.17}$$

As we will show in Sec. 4.6.2, the dimensionality of the ESFM parameters $\boldsymbol{\rho}$ can be reduced since the most significant variables are $\{a, b\}$ for our experiment, which greatly reduces the complexity of this calculation.

4.5 Human motion prediction

This section, as explained at the beginning of the chapter, makes use of the above explained tools and methods to characterize typically human behaviors and proposes a direct algorithm to integrate all the presented parts into a framework for enhancing the prediction of human motion.

Intentionality prediction is essential to understand human motion. We require the destinations, as explained in previous sections, to set points in a scene as goal-interesting places. Behavior estimation is also of vital importance for the correct prediction of human trajectories.

Therefore, we will update the probabilities $P\big(\mathcal{B}_{n,q}(t) = B_l | \, \boldsymbol{X}(t)\big)$ and $P\big(\mathcal{D}_n(t) = D_m | \, \boldsymbol{X}_n(t)\big)$ every instant t. For simplicity of the explanation, we assume that the estimations of $\mathcal{D}_n(t)$ and $\mathcal{B}_{n,q}(t)$ are known and available for the presentation of the trajectories' calculations, facilitating the formulation of human motion predictor. However, we have presented in previous sections an approach to calculate them and we are simplifying the problem by providing the most expectable $\mathcal{D}_n(t)$ and $\mathcal{B}_{n,q}(t)$. Moreover, we will explain later a multi-hypothesis prediction approach that contemplates different outcomes for a multiple estimations of destinations under the same given scene configuration.

Let $\boldsymbol{s}_n(t) = [\, \boldsymbol{x}_n(t), \boldsymbol{v}_n(t)]^\top$ be the augmented state vector for the nth person in the scene consisting of position and its derivate $\boldsymbol{v}_n(t) = \dot{\boldsymbol{x}}_n(t)$. More concretely, we define the person's state $\boldsymbol{s}_p(t) = [x(t), y(t), v_x(t), v_y(t)]^\top$ as a double integrator, a free moving particle subject to the

following differential constraints $dc()$ in the continuous domain:

$$\dot{\boldsymbol{s}}_n(t) = dc(t, \boldsymbol{s}_n(t), \boldsymbol{u}_n(t)) = \begin{bmatrix} v_x(t) \\ v_y(t) \\ a_x(t) \\ a_y(t) \end{bmatrix} \tag{4.18}$$

where the state $\boldsymbol{s}_n(t)$ is modified by the inputs $\boldsymbol{u}_n(t)$ which are the accelerations $\boldsymbol{u}_n(t) = [a_x(t), a_y(t)]^\top$ that are obtained by following (4.3) using the Behavior parameters as explained in Sec. 4.4. Although the values of the inputs $\boldsymbol{u}_n(t)$ must be discrete variables in the implementation, we have presented a formulation in which those inputs are expressed in a continuous time domain, as piecewise constant functions.

We can formulate this restriction more compactly into the function

$$\dot{\boldsymbol{s}}_n(t) = dc\big(t,\ \boldsymbol{s}_n(t),\ \boldsymbol{f}_n(t, \mathcal{D}_n(t), \mathcal{B}_n(t))\big), \tag{4.19}$$

which requires as inputs its own state $\boldsymbol{s}_n(t)$ and the virtual forces $\boldsymbol{f}_n(t, \mathcal{D}_n(t), \mathcal{B}_n(t))$. The differential constraint $dc\big(t,\ \boldsymbol{s}_n(t),\ \boldsymbol{f}_n(t, \mathcal{D}_n(t), \mathcal{B}_n(t))\big) = [\ \boldsymbol{v}_n(t),\ \boldsymbol{f}_n(t, \mathcal{D}_n(t), \mathcal{B}_n(t))]^\top$ is equal to the velocity of the state $\boldsymbol{v}_n(t)$ and the accelerations $\boldsymbol{u}_n(t) = \boldsymbol{f}_n(t, \mathcal{D}_n(t), \mathcal{B}_n(t))$ are calculated by the ESFM and improved by the behavior estimation.

Finally, we formulate a prediction trajectory for a time horizon of h and its correspondent covariance. Let

$$\hat{\boldsymbol{X}}_n(t+h) = \{\hat{\boldsymbol{x}}_n(t+\Delta t), \hat{\boldsymbol{x}}_n(t+2\Delta t), \ldots, \hat{\boldsymbol{x}}_n(t+h)\} \tag{4.20}$$

be the set of predicted positions starting in the current time t plus the time interval Δt, and finishing in the time horizon $t+h$, similarly as presented in (3.1). Thereby, its corresponding augmented vector $\hat{\boldsymbol{s}}_n = [\hat{\boldsymbol{x}}_n, \hat{\boldsymbol{v}}_n]$ of positions and velocities:

$$\hat{\boldsymbol{S}}_n(t+h) = \{\hat{\boldsymbol{s}}_n(t+\Delta t), \hat{\boldsymbol{s}}_n(t+2\Delta t), \ldots, \hat{\boldsymbol{s}}_n(t+h)\} \tag{4.21}$$

$$\hat{\Sigma}_n(t+h) = \{\hat{\Sigma}_n(t+\Delta t), \hat{\Sigma}_n(t+2\Delta t), \ldots, \hat{\Sigma}_n(t+h)\}. \tag{4.22}$$

As shown in Alg. 2, all the present targets in the scene propagate simultaneously and the expected propagations are utilized in the next iteration. Once a target succeeds on its intention to reach its destination $\mathcal{D}_n(t)$, it remains idle waiting for the rest of the targets to get to their corresponding destinations or until the time horizon h expires.

The ordinary differential equation (ODE) appearing in line 4 in Alg. 2 computes the update of the state $\hat{\boldsymbol{s}}_n(t' + \Delta t)$, which is solved analytically by considering the accelerations as constants throughout the time interval $[t', t' + \Delta t]$. In addition, it is subject to a limitation in velocity

Algorithm 2 Human trajectory prediction

for $t' = t, t + \Delta t \ldots, t + h$ **do**
  for $n = 1, \ldots, N$ **do**
    if $\hat{\boldsymbol{x}}_n(t') \nsubseteq \mathcal{D}_n(t)$ **then**
      $\hat{\boldsymbol{s}}_n(t' + \Delta t) = \hat{\boldsymbol{s}}_n(t') + \int_{\Delta t} \dot{\hat{\boldsymbol{s}}}_n(\tau) d\tau$
      $\hat{\Sigma}_n(t' + \Delta t) = \hat{\Sigma}_n(t') + \hat{\Sigma}_{dc}(t')$
    end if
  end for
end for

$\| \boldsymbol{v}_n \| < v_{max}$. The covariance $\hat{\Sigma}_{dc}(t')$ is calculated depending on the propagation values.

Regarding the multi-hypothesis issue, we should consider that the estimation of the target's intentionality (see Chapter 3) is not perfectly estimated and a certain degree of uncertainty is associated to the best expected destination, leading to possible association error, *i.e.* $\mathcal{D}_n(t) \neq D^*$. As it can be seen in Fig. 4.6, the target can move towards any of the mth destinations in the scene, with probability $P\big(\mathcal{D}_n(t){=}D_m | \, \boldsymbol{X}_n(t)\big)$. A hypothesis l is the set of combinations of people intentions, where each person has associated a single expected intentionality $\mathcal{D}_n(t) = D_{l_n}$. Thus, the joint probability for N people is

$$P\big(\mathcal{D}_1(t) = D_{l_1}, \ldots, \mathcal{D}_N(t) = D_{l_N} | \, \boldsymbol{X}_n(t)\big) = \prod_{n \in N} P\big(\mathcal{D}_n(t) = D_{l_n} | \, \boldsymbol{X}_n(t)\big), \tag{4.23}$$

where for each hypothesis l the prediction is performed following Alg. 2.

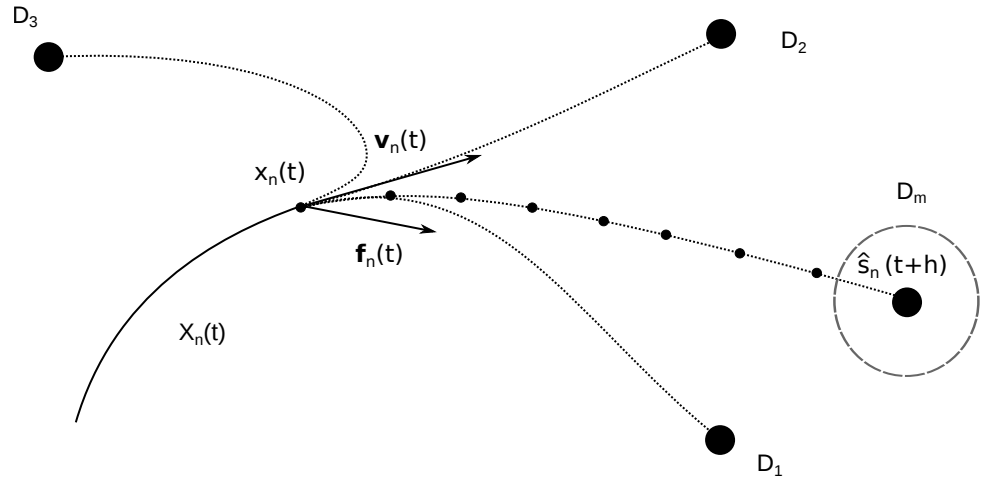

Figure 4.6: **Trajectory propagation.** An example of a single trajectory prediction trying to reach destination D_m.

If there are many targets in the scene, the number of hypothesis grows exponentially and we should branch and prune the hypothesis to those whose joint probabilities of (4.23) are more expectable, and proceed to apply Alg 2 with their respective parameters associated for each

hypothesis. In Fig. 4.7 is depicted an example of multiple targets propagating by using the best intentionality estimation.

In posterior chapters we will make use of the prediction algorithm as if the only hypothesis is the best hypothesis, although we have shown that it can be generalized to any number of hypothesis.

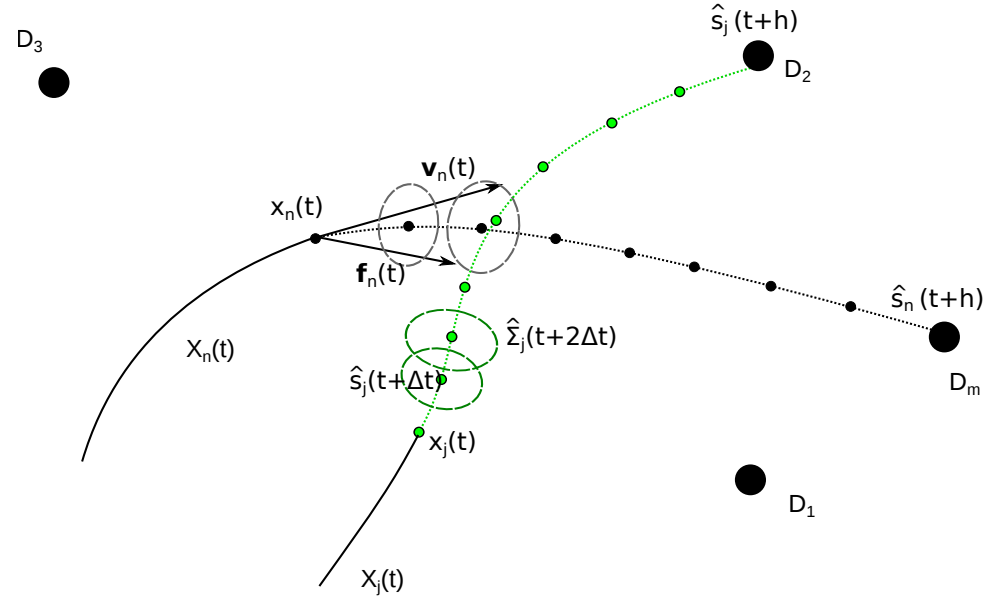

Figure 4.7: **Multiple trajectory propagations.** An example of a multiple trajectory prediction trying to reach their corresponding destinations at time $t + 2\Delta t$.

4.6 Experiments

In order to conduct all the experiments and to test the presented approach, we have used a mobile service robot, the Tibi&Dabo robotic platforms, designed to work in urban pedestrian areas and to interact with people (see Fig. 4.2).

The experimental areas are the BRL (Barcelona Robot Lab) and the FME (Facultat de Matemàtiques i Estadística), both outdoor and urban environments located at the university.

For the recording of the experiments, we have used two Hokuyo UTM-30LX 2D laser range sensors on-board the robotic platform. Human detection is done using laser information and the tracker helps out to maintain targets in the scene (for further details, see Appendix A).

We have divided this section in three different parts, one subsection for each of the corresponding experiments of Secs. 4.3-4.5.

4.6.1 ESFM parameters learning

The first part of the experiments is dedicated to the study of the ESFM parameters that governs human motion. We consider three kinds of interaction forces: person-to-person, person-obstacle and person-robot. The first and the second interactions have been studied in previous papers like [Helbing and Molnar, 1995; Zanlungo et al., 2011]. However, the person-robot interaction parameters were not directly obtained in any previous work, thereby, in this section we present the results obtained for the parameters $\boldsymbol{\rho}_{rp} = \{a_{rp}, a_{rp}, \lambda_{rp}, d_{rp}\}$.

As discussed in Sec. 4.3.1, we have divided the parameter estimation in two different parts, analyzing 80 trajectories described by 20 different volunteers between 20 and 54 years old. During the first part, we optimize (4.8) the intrinsic parameter of the ESFM $\{k\}$ describing the expected human trajectories under no external constrains. The experiment setting is as follows: the volunteers are told to walk towards a goal in a scene free of obstacles. A total of 4 different initial orientations are recorded in order to obtain more diverse trajectories.

The second part of the ESFM parameter learning was done under the influence of the Tibi robot. We optimize the parameters of the force interaction model $\boldsymbol{\rho}_{rp} = \{a_{rp}, b_{rp}, \lambda_{rp}, d_{rp}\}$ under the presence of a moving robot, asserting that it is the only external force altering the outcome of trajectory described by the person. The volunteers walk towards a given goal in a free obstacle scenario. Simultaneously, the teleoperated Tibi robot approaches the walking pedestrian and interacts with him/her. We observe and track their trajectories and process them in order to obtain the remaining ESFM parameters.

Interaction	k $[s^{-1}]$	a $[m/s^{-1}]$	b $[m]$	d $[m]$	λ
Per-Per [Luber et al., 2010]	2	1.25	0.1	0.2	0.5
Per-Per [Zanlungo et al., 2011]	4.9	10	0.34	0.16	1
Robot-to-Person (our approach)	2.3 ($\pm$ 0.37)	2.66 ($\pm$ 4.51)	0.79 ($\pm$ 0.21)	0.4 ($\pm$ 0.25)	0.59 ($\pm$ 0.36)

Table 4.1: Parameters of the SFM calculated in different works and our calculations for the robot-to-person interaction considered in the ESFM

Table 4.1 shows the parameters learned after applying the minimization process (see Sec. 4.3.1), using genetic algorithms, to all database trajectories. Each parameter includes a standard deviation obtained after estimating the parameters for each trajectory independently. Furthermore, in this table it can be seen the parameters proposed by Luber et al. [2010] and Zanlungo et al. [2011] are referred to the person-to-person SFM. The standard deviations of some parameters are high, because people behave differently when they interact with robots. Motivated to solve this problem, we have proposed the behavior-based estimation of the ESFM parameters for a more accurate prediction.

4.6.2 Behavior clustering

The second part of the experiments, performed in the FME, consisted of one robot and one person as obstacles, where a set of volunteers performed experiments in a controlled scene. The objective was to obtain data to calculate the behavior classes, as explained in Sec. 4.4.1. Over 40 volunteers were recorded during a full day of experiments. Men and women, ranging from 20 to 56 years old participated as volunteers and some of them had not any experience in robotics. In Fig. 4.8 is depicted a real example of an experiment, as observed by the robot GUI.

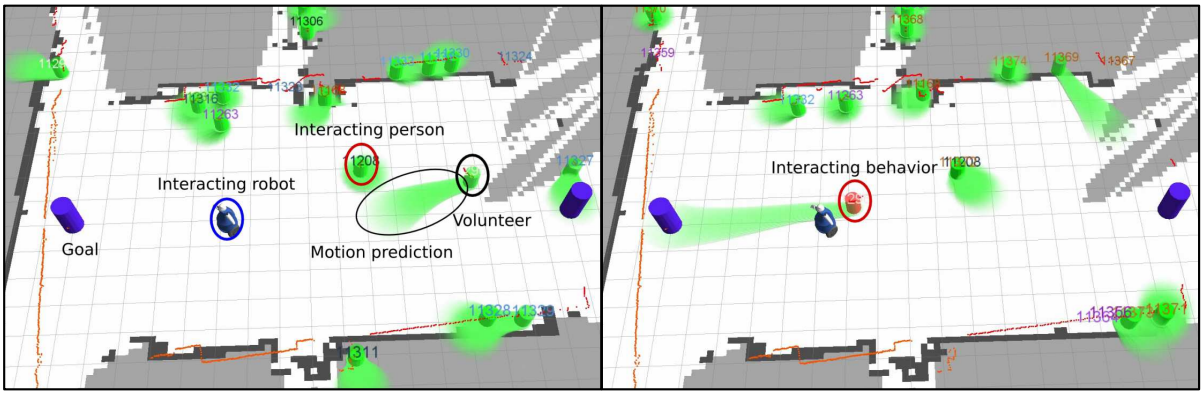

Figure 4.8: **Behavior clustering experiment.** On the *Left* the volunteer walks and interacts with the interacting obstacle while trying to reach the goal (lilac cylinder). On the *Right* takes place the second interaction with the robotic platform, that is teleoperated in order to provide interaction.

The experiment setting is simple: the volunteers are told to naturally walk towards a very visible destination (a huge lilac cylinder), while approaching their destination, a dynamic obstacle crosses his/her path. Two dynamic obstacles are used during the experiments, a person and the Dabo robot. During the experiment, it is very important not to interact with both obstacles at the same time, but the volunteers were not told anything regarding this condition.

Once obtained and processed the trajectories, the parameters $\boldsymbol{\rho}_k = \{k, a_k, b_k, \lambda_k, d_k\}$ can be calculated by simply applying the procedure described in Sec. 4.4.1. For plotting purposes, we have reduced the dimensionality of the SFM parameters $\boldsymbol{\rho}$ to the parameters $\{a, b\}$, as depicted in Fig. 4.9. A PCA analysis reveals that the two principal eigenvectors, were almost a linear combination of $\{a, b\}$ exclusively and their respective eigenvalues concentrated more than 99% of the "energy".

The results in Fig. 4.9 clearly show three basic behaviors. The *Aware* behavior in blue $\{k = 2.3, a = 4.78, b = 6.22, \lambda = 0.56, d = 0.20\}$, which is high both in a and b and represents all those trajectories of people extremely cautious, that exceed in consideration towards the other target. This behavior was clearly visible when some volunteers seemed to be afraid of the robot.

In green, the *Unaware* behavior $\{k = 2.3, a = 0.98, b = 0.16, \lambda = 0.56, d = 0.20\}$, correspond-

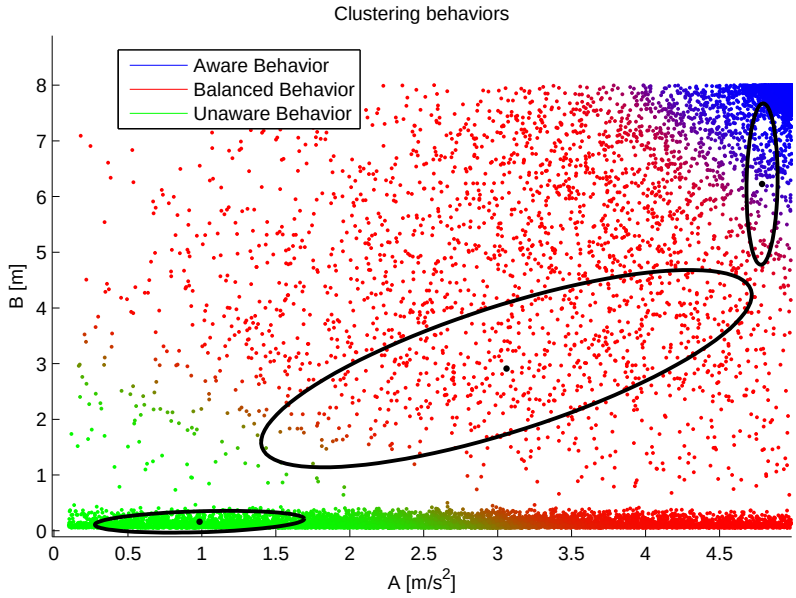

Figure 4.9: **Cluster of behaviors.** A projection of the most representative parameters $\{a, b\}$ in order to illustrate in a graphic the three basic behaviors detected.

ing to all those people that virtually ignored their obstacles and went to their destinations no matter what. This behavior is not atypical and it may happen often in daily life.

And finally in red we can observe the *Balanced* behavior $\{k = 2.3, a = 3.05, b = 2.91, \lambda = 0.56, d = 0.20\}$. This cluster describes all those behaviors that are not *Aware* or *Unaware* behaviors, and hence, it is a mixture of a great variety of behaviors.

The separability of clusters is not really significant, but this classification answers most of the questions arisen regarding the interaction of moving targets in a scene. It is not important the nature of the target, but the consideration of the person towards the target. An implication of this paradigm of interaction modeling is that it is no longer reciprocal, that is, an *Unaware* pedestrian may inflict great social-force stress to other pedestrians, but in response he or she gets almost no social-force feedback since the force exerted by other people to the *Unaware* pedestrian is much more smaller. On the contrary, an *Aware* pedestrian may suffer more social stress on a typically social environment. All those considerations greatly affect the deployment of social robots, being the first, the *Unaware* target a threaten to the integrity of the robot, and the *Aware* pedestrian would suffer a high social stress in the presence of a robot which should act accordingly to reduce that impact. For these reasons it is of vital importance to detect those behaviors if we want to deploy social robots on urban or social environments and being accepted by humans and facilitate their daily life and not in the contrary.

In Fig. 4.10 is depicted a function of the social-force module $|\hat{\boldsymbol{f}}_{obs}^{int}|$ for each set of parameters with respect to the distance to target. Additionally, we can observe the obtained social-force parameters for each $\boldsymbol{\rho}_k$ that resulted in the minimization of (4.13). We can appreciate that the

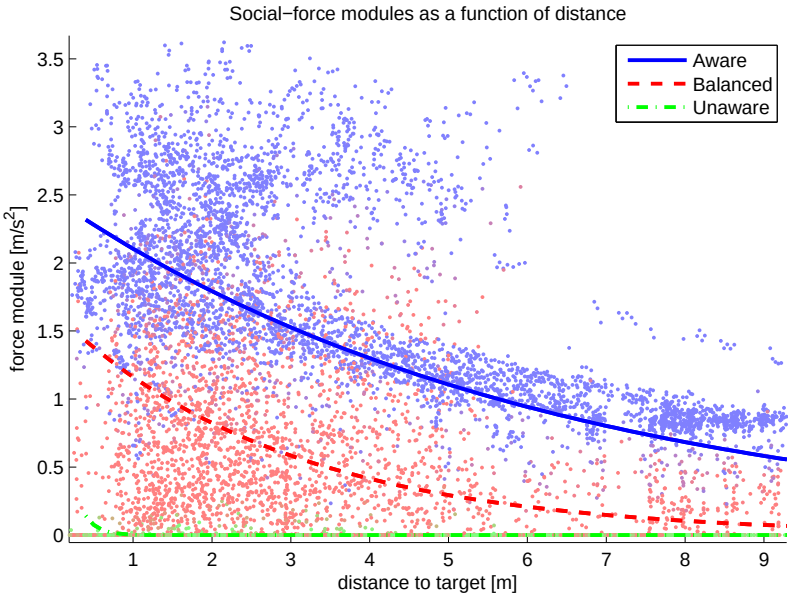

Figure 4.10: **Social-force modules clustered by behaviors.** The expected force of interaction $|\hat{\boldsymbol{f}}_{obs}^{int}|$ is plotted with respect to distance from interacting target and clustered into the three behaviors detected.

separation of the clusters is not so significant, despite the noisy conditions and the variability of humans.

4.6.3 Evaluation of predicted trajectories

The third part of the experiments was performed in the BRL. Using the parameters obtained before for each behavior, we tested the algorithm during a full morning of experiments. This time, the experiment setting was even more simple. We did not require any direct volunteer: the robot was navigating in the campus and meanwhile recording trajectories of people on their natural habitat.

The idea is to apply the algorithms explained before in a real scenario where nobody knows which kind of experiment the robot is performing. For all the trajectories observed, we have calculated the most expectable destination each target aims to. That is, we are selecting only the best destination, and thus, simplifying the multiple hypothesis that could be generated into a single hypothesis. The environment where the experiments are carried out, the BRL, is shown in Fig. 4.11.

An example of an interaction is depicted in Fig. 4.12. The robot slowly moves and three students quickly walk to attend a class. Each of the targets is depicted in the same color on each picture. On the left picture, the algorithm predicts that the green target may stop, due to the interaction with the blue target and the robot. As it can be seen in the complete trajectory, this never happens and green simply changes its direction and this time the algorithm predicts

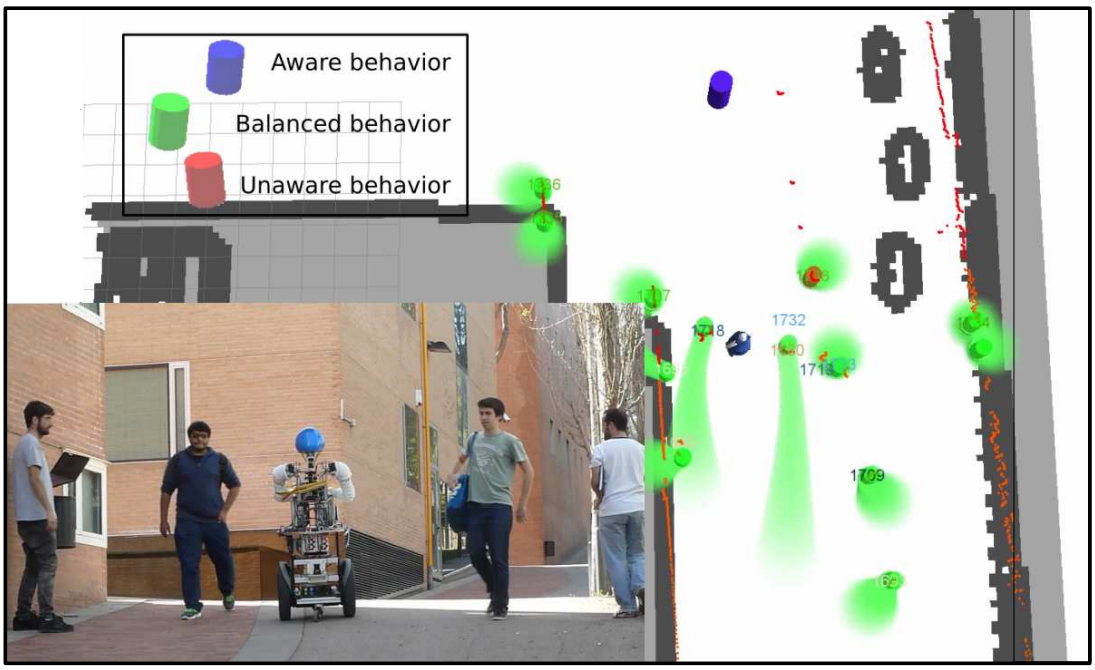

Figure 4.11: **Prediction example in a real environment.** In the image is depicted the real environment where this part of the experiments were carried out (BRL), and the robot GUI showing predictions as a series of green ellipses and behavior estimations.

correctly. All those prediction trajectories, and their corresponding covariances are calculated on a time horizon of two seconds.

Aiming to obtain reliable results, and not a single experiment of prediction, we have tested under the following circumstances. We have evaluated the performance of the prediction algorithm for each time of the interval, that is, starting just after the observation from a horizon of 0.1 seconds to the maximum horizon of 10 seconds.

In order to evaluate the accuracy of the prediction, we have set a binary function which returns a success if the prediction at time $t+h$ is within 1 meter of the real trajectory performed by the target. Additionally, we have compared various methods, as it can be seen in Fig. 4.13. In dashed blue is depicted the linear propagation as a prediction method. This method simply filters the velocity and propagates accordingly to the horizon time. In solid green is depicted the performance of the social-force approach, that is, making use of intentionality information and interaction forces, but using fixed parameters. It clearly outperforms the linear propagation, even for a short horizon time and for long horizons, it simply can not be compared. In dashed dotted red is drawn our complete approach, now using prediction information as well as behavior estimation. We can appreciate how the performance can be enhanced just by adding intentionality prediction and behavior information with respect to the linear propagation.

On average, the performance of the short-term velocity propagation method is 28.66%, for the social-force 78.47%, which only uses intentionality information and a 91.71% accuracy for

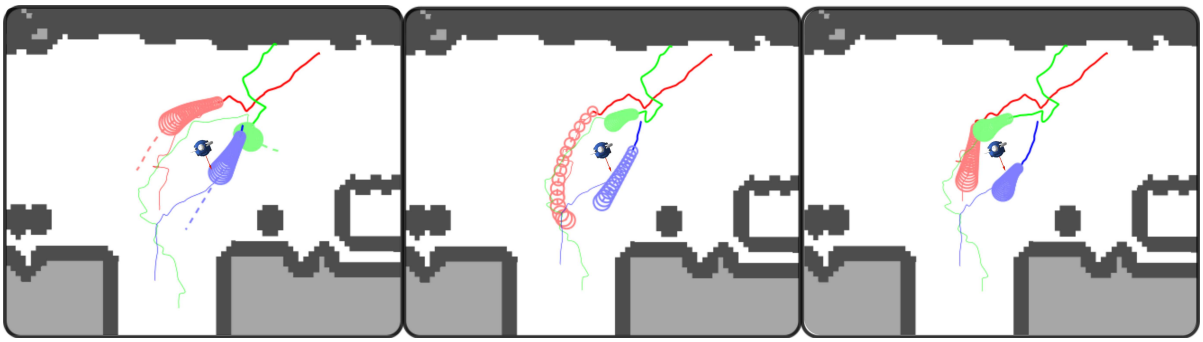

Figure 4.12: **Prediction example depicted in three frames.** Each of the targets is depicted in the same color on each picture. On the *Left* picture, the algorithm predicts that target green may stop, due to the interaction of the blue target and the robot. All those prediction trajectories, and their corresponding covariances are calculated on a time horizon of two seconds.

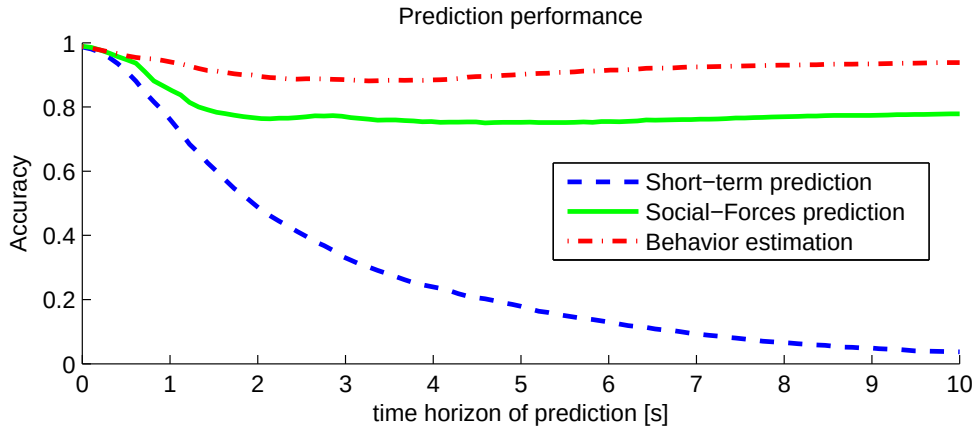

Figure 4.13: **Results on real environments.** The performance function of our proposed method, and a comparison with a short-term predictor and a prediction only based on forces.

the proposed method using behavior estimation and intentionality information.

4.7 Summary

In this part of the thesis we have presented a complete framework of human motion prediction in social environments. The framework consists of the intentionality predictor (BHMIP), the behavior estimator and the trajectory prediction algorithm that makes use of the two estimators to provide an enhanced prediction of human motion.

We have presented the Extended Social Force Model (ESFM) that considers robot-person interactions in addition to person-person and person-obstacle. The SFM by itself is not accurate enough and in this chapter we have provided estimation tools (the behavior estimation) in order to raise the prediction performance.

As a result of the study of the ESFM, we have suggested a behavior estimation to provide a

more precise prediction algorithm by proposing a set of basic behaviors or groups of $\boldsymbol{\rho}$ parameters, where three different basic behaviors have been detected: *Aware*, *Balanced* and *Unaware*. These clusters have been obtained during experimentation in a real environment using a wide diversity of volunteers and different kinds of interacting targets, such as a person and a robot.

The last part of the chapter corresponds to the trajectory prediction, where we have integrated the proposed estimators into the prediction model. We have called this structure the prediction framework. Real experimentation has demonstrated that the integration of intentionality prediction and motion behavior can greatly improve the accuracy of human motion prediction in real scenarios (BRL). However, it is important to note the limitations of the prediction approach, and accordingly, we provide covariances associates with predictions that increment over time.

A direct application as a future work for the behavior estimation is, for instance, the estimation of human behavior and its use as a human acceptance indicator, being specially useful in case of sensing an extreme *aware* behavior or to detect threatening pedestrians which may potentially collide with the robot.

In the context of this thesis, we will base our future contributions on many of the results presented here. It will be explained in more detail in the following chapters, but the next logical hypothesis is that the prediction system should improve the navigation approach.

Part II

Robot navigation

5

Social-aware reactive navigation

In our first approach to the robot navigation issue we propose a reactive scheme to solve the navigation problem in a urban environment considering people and obstacles. Unfortunately, in this early stage of our research, we treat the problem without considering the prediction framework defined in Part I, and a pure reactive approach is presented making use of the Extended Social Force Model.

The main idea of this chapter is to adapt the ESFM, that provides a realistic model of human motion, to a robot navigation algorithm, which is mainly driven by the social-forces centered at the robot. Since our navigation is based on the ESFM, our scheme becomes social-aware of the environment, seeing that we consider interactions with people and obstacles. The main hypothesis of this chapter is: a more humanized navigation, in the sense that the robot responds to the ESFM, will highly increase the acceptance over pedestrians, due to the similarities between the robot behavior and the expected behavior of other pedestrians. We will show in the following sections that this initial hypothesis does not hold when implemented in real scenarios. Luckily, this limitation has motivated us to further study robot navigation.

In the following sections is discussed our initial approach to the robot navigation problem, and this research has motivated the publication of this work in the *European Conference on Mobile Robotics* [Ferrer et al., 2013b].

5.1 Introduction

Nowadays, robots are expected to interact naturally in typically human environments. To this end, deploying urban robots safely in social environments and being accepted by people requires navigation algorithms capable of dealing successfully with such challenging scenarios.

In this chapter, we propose a novel robot social navigation for both indoor and outdoor environments. In order to model the social interactions, we use the Social Force Model (ESFM) introduced in Chapter 4. Specifically, this work presents a powerful scheme for a human-aware robot navigation based on the social-forces concept. Moreover, we introduce a new

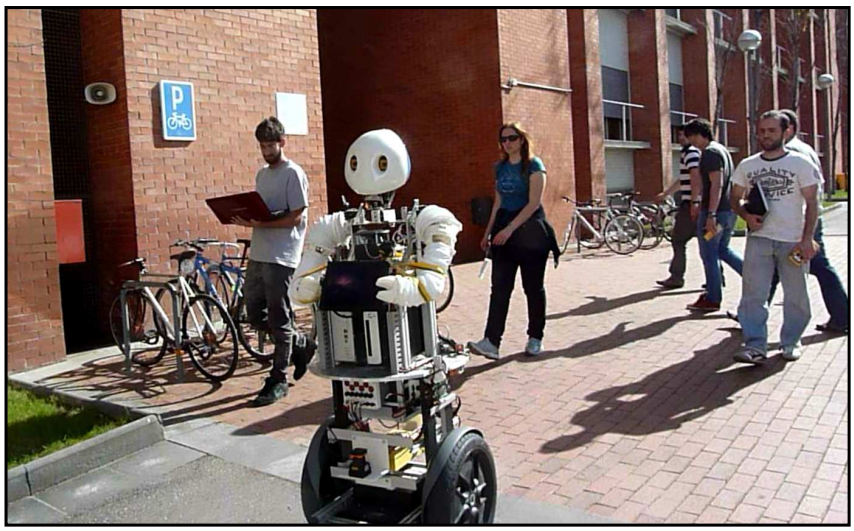

Figure 5.1: **Social robot navigation.** The Dabo robot navigating in the Barcelona Robot Lab. (BRL) with other pedestrians.

metric, inspired in the classical definition of mechanical work: the *social work*. This metric serves to evaluate the navigation performance in a social manner. Prior to carrying out real-life navigation experiments, where pedestrians are involved, it is required a previous stage making use of a simulation environment. With this purpose in mind, we use the MCMC Metropolis-Hastings [Andrieu et al., 2003] algorithm to learn the parameters values of the method, and afterwards we test it on real environments, as it can be seen in Fig. 5.1.

In order to navigate in a large urban environment, we construct a graph map with a set of destinations that completely describe the navigation environment.

The validation of the model is accomplished throughout a set of real-life experiments, where the *social work* is evaluated. We compared our approach with respect to a teleoperated robot by an expert controller. Both approaches were performed under the same conditions. We can conclude that our social-aware navigation model is efficient in semi-crowded environments. In the context of this thesis, we consider semi-crowded environments those setting where there is a reduced number of people, less than 8, that directly intervene in the scene, and thus are considered as dynamic obstacles. In most of the real experiments carried out during this work, the experiment environments were semi-crowded. Idle people are not considered as part of the dynamic obstacles.

5.2 Related work

Robot navigation is a mature field of robotics; there exist many works that demonstrate that robots are able to navigate in challenging environments [Kruse et al., 2013; Burgard et al.,

1999; Levitt and Lawton, 1990; Shatkay and Kaelbling, 2002]. However, more social-interactive approaches are required. Our work is greatly based on Potential Field methods [Khatib, 1986; Borenstein and Koren, 1991] as they keep a great synergy with the social force model, but focusing on the social acceptance. Alternative approaches from the learning perspective [Kuderer et al., 2012; Luber et al., 2012] have shed light into the human motion modeling problem.

More recent publications, such as [Trulls et al., 2011] have studied urban environments and complex environments, but they consider persons as obstacles, and consequently this kind of approaches are not centered in human acceptance. In [Luber et al., 2012; Henry et al., 2010], the authors have learned human-like motions based on example paths and simulate human trajectories, while Trautman and Krause [2010]; Trautman et al. [2013, 2015] have planed a robot navigation in semi-crowded indoor environments.

In [Foka and Trahanias, 2010], a human prediction of motion and navigation in a dynamic environment has been proposed. Other approaches have proposed a human aware navigation where a motion planner takes explicitly into account their human partners, and seeks social acceptance and safety of paths [Sisbot et al., 2007]. Other works have treated human movements as uncertainty propagation. Unlike them, we treat human movement as a response to exterior stimuli, based on the Social-Force model (SFM). Clearly, the SFM is not free of noise and inaccuracies, but it serves well for this purpose.

Because a mobile robot must be able to avoid obstacles in the environment where it is working, many different algorithms for obstacle avoidance have been developed. Often, dynamic obstacles are handled only in a reactive manner, and treated as static (non-moving) obstacles. Some works considering the vehicle velocities include the Curvature Velocity Method by Simmons [1996] or the Dynamic Window Approach by Fox et al. [1997].

Other algorithms consider obstacles moving over time [Kluge, 2003; Matveev et al., 2012]. Finally, several approaches consider both vehicles' velocities and obstacles' velocities [Foka and Trahanias, 2003; Owen and Montano, 2005]. While all of these algorithms may be used to generate varying degrees of safe and effective obstacle avoidance, none of them explicitly account for the pre-established social conventions that people use when moving around each other.

A number of methods have been developed to allow robots navigate around people in specific, typically non-generalizable tasks. Some of these tasks include standing in line [Nakauchi and Simmons, 2002]; tending toward the right side of a hallway, particularly when passing people [Olivera and Simmons, 2002]; and approaching people to join conversational groups [Althaus et al., 2004]. Museum tour guide robots are often given the capability to detect and attempt to handle people who are blocking their paths [Burgard et al., 1999; Nourbakhsh et al., 2003; Thrun et al., 1999]. In [Prassler et al., 2002], a robotic wheelchair that can follow a person was presented, but this method does not account for the social cues that the human might use in a certain situation, nor does it allow for any spontaneous social interaction. Some

researchers have begun studying how a robot might adapt its speed when traveling besides a person, but they have obtained mixed results, even in controlled laboratory settings [Sviestins et al., 2007].

Safety and reliability are key factors to the successful introduction of robots into human environments. In most studies, safety is assured by preventing humans from approaching the robots. But these methods are rendered ineffective whenever the robot is designated to directly assist a human individual. In [Alami et al., 2006], the notion of safety is studied in detail with respect to all relevant aspects of Human-Robot Interaction.

In the present chapter, a novel robot social navigation approach based on the SFM is introduced, which is capable of navigating in semi-crowded environments in an acceptable social way.

5.3 Global map

In this section we propose how to structure the environment in order to build a useful map for a social robotic navigation. To this end, we have obtained manually a set of destinations that completely describe our navigation environment, the Barcelona Robot Lab (BRL), although it is generalizable to any other environment. We have presented in Chapter 3 a different technique to obtain the set of destinations by using the EM algorithm. In this case, we manually label all those destinations, which produces the desired results, a map of destinations. Moreover, we consider the following hypothesis: the set of destinations, similar to those goals explained in Sec. 3.4, may be sufficient to a robot navigation in a urban environment.

Other classical navigation works like [Khatib, 1986] and [Borenstein and Koren, 1991] have proposed a similar navigation environment described by attractors. Our approach is not novel in this aspect, however, once obtained a set of these destinations in a urban environment, we will be ready to make use of the social forces to make the robot navigate in a social way, which is one of the main contributions of the present chapter.

The implementation of the global planning is a straightforward approach using a search algorithm (in our work we use an A* implementation) to solve the shortest path from one point of the scene to another. In Fig. 5.2 is depicted the scheme of the BRL and the graph representing the most significant destinations in the environment and their corresponding connections.

5.4 Social-aware navigation

Previously in Sec. 4.3, we have described a general social interaction model based on the ESFM. In this section, we provide the formulation to build a navigation algorithm using the following idea: the robot is considered as a social agent moving naturally in human environments

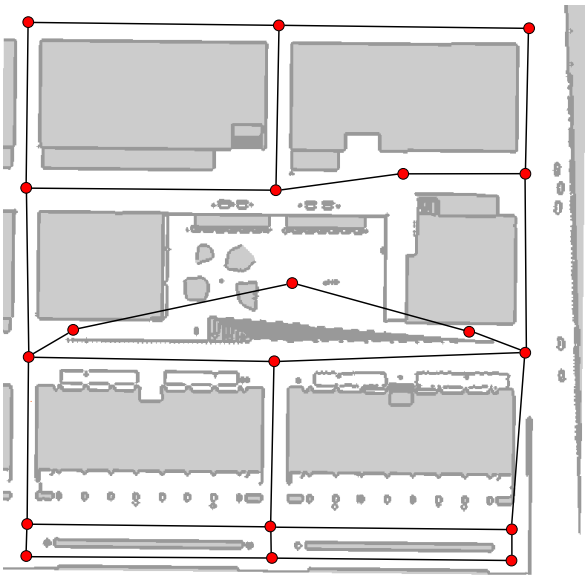

Figure 5.2: **Map scheme of the BRL.** Red dots are the set of destinations that describe the navigation environment and their corresponding connections.

according to the Extended Social Force Model, and thus, aiming to a destination and reacting to obstacles and people. Furthermore, as it has been remarked before, we believe that a more humanized navigation, in the sense that the robot responds to the ESFM, will highly increase the acceptance over pedestrians, due to the similarities between the robot behavior and the expected behavior of other pedestrians.

To this end, we propose a novel approach to the robot navigation issue, called the social-aware navigation, understood as an instantaneous reaction to sensory information, driven by the social forces centered at the robot. More precisely, we aim to obtain a short-term goal-driven robot navigation ruled by the ESFM.

Thereby, it is mandatory to clearly formulate again all the social forces, originally explained in Sec. 4.3, intervening in the social-aware navigation approach, but now centered in the robotic platform. The following equation is a straightforward derivation of (4.2). The robot destination is computed from the set of destinations in the global map and the force that drives the robot is

$$\boldsymbol{f}_r^{goal}(t, \mathcal{D}_r(t)) = k_r(\ \boldsymbol{v}_r^0(\mathcal{D}_r(t)) - \ \boldsymbol{v}_r(t)), \tag{5.1}$$

where the robot's desired velocity $\boldsymbol{v}_r^0$ is dependent on its intentionality $\mathcal{D}_r(t)$, that is, the calculated sequence of subgoals or destinations to reach its final goal.

Once the robot reaches its desired destination subgoal, the next destination calculated by the global planner becomes the new destination subgoal. The interaction forces due to the pedestrians are the repulsive forces that each person generates to the robot, and they can be calculated following two approaches, the ESFM describing a different kind of interaction for

people, obstacles and robots (Sec. 4.3) or the enhancement to the social forces by considering the behavior estimation (Sec. 4.4). We will present the interacting forces according to the ESFM, but we could substitute the equations by their corresponding behavior equivalents. Thus, the interacting forces to the robot due to people, according to (4.3)

$$\boldsymbol{f}_r^{per}(t) = \sum_{j \in P} \boldsymbol{f}_{r,j}^{int}(t), \tag{5.2}$$

are formulated as a summation of the forces $\boldsymbol{f}_{r,j}^{int}(t)$ which represent the interaction between the pedestrian j and the robot. Each one of these interactions between people and the robot

$$\boldsymbol{f}_{r,j}^{int}(t) = a_{rp} e^{(d_{rp} - d_{r,j}(t))/b_{rp}} w(\varphi_{r,j}, \lambda_{rp}), \tag{5.3}$$

which is the formulation of the spherical force (4.4) using the parameters $\{a_{pr}, b_{pr}, \lambda_{pr}, d_{pr}\}$. These parameters correspond to the person-to-robot interaction, and in general are dependent of the robotic platform used. We are assuming the following hypothesis: there is a symmetrical relation to the parameters robot-to-person, calculated in Sec. 4.6.1, and the parameters person-to-robot that we have described to model external human interactions to the robotic platform. Although we know that the robot is not reactive by nature to other people's interactions, we have modeled them under the same shape than in the inverse case. However, this hypothesis is not necessarily true, as we will discuss in the next chapters.

Correspondingly, the interaction between robot and obstacles is modeled as

$$\boldsymbol{f}_r^{obs}(t) = \sum_{o \in O} \boldsymbol{f}_{r,o}^{int}(t), \tag{5.4}$$

using part of (4.3). $\boldsymbol{f}_{r,o}^{int}(t)$ is calculated using (4.4)

$$\boldsymbol{f}_{r,o}^{int}(t) = a_{ro} e^{(d_{ro} - d_{r,o}(t))/b_{ro}} w(\varphi_{r,o}, \lambda_{ro}) \tag{5.5}$$

using the specific parameters $\{a_{ro}, b_{ro}, \lambda_{ro}, d_{ro}\}$ corresponding to the interaction obstacle-to-robot, which are calculated using the hypothesis that the parameters are equivalent to the obstacle-to-person parameters proposed in Sec. 4.3.

Similarly as presented in Sec. 4.3, repulsive effects from the influences of other people and obstacles in the environment are described by an interaction force which is a sum of forces either introduced by people or by static obstacles in the environment. The combination of the forces described above, which include goal and interacting forces, describes the resultant force governing the robot movement:

$$\boldsymbol{f}_r(t) = \alpha \boldsymbol{f}_r^{goal}(t, \mathcal{D}_r(t)) + \gamma \ \boldsymbol{f}_r^{per}(t) + \delta \ \boldsymbol{f}_r^{obs}(t). \tag{5.6}$$

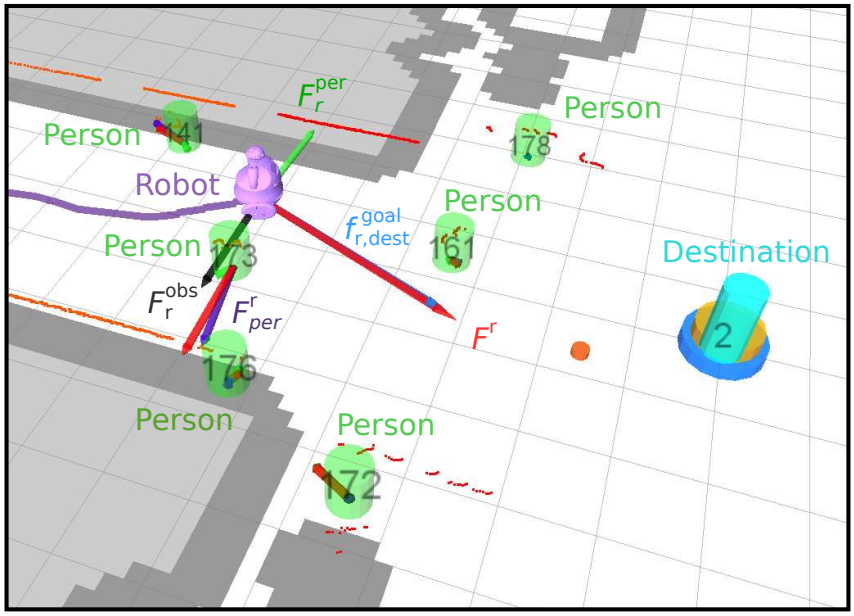

Figure 5.3: **The ESFM centered at the robot.** The ESFM forces applied to the robot while navigating in a urban environment.

where the parameters α, γ, δ, for simplification referred as the set $\boldsymbol{\theta} = \{\alpha, \gamma, \delta\}$, are the weights that determine the contribution of each component to the resultant force $\boldsymbol{f}_r(t)$. For clarity we are omitting the dependency on the robot intentionality $\mathcal{D}_r(t)$ on the resultant force. Once calculated the resultant social force, the robot behaves consequently to these external stimuli and propagates its state according to this force value. These additional parameters of the ESFM are proposed in order to guarantee a correct and acceptable navigation. As it will be explained later, we seek to minimize the "social work" through a correct calculation of $\boldsymbol{\theta}$.

Additional constraints are taken into account. All those robot propagations which result in a collision with an obstacle, are forbidden. Current robot maximum velocity is also a constraint and it depends on the robot navigation state, which is a function of the proximity of people:

$$v = \begin{cases} v_{safety} & \text{if } \frac{d_{r,p}}{w(\varphi_{r,p})} \leq \mu_{safety} \\ v_{cruise} & \text{if } \mu_{safety} < \frac{d_{r,p}}{w(\varphi_{r,p})} \leq \mu_{social} \\ v_{free} & \text{otherwise.} \end{cases} \tag{5.7}$$

The v_{safety} is the maximum velocity the robot can achieve when at least one person is inside its *inner zone*. We have proposed a *social distance* to define this region as $d_{r,p}w(\varphi_{r,p})$, similarly as described in Sec. 4.3, as a metric of the relative distance between the robot and a pedestrian and an asymmetric factor deforming the distance measure by $w(\varphi_{r,p})$, whose shape resembles a heart. This condition also corresponds to the *inner robot navigation* state. On the other hand, v_{cruise} is the cruise velocity when someone is inside its *social zone* and v_{free} is the

maximum robot velocity when there are no people inside its *inner zone* and *social zone*. The navigation states associated to this configurations are the *social robot navigation* and the *free robot navigation*, correspondingly. These velocities guarantee that the robotic platform is able to stop according to the resulting forces, before collision occurs.

Prior values of the velocity parameters are obtained from [Trulls et al., 2011], and during experimentation we redefine them according to our experience. Intuitively, these values are similar to people's velocities in urban areas when they are walking. The v_{free} is the highest velocity value, and thus, it is only desirable when there are no obstacles nor people near. If a person enters the *social zone*, then the maximum velocity becomes v_{cruise} and even in the case someone gets even nearer the robot, there is a third maximum value, the v_{safety}, which is even smaller. By doing this, we minimize the risk of collision with other pedestrians and minimize the "human perception" of thread in the proximity of other people.

The most interesting part of the system so far, resides in the fact that the proposed approach is able to navigate near moving people (dynamic environments) and successfully reach its goal. The following section discusses the procedure to obtain the value of the parameters $\boldsymbol{\theta} = \{\alpha, \gamma, \delta\}$.

5.4.1 Parameters learning

The computation of the weights of the system parameters, defined as $\boldsymbol{\theta} = \{\alpha, \gamma, \delta\}$, is a mandatory step, prior to the deployment of robots in real environments in a successful and safe way. To this end, we require an initial estimation to learn the magnitude of the $\boldsymbol{\theta}$ parameters.

In this case, we propose a cost function that takes into account the social forces intervening during the robot navigation. As stated before, we aim to obtain a social robot model capable of dealing with navigation issues in a more human-oriented manner. Consequently, we make use of a variation of the classical definition of *work* applied to social forces, similarly to the *social work* proposed in [Garrell and Sanfeliu, 2012]. The amount of *social work* corresponding to a time step Δt at time t is

$$W(t, \boldsymbol{\theta}) = W_r(t, \boldsymbol{\theta}) + \sum_{i \in P} W_{i,r}(t, \boldsymbol{\theta}). \tag{5.8}$$

This magnitude consists of the total work done by the robot $W_r(t, \boldsymbol{\theta}) = \boldsymbol{f}_r(t)\Delta\boldsymbol{l}_r$, where $\Delta\boldsymbol{l}_r$ is the variation in position along its trajectory, and the summation of the work done by each person i in the scene, enforced by the robot $W_{i,r}(t, \boldsymbol{\theta}) = |\boldsymbol{f}_{i,r}^{int}(t)\Delta\boldsymbol{l}_i|$ in absolute value in order to build a well-posed cost function.

Although the initial conditions can be identically copied throughout the simulations, given the interactive nature of the approach, the parameters $\boldsymbol{\theta}$ alter the outcome $W(\boldsymbol{\theta}) = \sum_t W(t, \boldsymbol{\theta})$ of each experiment (random variable). That is the main reason for considering as an appro-

Algorithm 3 MCMC-MH Learning

Initialize $\boldsymbol{\theta}^{(0)}$
for $i = 0$ to $N - 1$ **do**
  Sample $u \sim \mathcal{U}_{[0,1]}$
  Sample $\boldsymbol{\theta}^* \sim q(\boldsymbol{\theta}^* | \boldsymbol{\theta}^{(i)})$
  if $u < P(W(\boldsymbol{\theta}^*), W(\boldsymbol{\theta}^i))$ **then**
    $\boldsymbol{\theta}^{(i+1)} = \boldsymbol{\theta}^*$
  else
    $\boldsymbol{\theta}^{(i+1)} = \boldsymbol{\theta}^{(i)}$
  end if
end for

priate method for estimating the navigation parameters stochastic optimization. Monte Carlo methods are especially useful for simulating phenomena with significant uncertainty in inputs and systems with a large number of coupled degrees of freedom. More concretely, we have implemented a Markov Chain Monte Carlo Metropolis-Hastings (MCMC-MH) algorithm to find the best set of $\boldsymbol{\theta}$, implementing the Alg. 3.

The term $q(\boldsymbol{\theta}^* | \boldsymbol{\theta}^{(i)})$, appearing in the algorithm description, represents a Gaussian sampling for each parameter, centered at $\boldsymbol{\theta}^{(i)}$ and a determined variance for each of the variables, which are independent. The joint probability $P(W(\boldsymbol{\theta}^*), W(\boldsymbol{\theta}^i))$ is modeled as a Gaussian distribution.

5.5 Experiments

We have divided the experiments in two parts: simulations in order to learn the required parameters and experiments in the Barcelona Robot Lab. (BRL), a real environment.

We have implemented a simulated environment to model multiple people in scenarios, based on the ESFM, as well as static obstacles aiming to provide realistic conditions.

To conduct all the experiments in the BRL and to test the approach presented, we have used the Tibi&Dabo robotic platforms, that have been specifically designed to work in urban pedestrian areas and interact with people.

5.5.1 Parameters learning using the ESFM simulatior

Before deploying any real robot, we believe that is essential to grasp an initial idea of the navigation system in a controlled simulated environment. We could directly obtain the $\boldsymbol{\theta}$ navigation parameters in a real scenario, nevertheless, safety could not be guaranteed if we are exploring the limits of the navigation approach. To this end, we have implemented a simulation software that generates people's trajectories, static obstacles and all the requirements for a mobile robotic platform to simulate a urban-like environment. For more details, see Sec. 2.2.

A capture of the synthetic scenario used during the simulation step is depicted in Fig. 5.4, as a simplification of a urban environment. The studied environment consists of static obstacles and multiple people modeled as dynamical obstacles following the SFM, quite similar to a real urban dynamical environment.

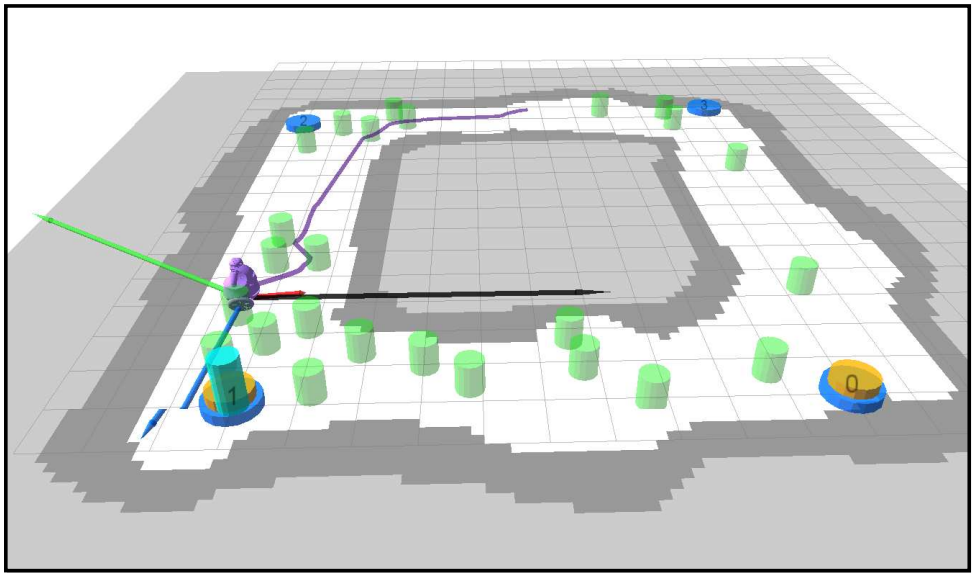

Figure 5.4: **Simulation environment.** In order to obtain the $\boldsymbol{\theta}$ parameters we make use of a reduced urban environment and a set of virtual dynamic people. The outcome of each simulation depends on its inner $\boldsymbol{\theta}$ parameters, and thus, we require a large number of experiments.

The results of the MCMC-MH optimization, explained above in Sec. 5.4.1, are obtained after more than a thousand simulations. The outcome of each experiment was dependent on the parameters $\boldsymbol{\theta}$, since the system reacts to the behavior of the robot navigation and vice versa. After following the proposed optimization method, we have obtained the values of $\boldsymbol{\theta}$ equal to $\{\alpha = 1.0, \gamma = 3.18, \delta = 0.20\}$, which will be the system parameters that we will use during the real experimentation.

The values obtained by using this approach are highly dependent on the learning environment, as we will discuss below. In this section of the chapter, we have chosen to learn the parameters on a dynamic scenario, considering a constant number of people and obstacles, though. For future simulation environments, we will diversify the composition of our learning environments in order to assure more robustness during real testing.

5.5.2 Experiments in real environments

Real experimentation was carried out in a urban environment, the Barcelona Robot Lab, which was described above. The $\boldsymbol{\theta}$ parameters have been obtained in the simulation learning stage, as explained in the previous subsection, and during all our real experiments, those social-aware

parameters calculated have remained unchanged.

A single experiment consisted in a query of the desired goal to the social-aware navigation system and the outcome of the robot navigation corresponds to the path executed in a urban environment with multiple static obstacles and pedestrians that were not given any instruction, they just walked naturally in the university campus as any other normal day. Some examples during the experimentation are shown in Fig. 5.5.

The set of experiments were carried out during a lapse of time equal to two hours, summing in total 20 queries to reach destinations within the BRL, as it can be seen in the map depicted in Fig. 5.2. Almost all navigations commands achieved successfully their goals, except for some cases (2 experiments) including narrow passages, were some oscillatory motions were detected. This problem is well known, as described in [Koren and Borenstein, 1991], and although there exist various solutions to this issue, none of them were implemented during the experimentation at that time. In Fig. 5.5-*Left* are depicted some shots of the robot navigating in the BRL and their corresponding sensor information and relevant information in the robot GUI, appearing in the right column of the figure. The navigation experiments succeed 90% of the times, including highly potentially problematic areas in the university campus.

In order to validate the model in real experiments, we have compared our approach with respect to a teleoperated robot by an expert controller. This experiment was performed under the same conditions as the social-aware navigation: a goal is provided, but instead of an autonomous solution to the navigation, we sought an expert controller to solve the navigation problem, while reaching its goal and dealing with any pedestrian or obstacle on the robot's path.

We have evaluated the performance of both approaches using the *social work* metric proposed in (5.8) for the parameter learning. As it can be seen in Fig. 5.6, we have drawn the average and the variance values of the robot's *social work*, the people's *social work* enforced by the robot and the total *social work* of the overall approach. However, the results of the *social work* were only taken into account if the robot navigation state was *social robot navigation* or *inner robot navigation*, that is, if there was at least one person within the social-navigation region, which represent the most interesting cases of study for human interaction purposes.

The social-aware generated less amount of *social work* both in the robot and people surrounding the robot. The comparison of the people's *social work* for both approaches is similar, both approaches generate a reduced and maybe unavoidable amount of *social work*. The trivial solution of "escaping" for the navigation problem, that is, stay as far as possible from potential social interactions, is not an option: this behavior would not solve the interaction with other people. Accordingly, we evaluate the *social work* carried out by the robot. In this case, the comparison between our approach and the teleoperated is quite significant, the social-aware approach outperforms the teleoperated approach and its variance is also greatly smaller, which represents more ability to cope more consistently with different situations requiring less *social work*.

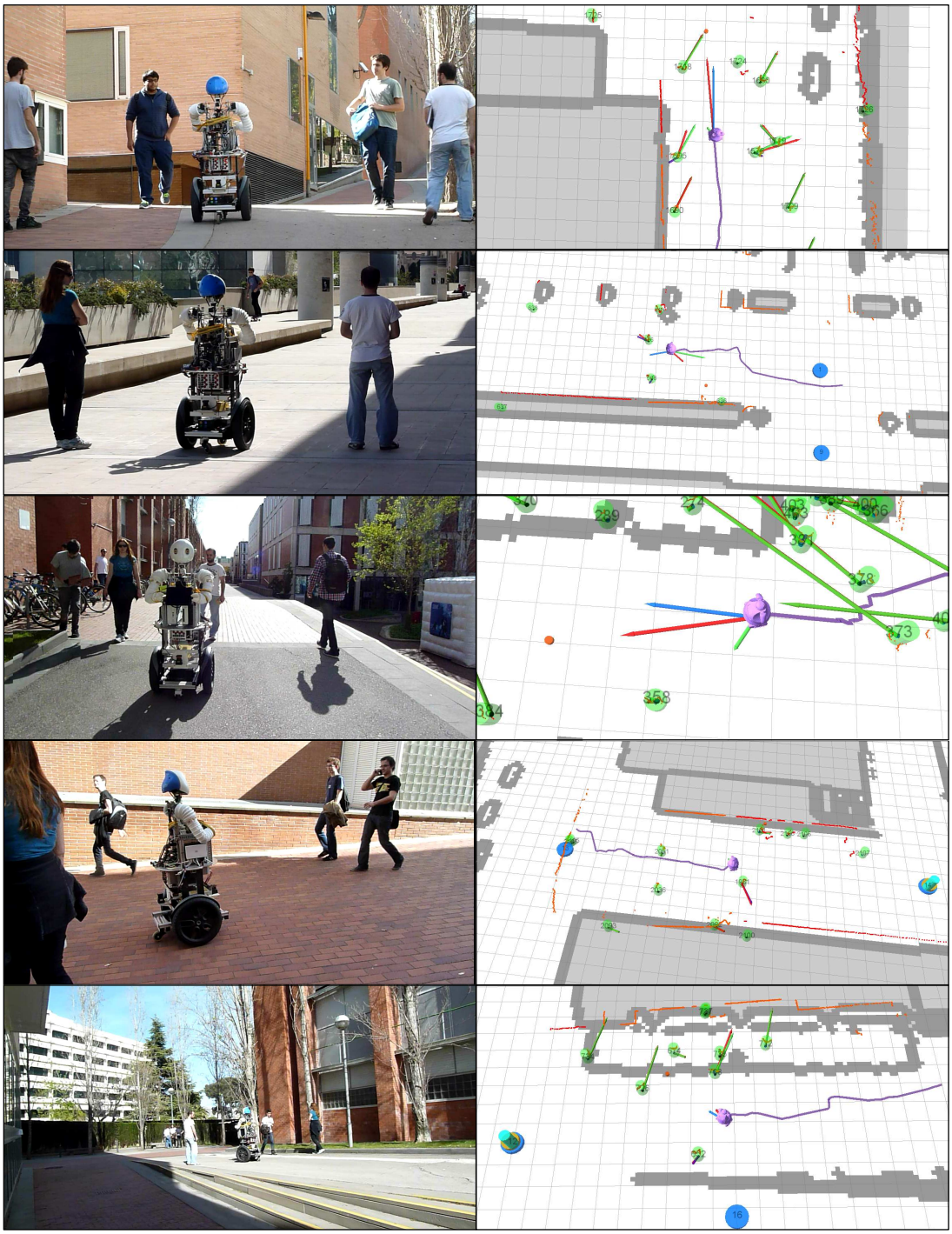

Figure 5.5: **Real experiments.** *Left*: some pictures of the social-aware approach navigating in the BRL. *Right*: their corresponding sensor information, virtual forces and trajectories in the robot GUI using ROS.

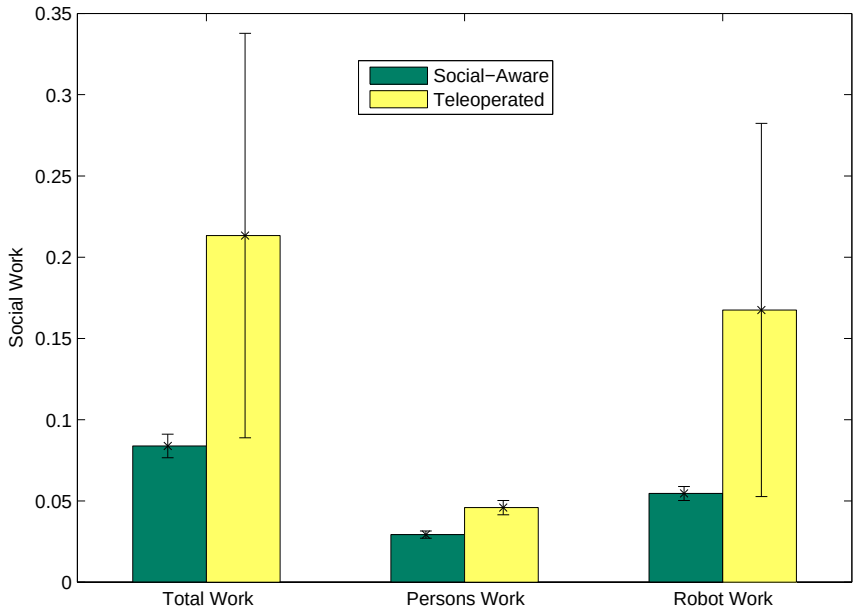

Figure 5.6: **Experiments results.** Average and standard deviation of the *social work* while performing real experiments. Green bars correspond to the social-aware approach and yellow bars correspond to the teleoperated approach, as a comparison to the proposed method.

For further information, check the videos of the experimental results and all code in the project web http://www.iri.upc.edu/groups/lrobots/social_aware_navigation/ecmr2013.php.

5.6 Summary

We have presented a novel robot navigation approach based on the ESFM. The navigation algorithm is socially-aware of interactions taking place with other pedestrians.

We have introduced a way to measure the impact of the robot navigation towards the social scene, the *social work* as explained in Sec. 5.4.1. Intuitively, this measure quantifies the quality of the navigation approach with respect to its social environment, and it has been the first step in this direction in this thesis. In future chapters we will stress on the importance on minimizing the social impact and its relation to other tasks, such as, time to achieve a goal or robot effort to navigate.

We have implemented a social simulation environment in order to verify the system and obtain the set of navigation parameters $\boldsymbol{\theta}$, as an essential prerequisite before any real experimentation is done. All the code of the simulation environment is available at the project webpage.

The validation of the model has been demonstrated throughout an extensive set of simulations and real-life experiments in a urban area. In contrast to other existing approaches, our

method can handle realistic situations, such as dealing with large environments with obstacles and semi-crowded scenes. For that reason, this work can be applied to certain specific real robot applications, for instance, guiding tourists or accompanying professional visitors.

The ESFM provides a realistic model of human motion to generate trajectories, though not exempt of limitations as discussed in previous chapters. The robot navigation approach is based on a human navigation model, the ESFM. However we have observed some limitations on the robot navigation in certain situations during real experiments, where the model is only able to behave like a person in simple situations, while in more complex configurations the system behaves abnormally. These limiting situations are oscillations or blocking states due to local minima, were already presented in [Koren and Borenstein, 1991].

In addition, robots are not pedestrians, and should not navigate as people, contrary to our initial hypothesis. We have built a navigation system, based on the ESFM, that failed to behave like a person. By providing a set of parameters $\boldsymbol{\theta} = \{\alpha, \gamma, \delta\}$, we guaranteed minimal social work, but only on the training scenarios, while we desire a successfully performance in multiple scenarios. After our study, we conclude that the ESFM should be taken as a feature that captures the interaction of human motion and not as a complete human navigation model. In the following chapters we will develop this idea.

6

Robot task: accompany people walking side-by-side

This chapter embodies our first step towards the integration of prediction information and a robot navigation approach. Particularly in this chapter, we integrate the BHMIP proposed in Chapter 3 and the reactive social-aware navigation approach presented in Chapter 5.

As a result we present a novel robot companion in semi-crowded urban areas. As explained before, the main contribution of this work falls back into the combination of these two topics presented in this thesis. This union highly improves the overall robotic performance, as we will show in a concrete example of the robot companion task. In addition, we present an interactive learning method using multimodal human feedback to compute the parameters of the social-aware navigation model. Finally, a quantitative metric based on people's personal spaces and comfortableness criteria is designed to evaluate the performance of the robot companion task. The validation of the model is accomplished throughout an extensive set of simulations and real-life experiments including a volunteers' survey to measure the acceptability of our robot companion's behavior.

This work has been published in the *IEEE/RSJ International Conference on Intelligent Robots and Systems* [Ferrer et al., 2013a], and we have submitted the extended version to the journal *Autonomous Robots*. Part of the present chapter appears in the thesis *Cooperative social robots: accompanying, guiding and interacting with people* [Garrell, 2013] where Dr. Garrell contributed to the evaluation of the companion task presenting a novel metric and the evaluation of the volunteers' poll and our contributions were in the adaptation of the reactive navigation to the companion task, integrating it with prediction and learning of parameters, as well as the coding to implement the algorithm in the robot.

6.1 Introduction

Nowadays, robots interact naturally with people and their environment and thus, urban robots require some skills to successfully serve people and being useful to them. The robot companion is a basic tool that every urban robot should have and it responds to the basic necessity of accompany people in a safety and natural way, see Fig. 6.1.

In this chapter, we define the "accompany" task as an enhancement of a "follow" task, where one agent replicates the trajectory of the followed agent. In the accompany task, the robot is supposed to walk side-by-side of the accompanied person in a more intelligent manner since the robot does not know which is the person's future path and needs to somehow infer it.

We propose to use a human intentionality predictor, the BHMIP presented in Chapter 3, to infer the target's most expectable destination and use it for improving the robot companion task. In this work, we are making use of prediction information to give the robot the ability to predict the trajectory that the target person is expected to do, and therefore, the robot is able to walk besides the human.

Figure 6.1: **Tibi accompanies a person.** A pedestrian is being accompanied by Tibi in a urban area in different scenarios.

This work goes one step further in terms of navigation, we aim to achieve a robot able to accompany a person in an acceptable social manner, while simultaneously navigate in a typically human environment. Our approach is inspired on human walk, and we incorporate the ESFM model to develop the robot's behavior. Moreover, we require a seamless integration of the navigation scheme with the accompany task and the formulation of the ESFM allows us to achieve it. To this end, additional considerations are required to make the system work properly, such as prediction information and a learning stage.

Moreover, we introduce a new metric to evaluate the robot companion's performance, based on vital spaces and comfortableness criteria. Since the verification of human-in-the-loop systems is usually subjective, we require an objective analytical metric that serves to validate the behavior of our robot companion approach.

Finally, we propose an interactive learning scheme to learn the social-aware navigation

parameters using the human feedback response in the companion system. The parameters are learned through an extensive analysis of the robot companion task in diverse situations, where the human feedback response enhances the accuracy of the robot companion performance, showing a better companion behavior.

The validation of the model is accomplished throughout an extensive set of simulations and real-life experiments, as well as a questionnaire to every participant in the experiments.

6.2 Related work

In recent years, human-robot interaction has become a very active research field, nevertheless, there is not extensive research on motion planning in the presence of humans. Some methods have been developed to allow robots to navigate around people while performing specific tasks. Some of these tasks include tending toward the right side of a hallway [Olivera and Simmons, 2002] and standing in line [Nakauchi and Simmons, 2002]. Museum tour guide robots are often given the capability to detect and attempt to deal with people who are blocking their paths on a case-by-case basis [Burgard et al., 1999].

Several groups have begun to address questions relating to plan complete paths around people, rather than relying on solely reactive behaviors. In [Shi et al., 2008], a method for a robot to change its velocity near people has been developed. While this method begins to address ideas of planning around people, it does not directly consider social conventions. In contrast, in [Sisbot et al., 2007], the Human-Aware Motion Planner considers both the safety and reliability of the robots movement and human comfort, it attempts to keep the robot in front of people and visible at all times. However, the paths that the planner generates may be very unnatural due to its attempts to stay visible to people.

In most works, unlike ours, safety is assured by not allowing humans to approach robots. However, these methods cannot be used if the robot has to assist a human. In [Alami et al., 2006], the notion of safety is studied in detail with all of its aspects in Human Robot Interaction.

Two different aspects of human's safety have been studied in [Zinn et al., 2004]: "physical" safety and "mental" safety. With this distinction, the notion of safety includes physical aspects and psychological effects of the robots motions on humans. Physical safety is necessary for the human-robot interaction. Normally, physical safety is assured by avoiding collisions with humans and by minimizing the intensity of the impact in case of a collision.

Introducing the science of "proxemics", Hall demonstrates how man's use of space can affect personal business relations, cross-cultural exchanges, city planning and urban renewal [Hall and Hall, 1969]. A robot should comply to similar conventions [Fong et al., 2003]. In human robot interaction, the spatial formation around a robot has been studied in relation to initiating interaction [Michalowski et al., 2006]. A classification of people's motion towards a robot was

presented in [Bergstrom et al., 2008]. In [Tasaki et al., 2004], a robot that chooses a target person based on distance was developed. In [Pacchierotti et al., 2006] a system for navigation in a hallway is presented, in this work the rules of proxemics are used to define the different strategies of interaction.

Another approach that deals not only with safety but also implicitly with comfort issues is the work on velocity along a planned trajectory [Madhava Krishna et al., 2006]. In this research, the robot adapts its trajectory and its speed in order to guarantee that no collision will occur in a dynamic environment. Although the human is not considered explicitly, this method guarantees a motion without collision by taking into account the dynamics of the environment.

Moreover, an increasing area of interest in the HRI field is in the development of autonomous companion robots [Dautenhahn et al., 2005]. Furthermore, researchers are making efforts on performing human-robot interaction in a more natural way. A robot companion should detect the human operator and conduct his/her commands [Haasch et al., 2004].

Human-robot interaction research in the field of companion robots is still new in comparison to traditional service robotics, such as robots serving food in hospitals or providing specific security services. Therefore, prior research in this particular field is relatively minimal [Wilkes et al., 1997].

Most of the current research predominantly studies robots that participate in social-human interactions as companions [Ishiguro et al., 2001]. Many studies have investigated people's attitudes towards robots and their perception of robots. In [Dautenhahn et al., 2006], it was shown that a seated person prefers to be approached by a robot in a fetch-and-carry task from the front left or right direction rather than frontally or from behind. Further research showed that there are other mediating factors, which can impact this preference, such as the person's experience with robots [Koay et al., 2007], gender [Dautenhahn et al., 2006] or in which part of the room she was standing or sitting [Walters et al., 2007]. [Satake et al., 2009] proposed a model for robots which should initiate interaction in a shopping mall.

In [Pransky, 2004], a new perspective to the different uses and identities of a companion robot has been brought, moreover it also describes the advantages and disadvantages of this type of companion. The "Robotic Butler/Maid" was able to perform domestic task, but also caused difficulties in relationships at home by being too efficient and making people feel redundant. In [Dautenhahn et al., 2005], a human-centered approach was adopted in order to look into people's perceptions and their desires for a companion robot. If social robots are going to be used in office and domestic environments, where they will have to interact with different individuals, they will have to be able to survive and perform tasks in dynamic, unpredictable environments and they must act safely and efficiently.

We present a novel robot companion approach based on the SFM. A model capable of approaching a person and accompanying him/her to a predicted goal. Moreover, this approach enables the robot to learn its behavior using a multimodal interaction feedback. We believe that

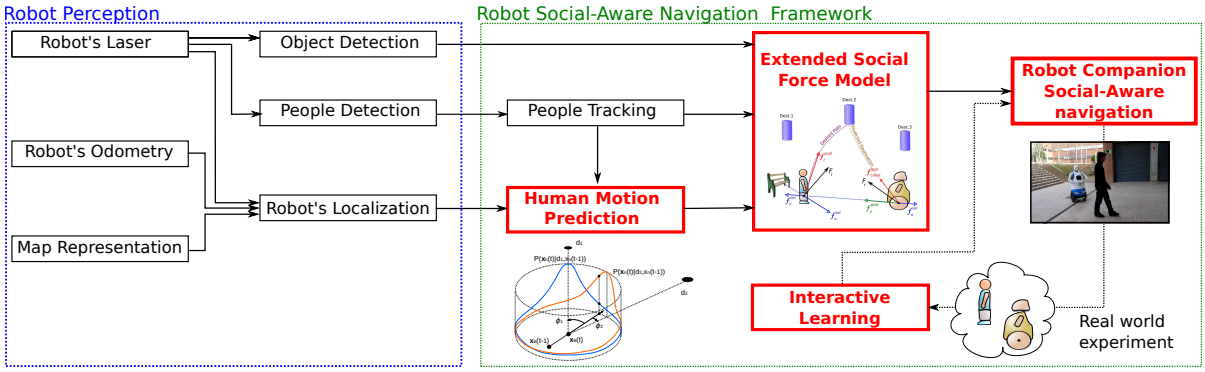

Figure 6.2: **Overview of the presented companion approach.** A general diagram of the robot companion approach is depicted, as well as its requirements. We have highlighted in red our contributions to advance the topics discussed later in the present work.

most of the limitations of state of the art methods are overcome by our method, as it will be discussed in the following sections.

6.3 Overview of the method

As stated earlier, this chapter describes the adaptation of the reactive navigation, presented in Chapter 5, to accompany people. One of the main issues which arises when humans are accompanied by robots is that the navigation must be socially accepted by people, therefore, robots need to be able to understand human's movements and understand human intentionality. In Fig. 6.2 is depicted a scheme of our proposed approach, where we are integrating the intentionality descriptor (BHMIP) proposed in Chapter 3

Intentionality Prediction: We use an indicator capable of quantifying the human motion intentionality (HMI) implicit on a trajectory with respect to the current position and orientation. This intentionality indicator captures the probability that a human trajectory reaches a destination point. This prediction is used by the robot to predict the destination of the person who is being accompanied.

ESFM-based Robot Companion Social-Aware Navigation: A robot model capable of approaching a person and accompanying him/her to a predicted goal is presented. The social force model described in [Helbing and Molnar, 1995] takes into account both destinations and interactions by defining a summation of existing forces determining people trajectories. The meaning of "social force model" does not refer to a social robot's behavior, but rather to the existence of a non-physical force that robots can exert to move or drag people. More specifically, this work proposes a robot's reactive navigation based on an extension of the social force model which results from the internal motivations of the individuals performing certain movements [Zanlungo

et al., 2011; Garrell and Sanfeliu, 2012]. A robot accompanying humans is one of the core capacities every service robot deployed in urban settings should have [Garrell and A. Sanfeliu, 2010; Garrell and Sanfeliu, 2012]. The proposed model is validated throughout simulations and a set of real-life experiments. We also demonstrate that prediction information and the interactive learning enhance the overall performance of the robot companion.

Interactive Robot Companion Parameters Learning: An interactive approach tests the model forces learned. At the same time, it learns which robot behavior is desired by humans. The provided feedback is a subjective measure, nevertheless, its purpose is to learn a general approaching rule that defines a better robot behavior. The proposed interactive learning helps to enlighten the nature of the model, in addition to generate controlled interaction forces that otherwise would be extremely complicated to generate. The on-line feedback comes from the target person to whom the robot tries to approach.

Robot Companion Performance Metric: In order to evaluate the performance of the task accomplished by the robot, a quantitative metric is defined. This assessment is based on "proxemics", proposed by Hall and Hall [1969].

6.4 Social-aware robot companion

Previously in this thesis we have presented several contributions, such as, a general social interaction model based on social-forces, in Sec. 4.3, a social-aware reactive navigation approach in Sec. 5.4 and a prediction algorithm to estimate the best destination a person aims to in Sec. 3.4. In this section, all these independent topics are integrated to build a robot companion task.

Following the same reasoning presented in Sec. 5.4, where we have considered the robot as a social agent moving naturally in human environments accordingly to the ESFM, we propose a robot companion system that not only considers the obstacles and people in the scene, but in addition considers prediction information in order to better execute the companion task.

In the navigation problem, the set of destinations that the robot was following was calculated from a global map. In the companion task, the robot destination is the accompanied person's destination, applying (4.2) centered at the robot

$$\boldsymbol{f}_{r,dest}^{goal}(t, \mathcal{D}_i(t)) = k_r(\, \boldsymbol{v}_r^0(\mathcal{D}_i(t)) - \, \boldsymbol{v}_r(t)), \tag{6.1}$$

where the desired velocity $\boldsymbol{v}_r^0$ is a function of the person's intentionality $\mathcal{D}_i(t)$.

As it can be seen in Fig. 6.3, the person's destination is the blue cylinder in the scene, and thus, we want the robot to navigate to that goal too. The force to the destination is a function of the intentionality $\mathcal{D}_i(T)$, since we have no information regarding the goal of the accompanied person. Accordingly, we calculate the ith person intentionality $P\big(\mathcal{D}_i(t) = D_i | \, \boldsymbol{X}_i(t)\big)$ following (3.8) to provide an estimation of the destination that the person is heading to. This probability

is calculated at the same rate that we receive observations from the environment, to ensure adaptability to changes of intentionality or wrong estimations.

In addition, we should guarantee that the robot is really accompanying a person, not just navigating to its estimated destination. To this end, we propose a variation of the social-aware navigation by introducing an extra heading force

$$\boldsymbol{f}_{r,i}^{goal}(t, \boldsymbol{x}_i) = k_r(\ \boldsymbol{v}_r^0(\boldsymbol{x}_i) - \ \boldsymbol{v}_r(t)), \tag{6.2}$$

which aims to the current position of the person $\boldsymbol{x}_i$. As it can be seen in Fig. 6.3, two destinations are contributing to the total force describing the robot's trajectory.

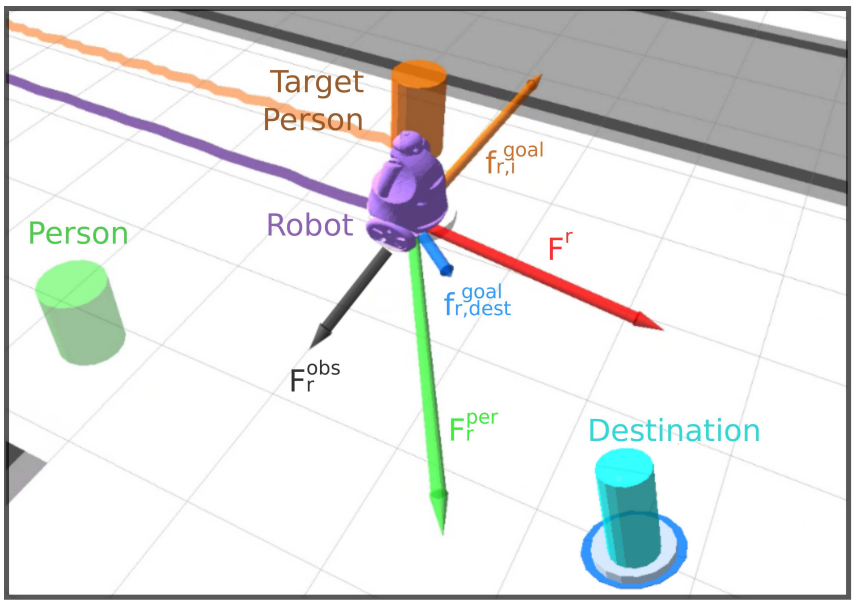

Figure 6.3: **ESFM adapted to the companion task.** Forces applied to the robot while accompanying a person.

The forces of interaction due to pedestrians are the repulsive forces each person generates to the robot $\boldsymbol{f}_r^{per}(t)$ calculated as proposed in (5.2), and the interaction forces corresponding to obstacles $\boldsymbol{f}_r^{obs}(t)$ are calculated using (5.4).

In contrast to the social force model, two different goals appear, therefore we combine both heading forces into a unified motion propagation. Firstly, the force $\boldsymbol{f}_{r,dest}^{goal}(t, \mathcal{D}_i)$ drives the robot towards the predicted destination. Furthermore, the robot must approach the person who accompanies, and hence, a second goal pushes the robot to move closer to the person p_i, $\boldsymbol{f}_{r,i}^{goal}(t, \boldsymbol{x}_i)$. The trade off of these forces, in addition to the interacting forces, describe the resultant force governing the robot movement

$$\boldsymbol{f}_r(t) = \alpha\, \boldsymbol{f}_{r,dest}^{goal}(t, \mathcal{D}_i) + \beta\ \boldsymbol{f}_{r,i}^{goal}(t, \boldsymbol{x}_i) + \gamma\ \boldsymbol{f}_r^{per}(t) + \delta\ \boldsymbol{f}_r^{obs}(t), \tag{6.3}$$

which reminds the formulation proposed in (5.6).

The following section discusses the procedure to obtain the value of the parameters $\boldsymbol{\theta} = \{\alpha, \beta, \gamma, \delta\}$ governing the robot companion task and how to update them. Once obtained the reactive force action, the system behaves consequently to these stimuli and propagates linearly its position and velocity according to this force value.

6.4.1 Quantitative metrics

To evaluate the performance of the task accomplished by the robot, a quantitative metric is defined. This assessment is based on "proxemics", proposed by Hall and Hall [1969] and the importance to walk side-by-side. This work considers the following taxonomy of distances between people:

- Intimate distance: the presence of another person is unmistakable, close friends or lovers (0-45cm).
- Personal distance: comfortable spacing, friends (45cm-1.22m).
- Social distance: limited involvement, non-friends interaction (1.22m-3m).
- Public distance: outside circle of involvement, public speaking ($>$ 3m).

To define the metric used in the present work, four different areas must be defined: *(i)* Personal space of the ith pedestrian $\mathcal{C}_i$, robot's navigation has to be socially accepted by the person being accompanied, it is necessary that the robot does not perturb the human's vital space and walks beside the person (6.4). *(ii)* Social distance area $\mathcal{A}$, the robot must be allocated in an acceptance social distance. *(iii)* The robot should be in the human's field of view as it interacts during the performance of the task and must walk beside the person $\mathcal{B}$. *(iv)* Finally, there are other pedestrians in the environment p_j, the robot is not allowed to perturb pedestrians' personal space $\bigcup_{p_j} \mathcal{C}_j$.

$$
\begin{aligned}
\mathcal{A} &= \left\{ \boldsymbol{x} \in \mathbb{R}^2 \setminus (\mathcal{B} \cup \mathcal{C}) \mid d(\boldsymbol{x}, \boldsymbol{x}_i) < 3 \right\} \\
\mathcal{B} &= \left\{ \boldsymbol{x} \in \mathbb{R}^2 \setminus \mathcal{C} \mid d(\boldsymbol{x}, \boldsymbol{x}_i) < 3w(\varphi_i) \right\} \\
\mathcal{C} &= \left\{ \boldsymbol{x} \in \mathbb{R}^2 \mid d(\boldsymbol{x}, \boldsymbol{x}_i) < w(\varphi_i) \right\}
\end{aligned} \tag{6.4}
$$

where $w(\varphi_i)$ is defined in (4.5) as the anisotropic element.

Moreover, the robot can be represented as a circle of 1 meter of diameter, with center at the robot's position $\boldsymbol{x}_r$, $\mathcal{R} = \{\boldsymbol{x} \in \mathbb{R}^2 \mid d(\boldsymbol{x}, \boldsymbol{x}_r) < 0.5\}$, whose area is $|\mathcal{R}| = \frac{\pi}{4}$.

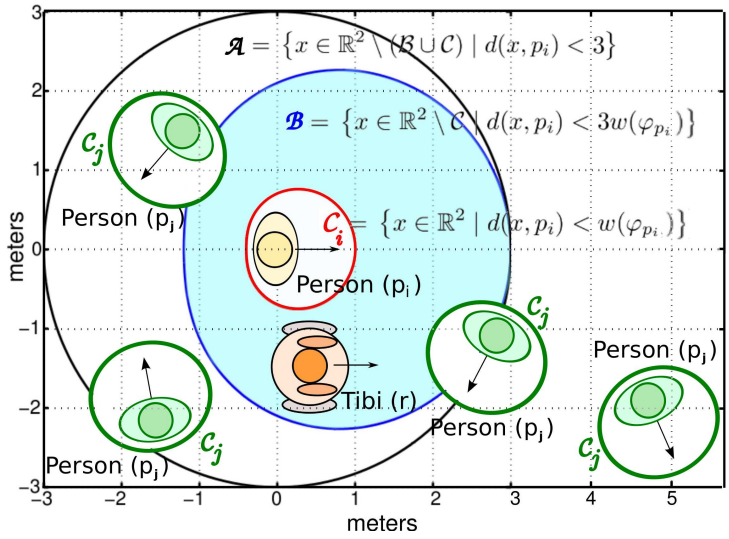

Figure 6.4: **Quantitative metrics.** Diagram of the areas used in the evaluation of the robot's performance. The areas represented by $\mathcal{C}_j$ are people's personal space, where the robot cannot get in, area named as $\mathcal{B}$ is the optimal area where the robot should be allocated in order to accompany a person. Finally, area $\mathcal{A}$ represents a social acceptable distance, but its performance is lower since if the robot is behind the person it would be out of the field of vision.

Thus, we can now define the performance of the task accomplished by the robot, depending on the human's position $\boldsymbol{x}_i$ and the robot's position $\boldsymbol{x}_r$

$$\rho(\boldsymbol{x}_r, \boldsymbol{x}_i) = \int_{(\mathcal{B} \setminus \bigcup_{p_j} \mathcal{C}_j) \cap \mathcal{R}} \frac{d\boldsymbol{x}}{|\mathcal{R}|} + \int_{(\mathcal{A} \setminus \bigcup_{p_j} \mathcal{C}_j) \cap \mathcal{R}} \frac{d\boldsymbol{x}}{2|\mathcal{R}|} \in [0, 1]. \tag{6.5}$$

The range of the performance function presented is defined between 0 and 1, if the complete area of the robot is allocated in zone $\mathcal{B}$, the performance is maximum, *e.g.*, 1. As the robot moves far from the person and enters zone $\mathcal{A}$, the performance decreases to 0.5. Finally, the performance in zones $\mathcal{C}_i$ is 0, as it is not allowed that the robot enters in people's personal space.

6.5 Parameters learning

In order to learn the values of the introduced parameters $\boldsymbol{\theta} = \{\alpha, \beta, \gamma, \delta\}$, we use a two-step learning approach. First, we require an initial estimation to learn the magnitude of the $\boldsymbol{\theta}$ parameters.

We calculate the best estimation, according to the companion metric defined in (6.5) presented in in Sec 6.4.1, of the $\boldsymbol{\theta}$ parameters in a simulated environment after thousands of simulations using a MCMC approach, very similar to the approach presented in Alg. 3, in Sec. 5.4.1. We will explain in Sec. 6.6.1 the details of the experimentation procedure.

The second step of the learning approach consist of an Interactive Learning [Katagami and Yamada, 2003]. Our approach is based on robots interacting with people, therefore, it requires people's feedback in order to refine the parameters values $\{\alpha, \beta, \gamma\}$, under the shape of the person's response to the stimuli generated by the robot. This method helps to enlighten the nature of the model, in addition to generate controlled interaction forces that would otherwise be extremely complicated to generate.

The on-line feedback comes from the target person to whom the robot tries to approach. The human agent provides the interaction by using a *wii* remote control. Here, we expect to receive a feedback measure of the subjective comfortableness of the target being approached.

This feedback is a subjective measure, nevertheless, we have modeled a system weighting the contribution of all active forces. Volunteers had a *wii* remote control. Participants were told to press the button '+' if they wanted the robot to get closer to them. However, if people preferred the robot to move directly to the destination, they should push button '-'. Below, the variation of parameters depending on people's feedback is presented.

Firstly, we can define the function $N(t)$ as the accumulated number of responses obtained from the person:

$$N(t) = \sum_{\tau=t_0}^{t} \epsilon(\tau) \tag{6.6}$$

where $\epsilon(\tau)$ is expressed as:

$$\epsilon(\tau) = \begin{cases} 0 & \text{if human does not press any button at time } \tau \\ +1 & \text{if human presses button '+' at time } \tau \\ -1 & \text{if human presses button '-' at time } \tau \end{cases} \tag{6.7}$$

$N(t)$ is the difference between the number of times the person presses button '+' and button '-' at the current time t. Then, $N(t) \geq 0$, if $N(t) < 0$ we impose $N(t) = 0$.

Secondly, the forces that appear during the process of accompanying vary according to the distance between the robot and the person. Then, the variation of the parameters will change depending on such distance.

Formally, if $h(N(t))$ denotes the function corresponding to human's response, it can be expressed as:

$$h(N(t)) = \begin{cases} \alpha(N(t)), \beta(N(t)) & \text{if } d_{r,i} \geq w(\varphi_{r,i}) \\ \gamma(N(t)) & \text{if } d_{r,i} < w(\varphi_{r,i}) \end{cases} \tag{6.8}$$

where, $\{\alpha(N(t)), \beta(N(t)), \gamma(N(t))\}$ is the set of weighting functions for the parameters $\{\alpha, \beta, \gamma\}$, $d_{r,i}$ is the distance between the robot and the person and $w(\varphi_{r,i})$ represents the personal space of a person, see (4.5).

Below, the definitions of the weighting functions are presented.

Force to the target destination α: We infer the target of the destination by using the intentionality prediction BHMIP described in Chapter 3, and thus the robot aims to the target's destination that is most expectable. As it has been described above, a parameter α controls the magnitude of the force $\boldsymbol{f}_{r,dest}^{goal}$. The value of this parameter is computed as follows:

$$\alpha(N(t)) = log(1 + N(t)/\sigma_\alpha) \tag{6.9}$$

Force to the person being accompanied β: An attractive force towards the accompanied person has been described. Either the current target position as well the expected motion prediction are known. The parameter β controls the magnitude of the force $\boldsymbol{f}_{r,i}^{goal}$. The value of this parameter is computed as follows:

$$\beta(N(t)) = 1 - \alpha(N(t)) \tag{6.10}$$

Force of interaction with people γ: A repulsive force due to the relative position and velocity between the robot and people must be considered, $\sum_{j \in P} \boldsymbol{f}_{r,j}^{int}$, this force is controlled by the parameter γ. The value of γ is defined as:

$$\gamma(N(t)) = log(1 + N(t)/\sigma_\gamma) \tag{6.11}$$

Force of interaction with obstacles δ: Finally, a repulsive force due to the relative position and velocity between the robot and obstacles has to be considered, $\sum_{o \in O} \boldsymbol{f}_{r,o}^{int}$, this force is controlled by the parameter δ. This parameter is not refined with human feedback since it only involves robot and obstacles.

The combination of these four forces determines the behavior of the robot while physically approaching a person. Although a general approaching rule must be obtained, it highly varies from person to person, in addition to the highly noisy environment in which we are working. While iteratively repeating the robot physical approach, the feedback provided refines the weights of the force parameters and we can infer an interactive behavior where the person feels comfortable under the presence of the robot.

6.6 Experiments

In this section, we present the corresponding experiments for the learning step and the complete robot companion task. In addition, we have included the experiments carried out in the simulation environment and real experimentation with people.

6.6.1 Parameters learning in simulations

We have devised different experiments to obtain the parameters that define the presented robot companion approach $\boldsymbol{\theta} = \{\alpha, \beta, \gamma, \delta\}$. In this section we will describe the experiments for the two proposed learning methods: a simulated environment and a posterior refinement in a real scenario with some volunteers.

In order to obtain a good initial estimation of the $\boldsymbol{\theta} = \{\alpha, \beta, \gamma, \delta\}$ parameters and to evaluate mathematically the correctness of the reactive navigation model, we have built a simulated social environment. This simulated environment serves two purposes: firstly, it allows an initial guess of the system parameters $\boldsymbol{\theta}$ and secondly, the simulated environment permits us to validate the performance of the approach using the function (6.5) in different scenarios and under different density of pedestrians.

To this end, we have implemented a complete social environment, depicted in the top row of Fig. 6.5. It takes into account pedestrians, obstacles and robots in an interactive way and each element is reactive to its surroundings, according to the ESFM. By doing this, we obtain a dynamical environment, in which each action of the robot alters the behavior of nearby pedestrians and vice versa.

According to previous human-based companion works [Garrell and Sanfeliu, 2012], we have set the accompany position at $1.5m$ from the target and 60° from the target's heading. Our approach for the robot companion task is evaluated in a simulated environment, which makes use of the social-aware robot companion and prediction information regarding the target destination. This simulated environment consists of a urban setting (inspired by the BRL), in which obstacles are present as well as a fixed number of pedestrians.

In order to obtain a good initial estimation of the system parameters, we have prepared a set of simulations, as explained above in Sec. 6.5, where we use more than two thousand MCMC-MH simulations. The outcome of each experiment is dependent on the parameters $\boldsymbol{\theta}$, since the system reacts to the behavior of the robot navigation and vice versa. After applying the optimization method proposed, we have obtained an initial guess of the magnitude of $\boldsymbol{\theta}$ roughly rounded to the values $\{\alpha = 0.1, \beta = 0.6, \gamma = 5.0, \delta = 0.50\}$. It is important to note that these parameters are obtained after random initializations in a virtual environment. However, this initial guess serves as a good estimation of $\boldsymbol{\theta}$ and their corresponding standard deviations, which will be the initial values of the system parameters that we will use for the interactive learning.

The second objective of the simulations is the validation of the parameters obtained before, in a challenging environment. Our method makes use of the ESFM of surrounding people and obstacles while approaching the target and additionally uses prediction information regarding the target destination to enhance its performance (red in Fig. 6.5). We have also implemented two additional methods to compare with our approach. A second configuration takes into

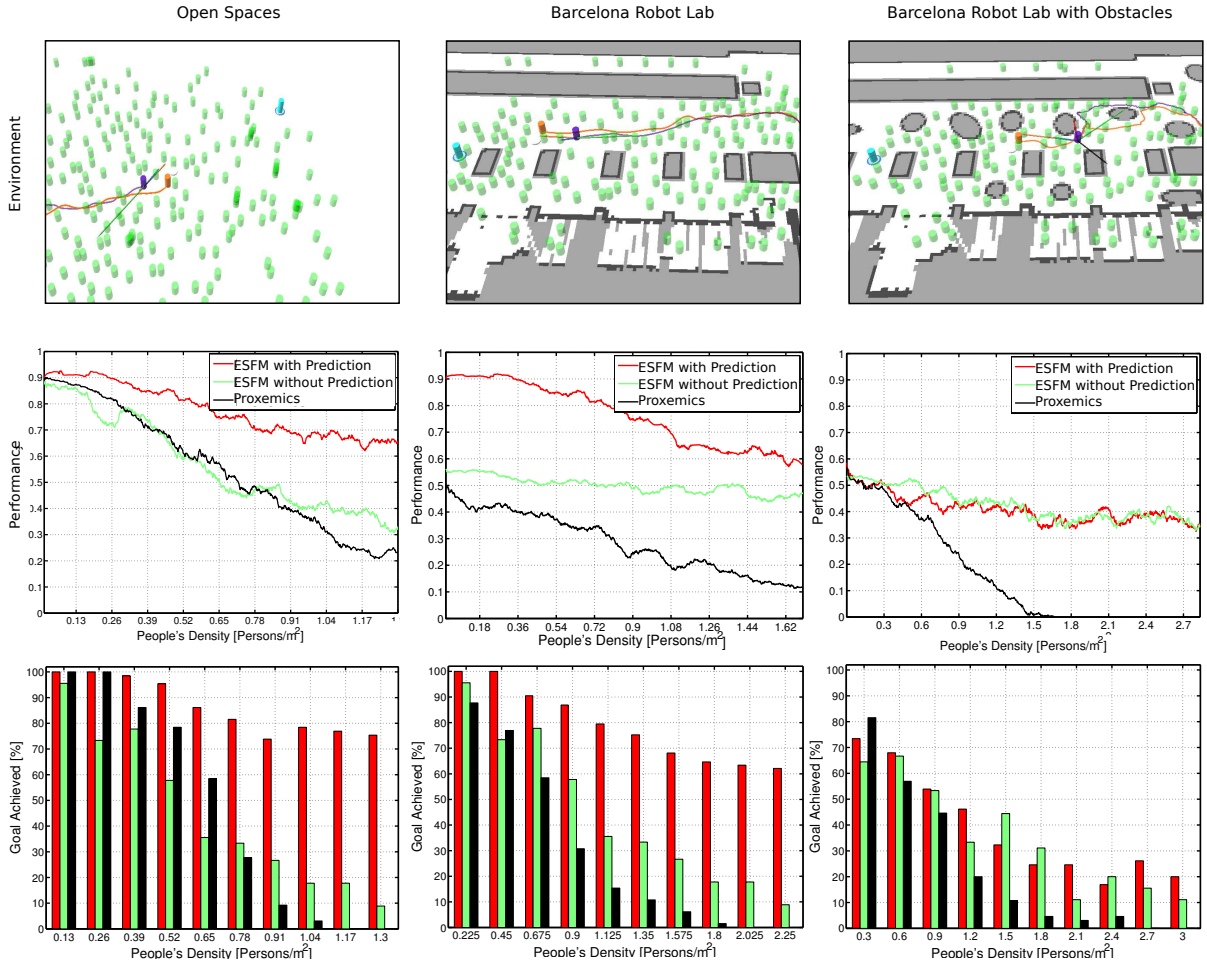

Figure 6.5: **Comparative of simulations.** *Left column:* unconstrained area with four destinations. *Central column:* urban settings, corresponding to the Barcelona Robot Lab. *Right column:* variation of the BRL with extra obstacles. *Top row:* different scenarios of the simulations, the blue cylinder corresponds to the destination, the orange one represents the person being accompanied by the robot and the purple one is the robot, the set of green cylinders are people in the environment. *Second row:* simulations performance, in black the proxemics approach, in green the ESFM companion and red the ESFM with prediction information. All results are function of the pedestrian density in the environment. *Third row:* rate of successful robot arrivals in bar diagrams. More info on the experiment videos in the project web (see Sec. 6.7).

account only the ESFM model (green in Fig. 6.5). For this reason, the avoidance of moving targets and obstacles is executed dynamically using the interaction forces in addition to the goal force. Our method is also compared to a robot companion based on proxemics, where the robot follows the target person, not considering the force of interactions with other people (black lines in Fig. 6.5). When some person enters the robot inner safety zone, the robot stops until the path is clear.

The experiment settings have been tested in three different scenarios, as it can be seen in the top row of Fig. 6.5. The first setting is an unconstrained area, free of obstacles, where four destinations are defined. The second is a urban setting, in which obstacles are present as well as pedestrians. The third is a variation of the previous setting, but increasing the number of obstacles in the scene.

For each environment, the algorithms have been tested depending on the density of persons in the unoccupied area. To give statistical consistency to the results, more than 50k experiments have been carried out, only varying the initial conditions, which are the initial positions of each pedestrian in the scene and the destination they are aiming to. These conditions are calculated randomly and the robot has to accompany a person under this uncertain environment. We would like to stress on the fact that the environment has a high density of people and each person aims to a random destination. This generates rapidly a chaotic and challenging environment for the robot companion testing (see video at the project web).

The second row of Fig. 6.5 shows the overall performance of the different methods with respect to the density of pedestrians in the scene (6.5), taking into account penalizations due to nearby people. As expected, using social interaction forces (red and green lines) highly increases the performance, it is natural to suppose that a more aware robot navigation would help to improve its efficiency. The predictive behavior clearly enhances the performance of the task, as it can be seen in the first and second columns. Under a low density of obstacles, the predictive information becomes of great utility. Nevertheless, under a high number of obstacles in the scene, the prediction strategy scores equally. This is due to the fact that acting predictively, specially in the third scenario, makes the robot decide alternative paths rather than just follow the target; *e.g.* while moving, surrounding a column to the right when the target goes to the left, but the destination would be more accessible by doing this. Although this behavior denotes some intelligence, its performance is punished based on our metric, as it can be seen in the figure. Anyways, the companion performance using prediction improves the overall performance of the system as it can be seen in Fig. 6.5, third row.

The third row of Fig. 6.5 shows average percentage of successful arrivals to the destinations, that is, if the robot is within the companion zone (zone A, see Sec. 6.4.1) at the moment the target achieves its destination. Although this metric is highly correlated, we observe that using prediction increases the arrival rate with respect to the other methods. That is, prediction information raises the probability to achieve its goal simultaneously with the target.

6.6.2 Interactive learning using volunteers

For the different real experiments we carried out, we considered a total of 61 volunteers between 20 and 40 (M = 27.4, SD = 5.78) years old. None of them had experience working or interacting with robots, they represented a variety of university majors and occupations including computer science, mathematics, biology, finance and chemistry. We separated them into two different groups. First, a group of 20 volunteers for the α, β, γ parameters using the interactive learning. Finally, we evaluated the performance of the system considering a qualitative and quantitative analysis using the second group of 41 volunteers as we will show in Sec. 6.6.3.

Aiming to refine the value of the $\boldsymbol{\theta}$ parameters, obtained in Sec. 6.6.1, we require to test the system in a real environment (the FME depicted in Fig. 2.3) with the first group of 20 volunteers. The experiment setting uses a robot in a real scenario as follows: we explain to each volunteer to naturally walk towards its chosen destination, among two options represented as red pylons. While approaching the desired destination, the robot accompanies the volunteers and they should behave naturally. In addition, and stressing on the predictive nature of the approach, we set an intermediate goal, not learned by the robot, to represent disturbances in people's trajectories and observe how our approach deals with them.

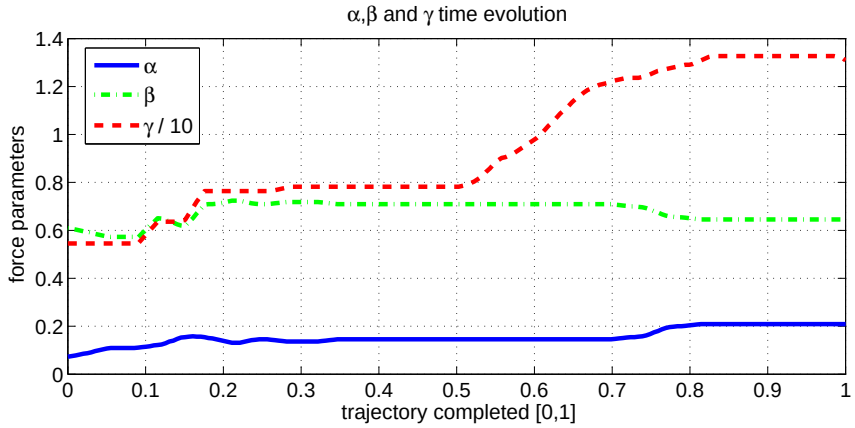

Figure 6.6: **Force parameters** α, β, γ**.** Evolution in time from start to end of each experiment of the force parameters α, β, γ. These variables are averaged using results chosen for each participant during the experiment.

As part of the interactive multimodal learning, the system learns the desired robot behavior as explained in Sec. 6.5. The feedback provided by the target is a subjective measure, nevertheless, its purpose is to learn a general approaching rule that defines a better robot behavior. It is provided directly by the target agent to be approached using a remote control, in this way the system automatically weights the contribution of the active forces (Sec. 6.5). An initial estimation of the $\boldsymbol{\theta}$ parameters is calculated in simulations (Sec. 6.6.1), and this information is useful although a readjustment is provided by the human feedback.

Fig. 6.6 shows the $\{\alpha, \beta, \gamma\}$ obtained from the user feedback that determines the robot behavior. It has been averaged for the 20 different volunteers and it is depicted as a function of time, normalized from the start of the experiment to its ending $t \in [0, 1]$. The δ parameter is not recalculated using this method since no obstacles were present in the experiment.

6.6.3 Robot companion validation in real scenarios

At this point of the experimentation, all the parameters of the system have been obtained and refined, as described previously. Consequently, we are ready to evaluate the performance of the robot companion approach in a real scenario, either using the quantitative metric explained in Sec. 6.4.1 or a qualitative method such a questionnaire to the volunteers.

A total of 41 volunteers carried out the experiments. The results were analyzed using both the quantitative metric (Sec. 6.4.1) and a questionnaire that reveals a qualitative metric for the approach. We have prepared a set of four experiments combining prediction characteristics and feedback information in order to evaluate the overall performance of each combination:

- Without prediction and without feedback
- With prediction and without feedback
- Without prediction and with feedback
- With prediction and with feedback

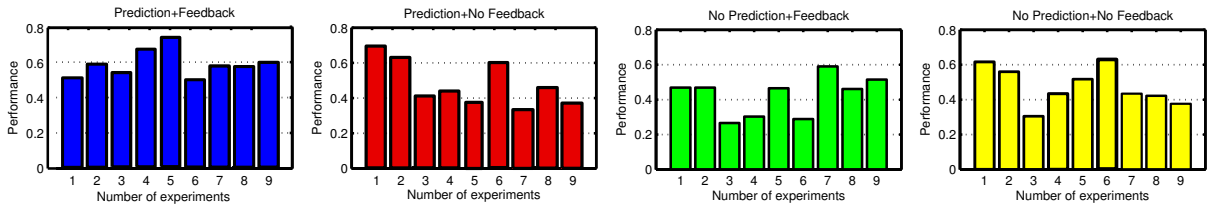

Figure 6.7: **Experiment results.** A bar diagram describing the average performance of each of the real experiments carried out. Each color corresponds to a different experiment setting.

We have kept the feedback in the system to probe if a direct control over the robot navigation parameters enhances the perception of people towards the system, specially for the questionnaires.

The robot was able to achieve its goal (the target's goal) in all conducted experiments. The volunteers were told to naturally walk and the robot accompanied the target using the social-aware companion described in Sec. 6.4. During the validation of the model in real experiments, we set unexpected obstacles and pedestrians in the targets' path, and the robot avoided them successfully.

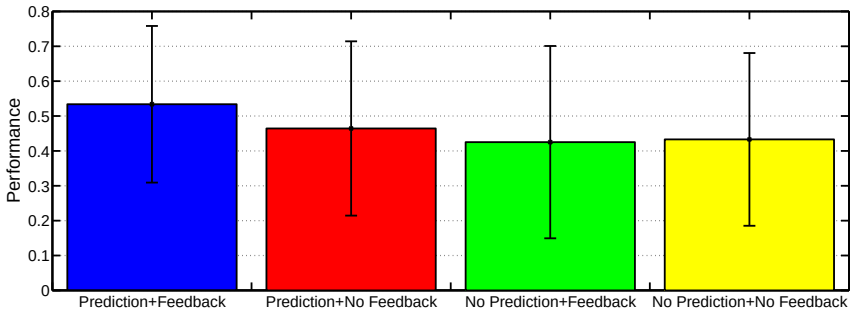

Figure 6.8: **Experiment results.** An average of the performance and its standard deviation for the experiments combination using prediction and feedback.

In Fig. 6.7 is depicted the average outcome of the performance during some experiments. Each group corresponds to a different configuration of the experiment settings. A summary of the overall performance for each setting is depicted in Fig. 6.8. The prediction information approach slightly enhances the robot companion approach. Below it will be discussed again this comparison using the human poll results, and it will be showed clearly the advantages of using prediction information.

During real world experimentation appeared unexpected difficulties that were not present during the simulations. We found severe limitations on the perception system, the laser people detector and tracker. People are not always detected and the data association may be wrong. A more detailed discussion of the perception system is explained in Appendix A.

This new set of experiments, are performed mostly in the BRL, under the interaction of multiple pedestrians and obstacles. Fig. 6.9 depicts examples of different experiments performed with volunteers in different urban environments. Moreover, it is shown several case scenarios where multiple objects and people are in the scene. In Fig. 6.10, an example of a single sequence is depicted, where a robot accompanies a person under the presence of a group of people in the scene.

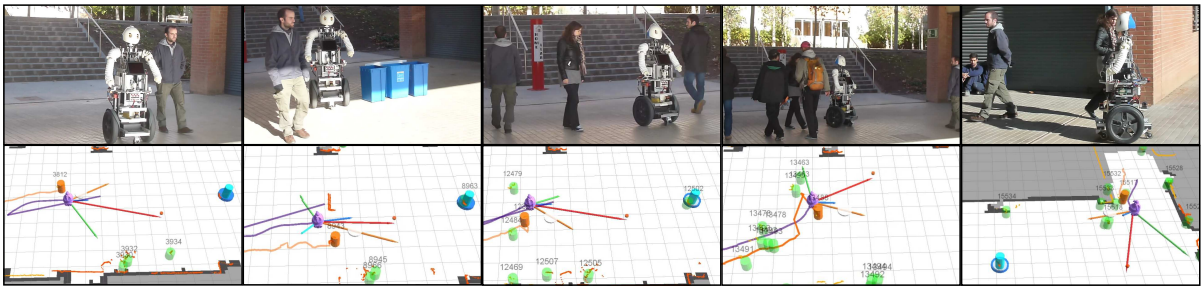

Figure 6.9: **Images of real experiments in the FME.** Some examples of the conducted real experiments. *Top:* Dabo accompanying a person to a desired goal. *Bottom:* The same scene using the system interface.

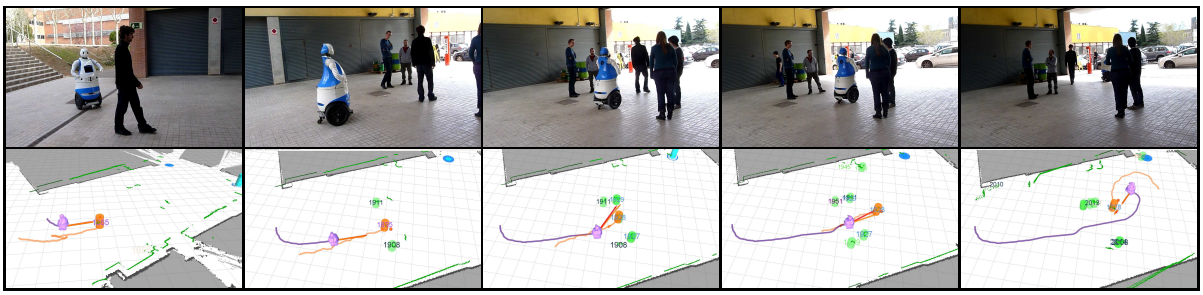

Figure 6.10: **Real-life experiments.** A single robot companion experiment. *Top:* Dabo accompanying a person to a desired goal. *Bottom:* The same scene using the system interface.

6.6.4 Qualitative validation in real scenarios

To further validate the performance of the robot companion task, we have evaluated the results using a poll of questions to the volunteers, as a qualitative and extra validation of the system.

As it has been mentioned previously, 41 real-life experiments with different volunteers have been carried out. Each participant filled out a questionnaire. The measurement was a simple rating on a Likert scale between 1 to 7. For the evaluation score, repeated ANOVA measurements were conducted. In this section, we provide two different results. On the one hand, it is desired to know if the prediction skill increases the perception of robot's abilities on humans. And, on the other hand, it is necessary to study if the use of the remote control enhances the interaction between the robot and a person.

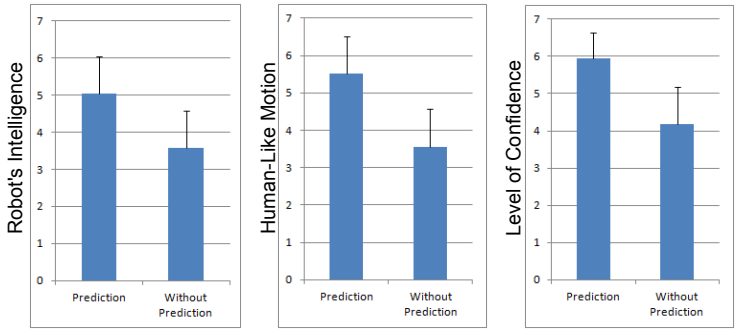

Figure 6.11: **Poll results.** People's perception of the prediction skill. *Left*: Robot's Intelligence. *Center:* Robot's Human-like motion. *Right:* Level of confidence.

Secondly, in order to analyze if the use of the remote control enhances the interaction between the robot and a person, three different scores were examined: "Robot's Intelligence", "Level of interaction" and "Level of confidence", plotted in Fig. 6.12. For robot's intelligence a repeated-measures analysis of variance revealed that no significance was found, $F(1, 44) = 1.88$, $p = 0.18$. For the level of interaction the ANOVA test do not revealed a significant main effect,

$F(1,44) = 0.48$ $p = 0.18$. And, finally, the analysis of variance showed that there is not a remarkable difference in the level of confidence $F(1,44) = 3.57$ $p = 0.07$.

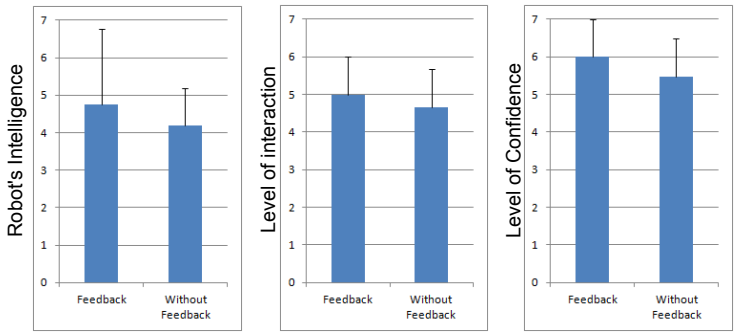

Figure 6.12: **Poll results.** People's perception of the use of the remote control. *Left*: Robot's Intelligence. *Center:* Level of interaction. *Right:* Level of confidence.

Firstly, human perception has been studied in the prediction skill. To analyze the source of the difference, three different scores were examined: "Robot's Intelligence", "Human-Like Motion" and "Level of confidence", plotted in Fig. 6.11. For robot's intelligence a repeated-measures analysis of variance revealed a significant main effect, $F(1,44) = 14.82$, $p < 0.001$. For robot's Human-like motion the ANOVA test revealed a great effect, $F(1,44) = 36.28$ $p < 0.001$. And, finally, the analysis of variance revealed a remarkable difference in the level of confidence $F(1,44) = 61.79$ $p < 0.001$.

As a summary, after analyzing these two components, we may conclude that when the robot has the ability to predict human motions it has the largest acceptance. People perceived the robot to be more intelligent, as it could detect and approach them, and, they felt that it had more social skills. Moreover, the use of the remote control does not enhance the interaction between the robot and a person.

We would like to point the reader to check the videos of the experimental results in the project web `http://www.iri.upc.edu/groups/lrobots/robot_companion/`.

6.7 Summary

We have presented a novel robot companion task based on the Extended Social Force Model. One of the contribution of this work has been the development of a new robot companion system based on the ESFM and human intentionality prediction. A social aware navigation is well suited for a robot companion task, and we have shown to improve its performance if human interactions through the ESFM are taken into account and intentionality prediction information, specially in open spaces.

We have introduced a model of human feedback that is able to obtain the set of weighting pa-

rameters for the robot companion behavior, after a prior calculation in a simulated environment. We believe that human feedback for parameter learning is a key point for the development of robots whose purpose is interacting with people.

Another important contribution is the proposed robot companion metric defined in Sec. 6.4.1. Since the verification of any system in which a human intervenes is hard to evaluate, and thus, we require an analytical metric that can evaluate the behavior of our robot companion approach.

The validation of the model has been demonstrated throughout an extensive set of simulations and real-life experiments in a urban area. In contrast to other existing approaches, our method can handle realistic situations, such as dealing with large environments with obstacles and semi-crowded scenes. For that reason, this work can be applied to certain specific real robot applications, for instance, guiding tourists or accompanying professional visitors. The overall validation of the approach in real scenarios is done by using feedback information directly from the volunteers. Moreover, we can determine that introducing a human intentionality predictor greatly increases the overall human-perceived performance of the system, according to the surveys.

Unfortunately, the robot companion approach is not free of limitations. We suffer the same problems as presented in Sec. 5.6, such as local minima due to the reactive nature of the approach, in addition to perception problems since we must detect and not loose track of the accompanied person in a real environment.

The most important contribution of the present chapter is the integration of intentionality prediction into the robot navigation scheme, which we have shown to clearly enhance the robotic task. We believe that it is a very promising line of research, and in future contributions presented in this thesis, we will focus our efforts into integrating navigation and prediction in a more effective manner.

7

Anticipative kinodynamic planning

This is the last chapter of Part II dedicated to the robot navigation topic. In the following sections are condensed most of the contributions of this thesis. We take fully advantage of the prediction framework presented in Part I and we integrate it into a planning scheme. We additionally make use of our findings in the previous Chapters 5 and 6 regarding the reactive navigation and the robot companion and present a new method that overcomes the limitations of our previous approaches. So in this chapter converge all of our previous contributions in a holistic approach consisting of the topics previously presented in this dissertation.

This chapter introduces the Anticipative Kinodynamic Planning (AKP) approach for robot navigation in semi-crowded urban environments, while satisfying both dynamic and nonholonomic constraints. To this end, we propose to integrate seamlessly a human motion prediction algorithm into the planning algorithm. The AKP generates a set of paths in a kinodynamic RRT fashion and chooses, among a set of candidates, the best path.

We go one step further and present a multi-objective cost function to consider different and independent criteria and a well-posed procedure to build a joint cost function in order to select the best path. Additionally, a *cost-to-go* function is proposed to measure the distance between states, that will be shown to outperform a classical Euclidean distance approach.

We have dramatically sped up the calculations by using a steering heuristic and at the same time, we have introduced a randomness factor to the steering method, to obtain more distinct paths, which is of great importance to the process of finding the best solution. Plenty of simulations and real experiments have been carried out to demonstrate the success of the AKP, compared to other navigation approaches.

This work has been published in the *IEEE/RSJ International Conference on Intelligent Robots and Systems* [Ferrer and Sanfeliu, 2014c] and we are preparing a journal version to be submitted.

7.1 Introduction

It is of the greatest importance that service robots can successfully navigate in typically urban environments, which are dynamic and constrained, and at the same time, people behavior should not be conditioned by the presence and the maneuvering of robots. We have reviewed this topic on previous chapters, however there were limitations on our approach. This chapter is a new iteration of the same issue, where we will propose relevant contributions.

Naturally, robots and people should interact if they share the same environment, as exemplified in Fig. 7.1. This issue becomes the main motivation of the present chapter: we aim to minimize the robot impact towards all those nearby pedestrians, while navigating and executing tasks. Our initial hypothesis is that there exists a trade-off between the robot navigation and its impact to the environment so we have to plan in advance. To this end, we propose an anticipative approach that is able to foresee people's trajectories and their corresponding reactions to each of the planned actions and accordingly act in advance of that information.

Figure 7.1: **Robot navigation.** *Left:* Simulation environment in a $space \times time$, where people are plotted as green cylinders and their predictions are drawn in the z axis, which corresponds to time. The tree of paths calculated by the robot appears in blue and the best path is a red line. *Right*: Example of robot navigation in a urban environment, the BRL. in a simplified visualization of the environment.

In addition, time restrictions are important in social environments: people walk and change their positions during time. A cost-based navigation path is calculated while satisfying both dynamic and nonholonomic constraints, also referred as kinodynamic constraints. Throughout this work, we consider people as dynamical obstacles and define a joint state of the system that takes into account the robot's state and the states for all the pedestrians in the scene.

In this chapter we use the framework for human motion prediction presented in Part I of this thesis, which consists of three concatenated elements: the intentionality predictor, the behavior estimator and finally the trajectory prediction. We analyze human trajectories un-

der the influence of dynamic semi-crowded and heterogeneous environments, where there are moving people, moving objects, robots and also static obstacles. Intuitively, prediction methods are of great importance for a better robot navigation. Unfortunately, most approaches separate planning and prediction and although a joint approach may seem to boost the problem complexity, we will present a simple method to jointly and seamlessly process predictions and planning into the same scheme.

The structure of our proposed algorithm is depicted in Fig. 7.2-*Left*. The white boxes represent well known methods necessary for a navigation scheme, such as a map and a global planner, and they are not presented in this chapter. Our contributions are within the blue boxes and include modifications to the local planner and an adjoint prediction module. Fig. 7.2-*Right* depicts the basic procedure to calculate the robot path:

- Get and track obstacles and people in the scene.
- Calculate a large set of paths by using a modified version of an RRT.
- Choose a set of possible path candidates and then calculate the best path.

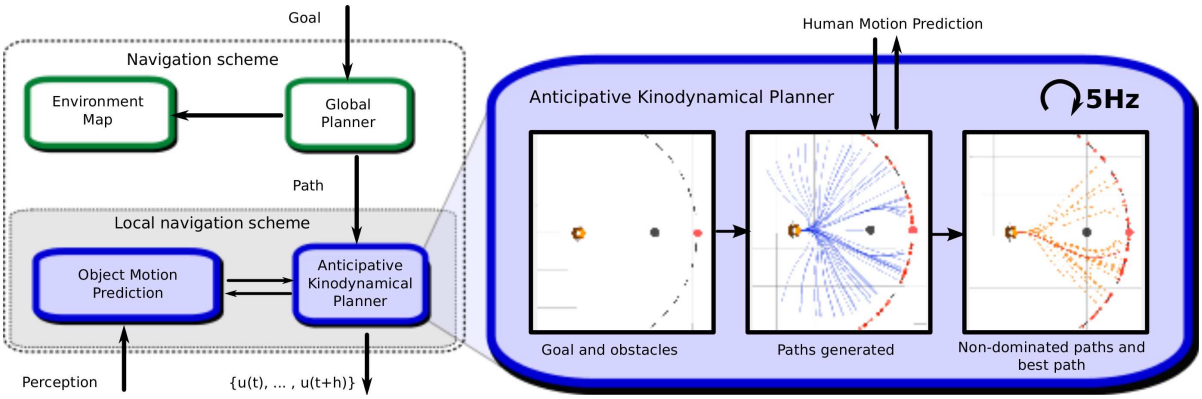

Figure 7.2: **Navigation scheme.** *Left*: Overview of the general AKP navigation scheme. The blue boxes are our contributions. *Right*: scheme of the procedure to calculate the best path.

Accordingly, we present a multi-objective function that considers different and independent objectives, such as the robot's cost, nearby people's cost, distance to goal, etc. Additionally, this technique permits us to correctly handle and compare different objectives into a single and well-posed function. We will discuss later the necessity to find the *non-dominated* set [Deb, 2014] of trajectories before finding the best candidate for the planning, inspired in Multi-Objective Optimization (MOO) techniques.

We propose a *cost-to-go* function, based on the multi-objective costs to calculate distances between states, instead of a Euclidean-based distance. The *cost-to-go* metric greatly enhances the area covered by the set of paths calculated by the planner, as it will be shown.

Our proposed algorithm is able to provide a real time execution thanks to steering methods that relax and simplify the calculations carried out by the planner. Our concern would be if

this technique introduces an important bias in the sampled solution space. This issue will be discussed in deep in the following sections.

7.2 Related work

Dynamic planning can only be understood if there exists a precise motion prediction system. Aimed by this idea, we have presented state of the art techniques in prediction in Chapter 4 and discussed how we have integrated some of them into a planning scheme in Chapter 6.

In this chapter, we apply geometrical based predictors as presented in Chapter 3 that infer human motion intentions and afterwards predict human motion in a continuous space, according to the Extended Social Force Model (ESFM) as presented earlier in Chapter 4.

The ESFM can be defined as a kind of Potential Field (PF), and thus, directly applied to the robot navigation issue as a navigation function. The literature has already extensively studied PF [Khatib, 1986] for navigation algorithms, mostly for static environments, since a couple of decades ago. Despite their advantages, there exist many well known limitations [Koren and Borenstein, 1991], such as local minima or oscillations. Several approaches try to overcome these limitations, such as [Barraquand and Latombe, 1991], by using a randomized walking path when a local minimum is reached.

The dynamic window approach [Fox et al., 1997] and other velocity constrained approaches [Simmons, 1996] permitted to consider obstacles and collisions. Unfortunately, they suffer from local minima as well. Approaches combining a DWA with a global planner like [Brock and Khatib, 1999] solve the problem by introducing a global function. Our approach also relies on a global planner as it can be seen in Fig. 7.2.

During the last decade, sampling-based techniques have become quite popular when solving planning problems. Furthermore, sampling-based methods may take into account kinematic and dynamic constraints such as [LaValle and Kuffner, 2001a,b] and [Hsu et al., 2002], which are very appropriate for dynamic environments, and thus for our approach. In [Stachniss and Burgard, 2002] they obtain a kinodynamic compliant trajectory by decoupling the problem into a search in space and a posterior optimization of the path satisfying the restrictions. Our approach directly plans in the action space, it integrates the search of a path avoiding obstacles as well as provides the inputs required to execute that trajectory considering kinodynamic constraints.

A special case of dynamic environments include robot navigation among humans, and it has been studied intensively by the mobile robotics community during the last years. Works such as [Sisbot et al., 2007] have proposed to model people as a summation of a Potential Field (PF). In [Svenstrup et al., 2010] the authors have used a navigation PF and minimized its cost through people's Potential Fields. Fulgenzi et al. [2009] calculate probabilities of collision and plans

using a set of motion primitives under a limited time horizon, very similar to our approach. A pure *reactive* approach based on the ESFM, a kind of PF, has been proposed in Chapter 5, where we plan socially-aware in human environments.

A joint calculation of people's paths and the robot's path has been proposed in [Trautman and Krause, 2010; Trautman et al., 2013, 2015] using Gaussian processes and a distance-based *interaction potential* between people. This method is able to provide an approximation to an anticipative behavior finding the less occupied robot trajectory, but unlike our approach, we are able to quantify the magnitude of the alterations to nearby pedestrians and plan accordingly.

Finding a cost function to correctly characterize robot navigation among people may become an ill-posed problem, *e.g.* local minima, etc. Jaillet et al. [2010] demonstrate the importance of a correct cost function to solve planning problems. In [Kuderer et al., 2014], the authors have addressed this problem and proposed a set of homotopically distinct trajectories. Sharing this same goal, we tackle this problem by proposing a multi-objective cost function where we optimize different independent criteria, such as the distance to the goal or the cost to navigate for pedestrians. A Multi-Objective Optimization (MOO) method [Marler and Arora, 2004; Deb, 2014] has inspired a solution to the minimization problem that selects the best path, and at the same time, we provide a distance function between states, a *cost-to-go* function, based on multiple cost functions.

Some of the above approaches, ourselves included, have chosen to use sampling-based techniques to solve the planning problem. These popular methods [LaValle and Kuffner, 2001a; Hsu et al., 2002] can take into account kinematic and dynamic constraints, which is of great relevance in dynamic environments. However, the distance function used can change completely the outcome of the planner. Several works [Glassman and Tedrake, 2010; Perez et al., 2012; Kunz and Stilman, 2014] make use of *cost-to-go* functions as a distance function between states. We propose a *cost-to-go* function based on the same multi-objective cost function mentioned above and calculate distances between states for the RRT planning.

We aim to obtain a fast method to deploy robots in real dynamic environments. Some steering heuristics used in state of the art methods consider control approaches [Palmieri and Arras, 2014] or analytical solutions through relaxation of constraints [Kunz and Stilman, 2014]. The objective is the same, reduce the computational cost drastically. Although it may seem appealing, the price to pay may be a shrinking of the search space. We propose a technique to minimize this problem by introducing some randomness into the steering function, as presented below.

7.3 State-space formulation

We consider that both robots and people move in a two-dimensional space which represents the urban environment. Let $\mathcal{X}$ denote the workspace and $\boldsymbol{x} \in \mathcal{X}$ describes the position $\boldsymbol{x} = [x, y]^\top$ in a two dimensional space, for moving objects (including people) and robots. The configuration space $\mathcal{C}_z$ is defined as a configuration $\boldsymbol{q}_z \in \mathcal{C}_z$, where z denotes either people p or robots r.

We define the augmented phase space $\mathcal{S}_z$ for the kinodynamic treatment of the states, that considers the first order derivative plus time: $s_z \in \mathcal{S}_z$ is a state $s_z = [\, \boldsymbol{q}_z, \dot{\boldsymbol{q}}_z, t]^\top$. And $S_z = \{\, \boldsymbol{s}_z\}$ is a set of states $\boldsymbol{s}_z \in \mathcal{S}_z$.

The action $\boldsymbol{u}_z \in \mathcal{U}_z$ modifies the states $\boldsymbol{s}_z$, and is the acceleration calculated by the steering method, the ESFM (Sec. 4.3). Similarly, $U_z = \{\, \boldsymbol{u}_z\}$ is a set of inputs $\boldsymbol{u}_z \in \mathcal{U}_z$. The following differential constraints

$$\dot{\boldsymbol{s}}_z = dc(\, \boldsymbol{s}_z,\ \boldsymbol{u}_z) \tag{7.1}$$

are in general the propagation restrictions depending on z being a robot or a person.

More concretely, we define the person state $\boldsymbol{s}_p = [x, y, v_x, v_y, t]^\top$ as the phase state consisting on position and velocity. The differential constrains that determine the evolution of the system resemble a double integrator, a free moving particle:

$$\dot{\boldsymbol{s}}_p = dc(\, \boldsymbol{s}_p,\ \boldsymbol{u}_p) = \begin{bmatrix} v_x \\ v_y \\ a_x \\ a_y \\ 1 \end{bmatrix}, \tag{7.2}$$

which are expressed in the continuous domain.

In the same manner, the robot state $\boldsymbol{s}_r = [x, y, \theta, v, \omega, t]^\top$ is a unicycle model presenting the following nonholonomic constraints:

$$\dot{\boldsymbol{s}}_r = dc(\, \boldsymbol{s}_r,\ \boldsymbol{u}_r) = \begin{bmatrix} v\cos(\theta) \\ v\sin(\theta) \\ \omega \\ a_v \\ a_\omega \\ 1 \end{bmatrix}. \tag{7.3}$$

7.3.1 Joint state-space

The joint state space $\mathcal{S}$ consists of $\mathcal{S} = \mathcal{S}_r \times \bigcup \mathcal{S}_{p_i}$, which considers the robot phase space $\mathcal{S}_r$ and the union of every person's phase space $\mathcal{S}_p$. Correspondingly, the joint state $\boldsymbol{s} \in \mathcal{S}$ is defined as $\boldsymbol{s} = [\, \boldsymbol{s}_r,\ \boldsymbol{s}_{p_1}, \ldots,\ \boldsymbol{s}_{p_N}]^\top$.

The variable time $t = t(\boldsymbol{s})$ is equal for all the states that $\boldsymbol{s}$ consists of. We will refer to $S = \{\boldsymbol{s}\}$ as a set of states $s \in \mathcal{S}$ and $U = \{\boldsymbol{u}\}$ a set of inputs $\boldsymbol{u} \in \mathcal{U}$.

7.3.2 ESFM applied to the robot

The objective is to treat the robot as a free moving particle in the space, similarly to a person as explained above. Unfortunately, nonholonomic constraints reduce the robotic platform mobility. We need to bridge the gap and provide an adjustment that permits the robot being compatible with the ESFM. The resultant robot force $\boldsymbol{f}_r = \boldsymbol{f}_{r||\theta} + \boldsymbol{f}_{r\perp\theta}$ consists of a component in the direction of translation $\boldsymbol{f}_{r||\theta}$, which directly transforms into a translational acceleration and an orthogonal force $\boldsymbol{f}_{r\perp\theta}$ that does not contribute to the robot translation. In order to solve this, the robot rotation acceleration is computed considering the orthogonal force component in the following way:

$$\tau_r = \boldsymbol{r} \times \boldsymbol{f}_{r\perp\theta} + k_\tau \omega, \tag{7.4}$$

where $\boldsymbol{r}$ is the vector radius of our platform, oriented to θ and k_τ is a damping factor in order to avoid oscillations.

7.4 The Anticipative Kinodynamic Panning

As stated before, our main objective is to navigate in urban environments where dynamic obstacles, such as people, naturally stay. The general scheme of our approach can be seen in Fig. 7.2, where we contextualize the contributions of our work (blue boxes) into the general navigation framework.

We use the ESFM in the planning algorithm, since other methods only solve the Boundary Value Problem to connect a pair of poses and they are not capable of capturing the interacting nature of the environment.

We use the basic mechanics of the kinodynamic RRT [LaValle and Kuffner, 2001a] to extend paths, in order to generate a large set of feasible paths and choose the best path according to multiple minimization criteria.

The following is a list of the most important features from the proposed approach, the AKP:

1. Human motion prediction is integrated into the planning scheme.

Algorithm 4 AKP($\boldsymbol{q}_r^{goal}$, $\boldsymbol{s}_{ini}, t_{horizon}, K$)

```
Initialize T(V, E) ← {}
V ← s_ini
{ q_pi^goal } = PEOPLE_INTENTIONALITY(X(t), D)
for j = 1 to K do
    [ q_r^g, β] = SAMPLE( q_r^goal )
    s_parent = FIND_NEAREST_VERTEX( q_r^g, T, β)
    [U^new, S^new] = EXTEND( s_parent, q_r^g, { q_pi^goal })
    J^new = COST_TO_GO(U^new, S^new, q_r^goal, T)
    if NO_COLLISION(S_new) then
        V ← V ∪ {S^new, J^new}
        E ← E ∪ {U^new}
    end if
end for
return MINIMUM_COST_BRANCH(T)
```

2. The approach is anticipative, in the sense that each action of the robot results in different people's predictions.

3. Steering function to solve the kinodynamic planning in real time.

4. A multi-objective cost function to find the best trajectory among a set of candidates.

5. A *cost-to-go* function to measure the cost to connect a pair of states, instead of a Euclidean distance.

6. Randomness is introduced into the steering method.

We are highly concerned to provide a good representation of the solution space if we want to obtain the "best trajectory" solution. It will be later shown the performance of our contributions, either in simulations as well as in real experiments.

We present the basics of the algorithm to compute the AKP, as depicted in Alg. 4. Four inputs are required: the goal $\boldsymbol{q}_r^{goal}$, the initial state $\boldsymbol{s}_{ini}$, the horizon time $t_{horizon} = t + h$, and the number of vertices K. The $\boldsymbol{q}_r^{goal}$ provides the position and orientation of the final robot configuration. The initial state $\boldsymbol{s}_{ini} \in \mathcal{S}$ contains the information of the robot state plus all the people's states considered on the scene. The horizon time $t_{horizon}$ specifies the temporal window used to forecast the plan and the predictions.

The algorithm builds a tree $\mathcal{T}(\mathcal{V}, \mathcal{E})$ and returns the minimum cost branch. The edges $\mathcal{E}$ are the control inputs $\boldsymbol{u} \in \mathcal{U}$, the vertices $\mathcal{V}$ consist of the joint state $\boldsymbol{s} \in \mathcal{S}$ and the accumulated multivariable cost $\boldsymbol{J}$ to reach that vertex (see Sec. 7.5).

The general algorithm scheme is shown in Alg. 4, which is quite similar to the original RRT, although we have added some modifications, that are described in the following subsections.

7.4.1 Horizon time

The horizon time parameter sets the amount of time that the planner forecasts in order to obtain a path similar to a model predictive control (MPC). Although the inputs $\{\, \boldsymbol{u}_r(t),\ \boldsymbol{u}_r(t+\Delta t), \ldots,\ \boldsymbol{u}_r(t+h)\}$ are calculated, only the first input command is executed and a new set of inputs is calculated in the next iteration.

7.4.2 Sampling

The horizon time bounds the region of exploration $\mathcal{C}_r$ to a circle radius equal to $h \cdot v_{max}$ as depicted in Fig. 7.3. Since there is a strong time restriction, $\boldsymbol{q}_r^g$ is sampled using a Gaussian distribution, over the boundary of $\mathcal{C}_r$ to ensure that the paths generated indeed expand $\mathcal{T}$. If the density of nearby obstacles on the scene is high, the $\boldsymbol{q}_r^g$ sampling distribution is widespread.

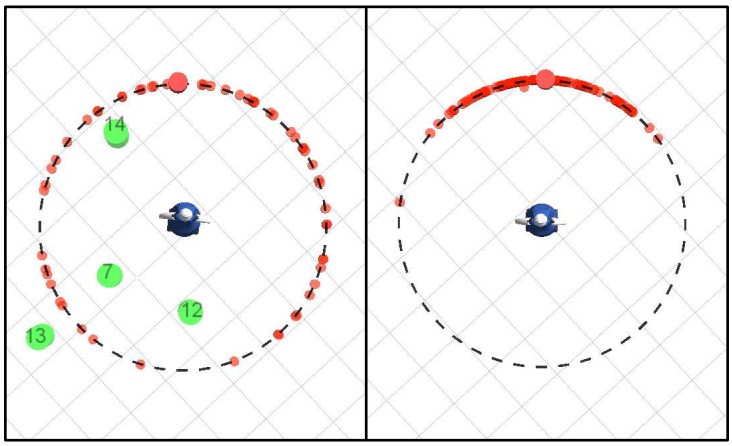

Figure 7.3: **Distribution of random goals $\boldsymbol{q}_r^g$.** On the *Right* there are no people in $\mathcal{C}_R$ and the search is concentrated on the goal direction. On the *Left* the density of nearby people on the scene is higher, and thus, the $\boldsymbol{q}_r^g$ sampling distribution is widespread.

7.4.3 RRT extend: ESFM steering heuristic

As explained before, the prediction algorithm used by our approach is based on the ESFM. We additionally make use of this model in order to build a steering heuristic that permits us to connect a pair of poses $\boldsymbol{q}_{ini}$ and $\boldsymbol{q}_f$, in a computationally fast manner. In the context of this work we define "steering" as a method to relax the connection of two states in a computationally fast manner. Typically, it is needed to solve the Boundary Value Problem (BVP) to connect a new state $\boldsymbol{s}_{new}$ with a state $\boldsymbol{s}_k$ belonging to the tree $\mathcal{T}$. The "steering" method provides a simplification to the problem of finding the set of inputs U that connect both states $U =$ BVP$(\, \boldsymbol{s}_k,\ \boldsymbol{s}_{new})$.

We calculate the resultant robot force $\boldsymbol{f}_r$ using (4.3), which takes into account its environment $[\, \boldsymbol{s}_{p_1}, \ldots,\ \boldsymbol{s}_{p_N}]$, while at the same time tries to reach the given random goal $\boldsymbol{q}_r^g$, that

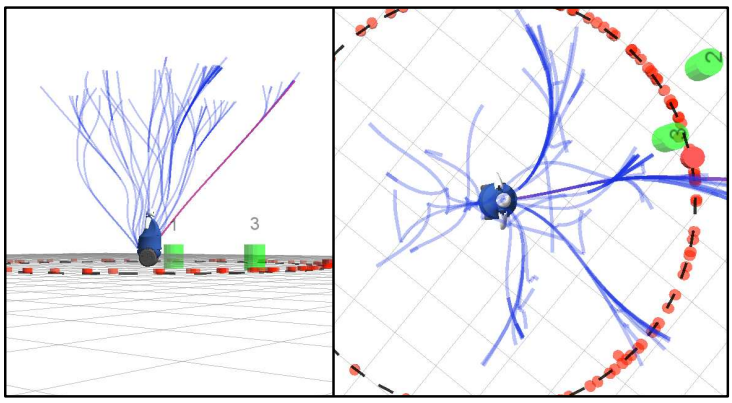

Figure 7.4: **Set of trajectories generated.** Representation of the set of trajectories included in $\mathcal{T}$ drawn in the space $\mathcal{X} \times time$. On the *left*, the z axis represents time. On the *right* projection of $\mathcal{T}$ in $\mathcal{X}$.

represents its inner intentionality $\mathcal{D}_r$. In Fig. 7.4 is depicted an example of depth propagation, where each path tries to reach its corresponding random goal.

Since the action space is limited to $\mathcal{U}_r$ and we cannot control the environment, that is, we cannot send commands to nearby people. Nonetheless, we can infer those pedestrians's intentions in order to calculate their expected motion commands. As proposed in Chapter 3, we calculate the most expectable $\boldsymbol{q}_{p_i}^{goal}$ for every person on the scene (line 3 in Alg. 4).

The EXTEND function is depicted in Alg. 5, where it firstly propagates the robot state $\boldsymbol{s}_r(\boldsymbol{s}_{parent})$ accordingly to $\boldsymbol{u}_r^{new}$ and integrates the differential equation (7.3) by using a numerical integration method. Then, for every person on the scene, and if the person has not reached its inferred goal $\boldsymbol{q}_{p_i}^{goal}$ (line 5 in Alg. 5), an action $\boldsymbol{u}_{p_i}^{new}$ is calculated depending on the rest of the dynamic obstacles on the scene and the new robot state $\boldsymbol{s}_r^{new}$ (line 6 in Alg. 5).

Algorithm 5 EXTEND$(\boldsymbol{s}_{parent}, \boldsymbol{q}_r^g, \{\boldsymbol{q}_{p_i}^{goal}\}, \boldsymbol{\beta})$

1: **while** $t(\boldsymbol{s}_{parent}) < t_{horizon}$ & $\boldsymbol{s}_r(\boldsymbol{s}_{parent}) \notin \boldsymbol{q}_r^g$ **do**
2: $\quad \boldsymbol{u}_r^{new} = \boldsymbol{f}_r(\boldsymbol{s}_{parent}, \boldsymbol{q}_r^g)/m_r$
3: $\quad \boldsymbol{s}_r^{new} = \boldsymbol{s}_r(\boldsymbol{s}_{parent}) + \int_{\Delta t} \dot{\boldsymbol{s}}_r$
4: $\quad$ **for** $i = 1, \ldots, N$ **do**
5: $\quad\quad$ **if** $\boldsymbol{s}_{p_i}(\boldsymbol{s}_{parent}) \notin \boldsymbol{q}_{p_i}^{goal}$ **then**
6: $\quad\quad\quad \boldsymbol{u}_{p_i}^{new} = \boldsymbol{f}(\boldsymbol{q}_{p_i}^{goal}, \boldsymbol{s}_{parent}, \boldsymbol{s}_r^{new})/m_i$
7: $\quad\quad\quad \boldsymbol{s}_{p_i}^{new} = \boldsymbol{s}_{p_i}(\boldsymbol{s}_{parent}) + \int_{\Delta t} \dot{\boldsymbol{s}}_{p_i}$
8: $\quad\quad$ **end if**
9: $\quad$ **end for**
10: $\quad \boldsymbol{s}_{parent} = [\boldsymbol{s}_r^{new}, \boldsymbol{s}_{p_1}^{new}, \ldots, \boldsymbol{s}_{p_N}^{new}]$
11: $\quad S^{new} \leftarrow S^{new} \cup \boldsymbol{s}_{parent}$
12: $\quad U^{new} \leftarrow U^{new} \cup [\boldsymbol{u}_r^{new}, \boldsymbol{u}_{p_1}^{new}, \ldots, \boldsymbol{u}_{p_N}^{new}]$
13: **end while**
14: **return** $[S^{new}, U^{new}]$

The EXTEND function calculates consecutively for each instant of time the propagation for all the people and propagates the state of the system until $t_{horizon}$ is reached or the robot has reached the random goal $\boldsymbol{q}_r^g$. The EXTEND function closely resembles Alg. 2, but introducing the calculation of the new robot state $\boldsymbol{s}_r^{new}$, in which the computed planning action U^{new} is seamlessly integrated with the prediction algorithm in an anticipative approach.

By doing so, our approach shows anticipative traits since the robot tends to plan in advance and modify predictions accordingly, rather than reacting to events. The cost for being anticipative is a more intensive processing, since we must propagate the state of the robot and the considered moving obstacles accordingly to the robot propagation.

As explained in previous sections, steering methods present excellent characteristics to drastically reduce the computational cost of kinodynamic planners, both in the EXTEND function as well as the COST-TO-GO. However, there is an important drawback for such methods: the set of trajectories that can be obtained is highly dependent on the environment configuration, and thus, we may be biasing the search space into only a subset of it.

Since we need a set of paths that cover as much of the solution space as possible, the sampling of $\boldsymbol{q}_r^g$ expands the paths in many different directions, and additionally, we propose to introduce randomness into the steering function, in order to obtain more diverse solution paths.

Normal pedestrians behaviors while walking can be classified into three different classes: {*Aware,Unaware,Balanced*}, as introduced in Chapter 4. We aim to introduce some randomness in the generation of robot trajectories by attributing random behaviors to the robot when trying to reach a destination $\boldsymbol{q}_r^g$. The resultant force

$$\boldsymbol{f}_r(t) = \beta_1 \boldsymbol{f}_r^{goal}(t) + \beta_2 \boldsymbol{f}_{people}^{int}(t) + \beta_3 \boldsymbol{f}_{obstacles}^{int}(t) \tag{7.5}$$

determines the generated trajectory, being $\boldsymbol{\beta} = [\beta_1, \beta_2, \beta_3]$ a set of values associated to each behavior $\boldsymbol{\beta} \sim \{\boldsymbol{\beta}_{aw}, \boldsymbol{\beta}_{un}, \boldsymbol{\beta}_{bal}\}$, which is a discrete uniform sampling among the three behaviors as part of the sample function in Alg. 4, line 5. Sampling $\boldsymbol{\beta}$ will enrich the generation of paths to be evaluated by the planner.

7.4.4 Cost functions and *cost-to-go*

We have defined in previous chapters a *social work* function (5.8) to measure the impact of the robot navigation into the environment. However, this function presented limitations as explained before, and those limitations have motivated us to further consider other options. As stated before, we aim to obtain a navigation algorithm that considers different cost functions. In this subsection, these costs functions are defined. The cost J_d to reach a goal $\boldsymbol{q}_r^{goal}$ is defined

as

$$J_d(S,\ \boldsymbol{q}_r^{goal}) = \sum_{t=t_{ini}}^{t_{end}} \| \boldsymbol{x}_r(t) - \boldsymbol{x}_r^{goal} \|^2, \tag{7.6}$$

where we obtain the accumulated square distance value from the initial state at time t_{ini} in the set of states S, to the final state at time t_{end}.

The cost orientation J_{or} expresses the difference between the desired orientation and the current orientation

$$J_{or}(S,\ \boldsymbol{q}_r^{goal}) = \sum_{t=t_{ini}}^{t_{end}} \|\theta_r(t) - \theta_r^{goal}\|^2, \tag{7.7}$$

representing the accumulated distance to the desired goal orientation θ_r^{goal}.

We additionally measure the cost associated to the robot control J_r in the following way

$$J_r(U) = \sum_{t=t_{ini}}^{t_{end}} \| \boldsymbol{u}_r(t)\|^2, \tag{7.8}$$

that sums the robot inputs $\boldsymbol{u}_r$ throughout the calculated trajectory.

Similarly, we define the cost function for the pedestrians J_p as

$$J_p(U) = \sum_{t=t_{ini}}^{t_{end}} \sum_{i=1}^{N} \| \boldsymbol{u}_{p_i}(t)\|^2, \tag{7.9}$$

where the inputs due to the robot influence to other pedestrians $\boldsymbol{u}_{p_i}$ is summed over time for each person when naturally walking towards their goals, according to the ESFM.

We also take into account the cost produced by nearby obstacles to the robot J_o as

$$J_o(U) = \sum_{t=t_{ini}}^{t_{end}} \sum_{i=1}^{O} \| \boldsymbol{u}_{o_i}(t)\|^2, \tag{7.10}$$

where again we consider the perturbation occasioned to the robot due to nearby obstacles $\boldsymbol{u}_{o_i}$, since we want to avoid collisions. It will be explained below how to combine these different metrics in order to obtain the best path and the minimum distance between vertices.

We have defined different cost functions, and thus a multi-objective problem, that can also be used to evaluate the *cost-to-go* from a state to another state.

Euclidean distance is a good metric in a geometrical planning problem, nevertheless, it has proven to be inefficient in certain planning schemes and *cost-to-go* functions work better in kinodynamic planning, as we will demonstrate later.

Many works [Glassman and Tedrake, 2010; Perez et al., 2012; Kunz and Stilman, 2014] calculate the *cost-to-go* in the absence of obstacles. In our case, we consider dynamic obstacles and include these interactions, thanks to the ESFM. In Fig. 7.5 is drawn the process to calculate

the nearest vertex in the search tree. We extend a virtual path towards the goal $\boldsymbol{q}_{new}$ from each of the vertices, and calculate the accumulated cost to reach it plus the previous costs.

We will discuss in Sec. 7.6 the coverage of the solution space explored using a *cost-to-go* function to find the nearest vertex and compare it to a Euclidean approach.

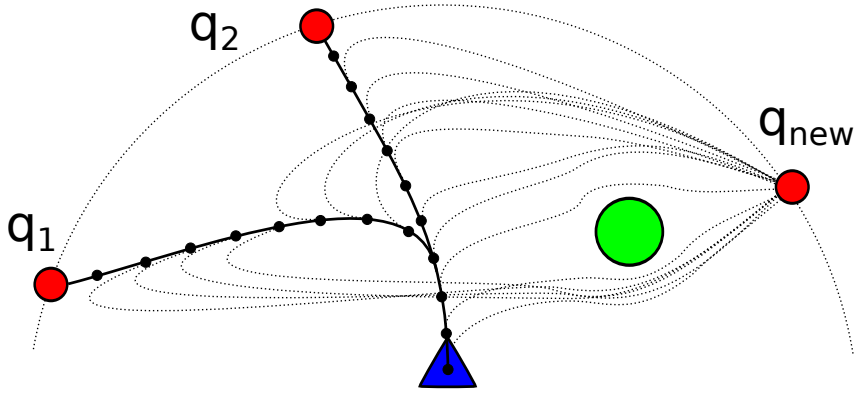

Figure 7.5: **Scheme of the *cost-to-go* function.** Set of trajectories to reach $\boldsymbol{q}_{new}$ from each of the vertices in the tree.

7.5 Multi-objective optimization

Commonly, cost functions are built after a scalarization of different variables, expressed in a function like $J = c_1 \cdot J_1 + c_2 \cdot J_2 + \ldots + c_I \cdot J_I$. Each of the J_i may be expressed in different units, and they are projected into the real space $J : \mathbb{R}^I \rightarrow \mathbb{R}$. Our initial work [Ferrer and Sanfeliu, 2014c] followed a similar approach; at the end, it becomes a problem of tunning weight parameters and this solution is only valid in a limited number of situations.

There are multiple objectives to be minimized in dynamic planning expressed as a vector function consisting of I components

$$\boldsymbol{J}(S,\ \boldsymbol{q}_r^{goal}, U) = [J_d, J_{or}, J_r, J_p, J_o], \tag{7.11}$$

in our case $I = 5$, and we should use different and independent criteria instead of a single-objective composed of different variables. In our problem, these functions are described in (7.6)-(7.10).

To this end, inspired by a multi-objective optimization technique, we solve the problem of finding a set of optimal solutions. The weighted-sum method is a popular and simple approach, although it also presents limitations. We propose to avoid the scaling effect by normalizing the objective functions according to:

$$\bar{J}_i(X) = erf\left(\frac{x - \mu_x}{\sigma_x}\right). \tag{7.12}$$

The variables μ_x, σ_x are estimated after the tree $\mathcal{T}$ is built. The multi-objective cost function becomes a single-objective by applying a three step calculation: first, the individual costs for each criteria to be considered $\boldsymbol{J} : \mathcal{S} \times \mathcal{U} \rightarrow \mathbb{R}^I$. Second, a normalization to $(-1, 1)$ for each of the costs (7.12), and finally, a projection via a weighted sum $J : \mathbb{R}^I \rightarrow \mathbb{R}$ as follows

$$J(S,\ \boldsymbol{q}_r^{goal}, U) = \sum_i w_i \bar{J}_i(S,\ \boldsymbol{q}_r^{goal}, U). \tag{7.13}$$

At the end, we have obtained a cost $J \in \mathbb{R}$, but after a normalization and a projection that guarantee a more convenient construction of the joint cost function since the results obtained by this approach are slightly different than a direct scalarization. We will demonstrate in Sec. 7.6.1 that the $\boldsymbol{w} = [w_d, w_{or}, w_r, w_p, w_o]$ parameters are valid for a large number of different scenarios, which is one of our initial motivations.

7.5.1 Identifying the non-dominated set

Our algorithm is inspired in a multi-objective approach in order to calculate the best trajectory among the paths calculated during the planning step. Prior to provide a solution, we seek to obtain the set of *non-dominated* solutions depending on the different cost functions J_i defined in Sec. 7.4.4.

In general, a solution x_1 is said to dominate other solution x_2 if both of the following conditions are true:

1. $J_i(x_1) \leq J_i(x_2), \quad \forall i \in I$
2. $J_i(x_1) < J_i(x_2)$ for at least one $i \in I$

If both conditions are asserted, then x_1 dominates x_2 and we formulate it mathematically $x_1 \preceq x_2$. In Alg. 6 is explained the procedure to iteratively compare pairs of trajectory solutions $traj_i$ and increase or decrease the *non-dominated* set.

If we obtain the set of *non-dominated* solutions, then any pair of solutions do not dominate each other. Ideally, if we could calculate all the solutions in the solution space, then the *non-dominated* set would be *Pareto-optimal set* [Deb, 2014]. No solution of this set is by itself better than other, we have only discarded those solutions that are dominated.

In Fig. 7.6 is depicted the Pareto front obtained during the AKP simulations trying to minimize only two costs, people and distance. Minimizing both functions entails that the Pareto front is located in the lower-left part of the figure, represented by red circles. We have not calculated the complete front, since it is a curve, but this image gives us an idea of the shape of optimal solutions. Once calculated the Pareto front, the multi-objective optimization (MOO) is solved and we can obtain information of the solutions for this problem.

Algorithm 6 Identifying the non-dominated set

1: $P' \leftarrow \{\}$
2: **for** $i = 1$ to K **do**
3: **for** $j = 1$ to elements_in(P') **do**
4: **if** $traj_i \preceq traj_j$ **then**
5: $P' = P' \setminus \{traj_j\}$
6: **end if**
7: **if** $traj_j \preceq traj_i$ **then**
8: go_to_line 2
9: **end if**
10: **end for**
11: $P' = P' \bigcup \{traj_i\}$
12: **end for**

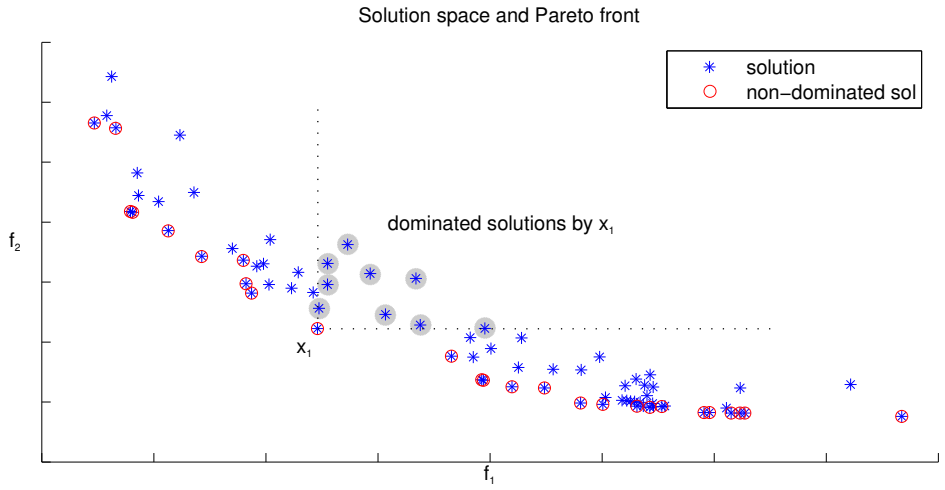

Figure 7.6: **Pareto front.** In blue the solutions calculated by the AKP for two cost functions. Example of the non-dominated solution x_1, inscribed in a red circle, dominates the set of solutions shaded in gray.

Obtaining a set of *non-dominated* solutions is of great importance [Marler and Arora, 2004; Deb, 2014], since the algorithm uses this information to choose a better solution. The selection of the *non-dominated* is done before any scalarization or normalization and this fact is useful specially when dealing with non-convex sets of solutions since it allows us to discard local-optimal solutions in front of global ones, before reprojecting into $J \in \mathbb{R}$.

7.6 Simulations

We will follow the same methodology presented in Chapters 5 and 6 where we have pointed out the importance of a previous testing in the simulated environment. It is of the greatest utility to validate the AKP algorithm in a simulated environment before any interaction with people takes place.

We combine a different number of obstacles and pedestrians walking in the area and under this dynamic environment, we send a goal query to the robot.

In this section we will discuss, by using different simulated scenarios, some of the most relevant topics regarding the AKP, such as the initial learning of the weighting parameters $\boldsymbol{w}$, the importance of a correct *cost-to-go* function compared to a Euclidean metric, and finally the multi-objective optimization performance with respect to a reactive approach.

7.6.1 Parameters learning

In order to correctly characterize the effect of the $\boldsymbol{w} = [w_d, w_{or}, w_r, w_p, w_o]$ parameters, we have used a Monte Carlo approach to sample the weights of the normalized costs, carrying out more than 20k simulations. We have used many different scenarios which consist of a variable number of people and obstacles, and we have calculated the costs associated to the sampled $\boldsymbol{w}$ parameters for each configuration.

The results of the simulations have been averaged in order to address the fact that the scenario is dynamic and the outcome for the same set of parameters can be different depending on the initial conditions, those are, the position of the simulated pedestrians and their corresponding destinations.

In Fig. 7.7 is depicted the expectation for two costs results (distance and obstacles) depending on the same parameter w_{obs}. As it can be seen, there is not a clear value for the weight cost that can minimize simultaneously for the obstacle and people costs. In addition, there is a high variance in the results, since we are testing a highly dynamic environment.

For these reasons, we have used a heuristic method to select which are the most convenient values of $\boldsymbol{w}$. Each of the costs considered in this work is drawn as a function of a weight parameter, in the case of Fig. 7.7, the parameter is w_{obs}. Then, we describe an *acceptable* region starting at 80% of the maximum cost value to the 20% of the minimum value. The intersection,

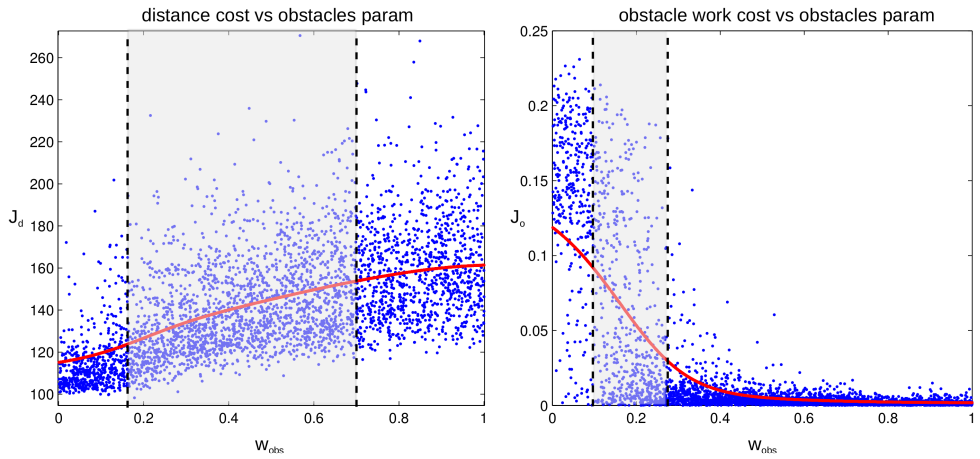

Figure 7.7: **Learning simulation results.** On the *Left* distance cost and on the *Right* obstacle cost w.r.t. the w_{obs} weight parameter. Blue dots correspond to single experiments and the red line is the calculated expectation using a Gaussian likelihood. In both graphics appear the interval of the *acceptable* region, intersection around $w_{obs} = 0.2$.

if possible, of the different regions leads to an approximate value for the parameter, after some adjusting by try and error.

The parameters used throughout the remaining of the work are $w_{distance} = 0.7$, $w_{orientation} = 0.4$, $w_{robot} = 0.5$, $w_{ppl} = 0.3$ and $w_{obs} = 0.2$.

In Fig. 7.8 we can observe the distribution of the cost parameters, prior to normalization, and the corresponding normalization function. The magnitudes of the variables are too different, and any attempt to scale them and sum (former approach) represents a real challenge, if not an ill-posed problem.

We have observed an interesting feature after comparing the graphical results for the cost functions in different scenarios: the expectation curves obtained are very similar for the same cost in different scenarios, *e.g.* one person, two people and two obstacles, etc. In other words, they are not dependent on the number of interacting obstacles or people, when there is a reduced number of obstacles. Accordingly, we choose the same set of parameters $\boldsymbol{w}$ for all the navigation situations, and thus, we can make use of the same weigh values in all situations for future experiments and simulations.

7.6.2 Coverage of the solution space

In this subsection we measure the coverage of the workspace that the planner is able to reach. Ideally, the RRT is probabilistic complete, however, this statement may not hold when considering kinodynamic constraints. In Fig. 7.9-*Left* is depicted two of the scenarios chosen, among many, to illustrate the problem. On the *Top*, there is an obstacle free scenario and on the *Bottom* an scenario with some obstacles. The tree generated by a Euclidean function, as formulated

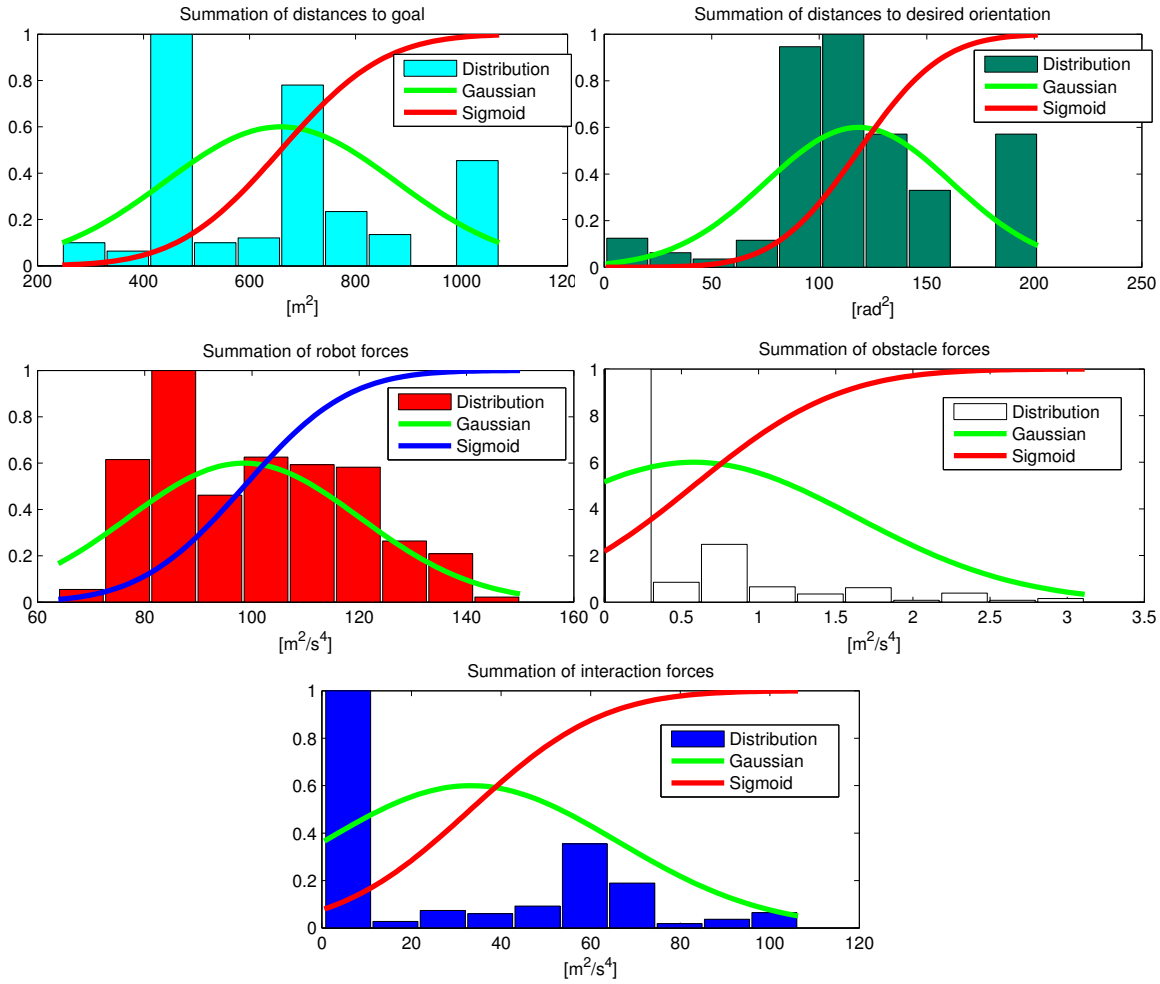

Figure 7.8: **Distributions of the cost parameters J_i.** For each cost J_i is depicted the histogram of their raw values, and superposed, the estimated Gaussian distribution and the sigmoid *erf* function that adaptively normalizes the different cost values into $(-1, 1)$.

in [Ferrer and Sanfeliu, 2014c], can be seen in Fig. 7.9-*Right* and the tree generated by the *cost-to-go* metric and randomness in the ESFM is depicted in Fig. 7.9-*center*.

The area in red corresponds to an average of visited regions and the blue area corresponds to non visited. It is not possible to generate paths that can cover all the solution space since there is a strong time restriction $t_{horizon} = 5s$. We observe that there is no difference in the obstacle free scenario. Both approaches visit a similar area. However, in the scenario with some obstacles, there is a great difference: the Euclidean approach presents more difficulties to scape the obstacle area. The *cost-to-go* and the randomness to the resultant force make possible to explore a wider region of the solution space.

These qualitative measures need to be quantified. To this end, we have run another experiment that measures the area visited in the obstacle scenario, while growing the number of vertices in the AKP.

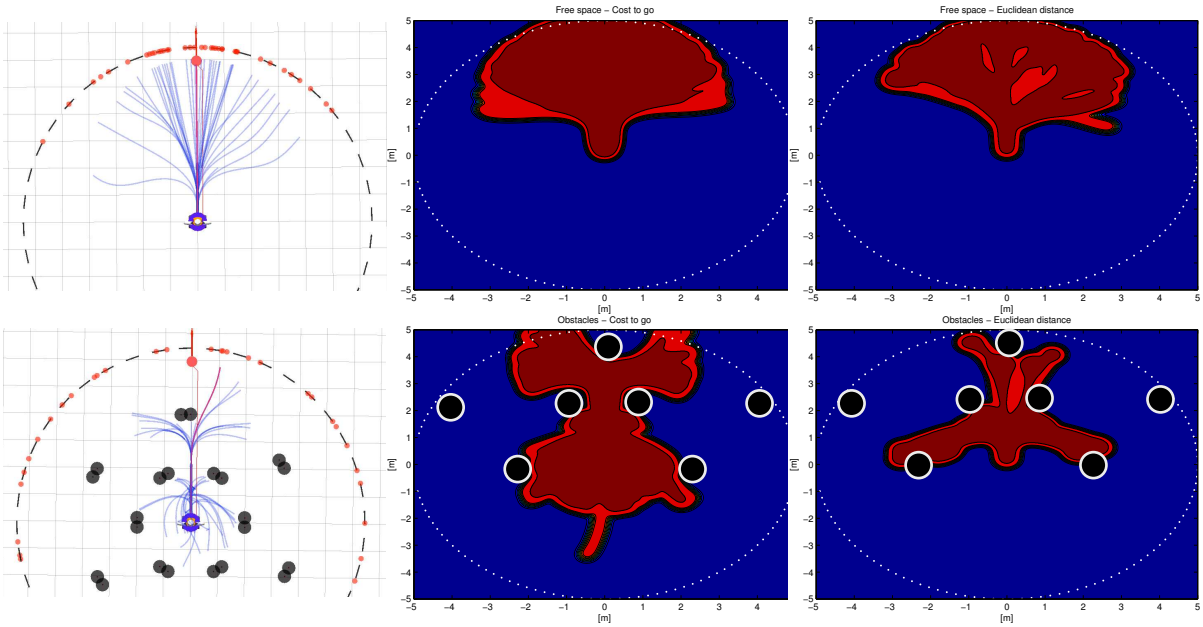

Figure 7.9: **Coverage of the workspace.** According to the *cost-to-go* and randomness in the ESFM and the Euclidean metric for the same number of vertices and obstacles. In red, typically visited areas averaged over a large number of iterations, and in blue, typically non visited regions. The gradient between red and blue represents rarely explored regions by the AKP. On the *Left*, the simulated scene and the configuration of obstacles, some of them are plotted in the coverage figure as black circles.

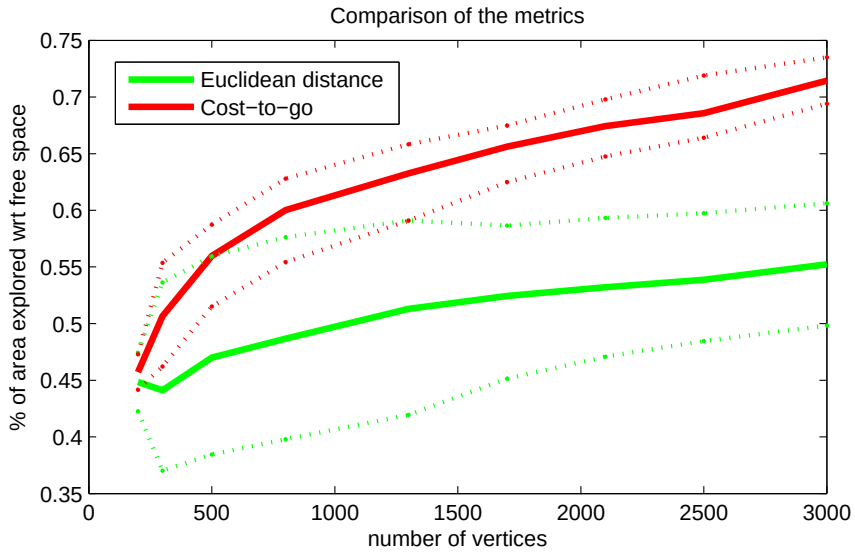

Figure 7.10: **Coverage of the workspace.** The results are drawn with respect to the number of vertices used in the scenario with obstacles. Results normalized to the coverage of a free obstacle scenario. The standard deviations of the results are also plotted as dotted lines.

The results are depicted in Fig. 7.10. Clearly, the *cost-to-go* and randomness approach outperforms the Euclidean distance, at least under this configuration. The computation overhead generated by using the *cost-to-go* metric to find the nearest vertex compensates when considering that to obtain the same area covered by the Euclidean approach, we require multiple times the number of vertices used.

7.6.3 Performance

We have conducted a large number of simulations in different environments as described above: with multiple obstacles, multiple people, very near obstacles while navigating with people, etc. We want to provide a challenging testing for diverse environments.

To illustrate this idea, we have performed more than $5k$ experiments per method, comparing our approach, the AKP using the *cost-to-go* distance, with the AKP using Euclidean metrics and a third approach: the pure reactive planning presented in Chapter 5. We have set the number of vertices to $K = 800$ for both AKP approaches, and the planner was able to provide a path at a rate not lower than 5Hz.

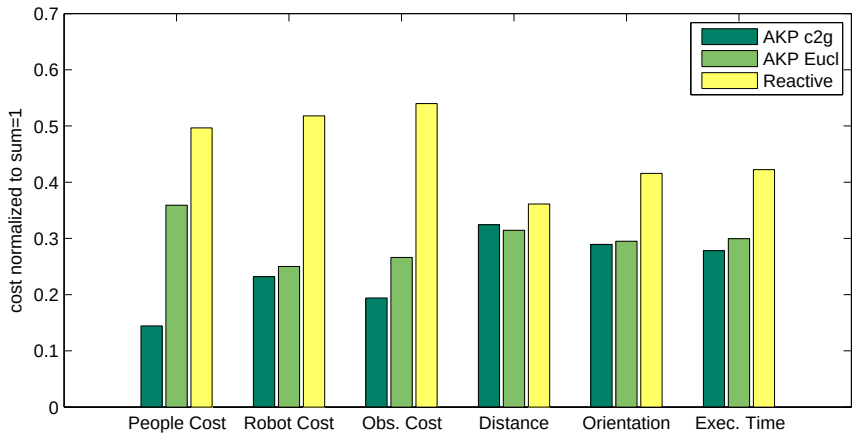

Figure 7.11: **Simulation results: a comparison.** Different cost functions J_i for the AKP using *cost-to-go* function, compared with the AKP with Euclidean metrics and a pure reactive approach. All the results have been normalized to sum 1 for visualization reasons.

All the objective cost functions are plotted in Fig. 7.11, averaged for the different scenarios analyzed, which are presented jointly. Both of our approaches clearly outperform in all objectives the reactive approach, which has demonstrated to behave badly in dynamic environments, since we often observed a *go-stop-go* strategy.

Both AKP behave similarly in simple scenarios, however the AKP with Euclidean metric presents a more "straight behavior" towards its goal, specially in complicated environments (lots of obstacles). Under this circumstances is where the AKP with *cost-to-go* really shines. The AKP is able to explore more solutions and to provide more candidates that result in a better choice

for the best trajectory. Observing these results we can conclude that our algorithm performs successfully in many situations with the same set of parameters $\boldsymbol{w}$.

7.7 Experiments

In the second part of the testing, the real experimentation, we have evaluated the AKP in real scenarios with volunteers and normal pedestrians, as we believe that social robot navigation should be largely tested in real situations, since all the simulations have limitations. The two environments used for the experimentation are a controlled environment consisting of a limited number of obstacles and people and a real environment were no instructions are given to pedestrians.

The Tibi&Dabo robots, as presented in Sec. 2.1, are a two-wheeled robotic platform built on the Segway RMP200 platform, which are very agile and suitable for a dynamic navigation. To perceive the environment they are equipped with two Hokuyo UTM-30LX 2D laser range sensors used to detect obstacles and people, giving scans over a local horizontal plane at 40cm above the ground, facing forward and backward. We use range information to navigate as well as to generate people's detections needed for the AKP.

7.7.1 Comparison in a controlled environment

Using the Tibi platform, we have conducted 52 experiments in a controlled environment, the *Facultat de Matemàtiques* (FME), which consists of an open space surrounded by some walls. The volunteers were told to walk towards a destinations in the scene, while simultaneously the robot performed a *go-to* query that entailed an interaction with the pedestrian. The idea behind these scenarios is to provide an isolated and unconditioned interaction between a person and the robot, and thus, analyze the corresponding results which are guaranteed to eliminate other disturbances.

We have tested three different scenarios: on the Fig. 7.12-*Top* is depicted the first scenario, where the volunteer, in green, is told to walk towards a destination in a straight line, while the robot approaches the person from behind, just in time to intersect with the volunteer path. Two additional configurations are evaluated, a side-frontal interaction, see Fig. 7.12-*Center*, and a completely frontal interaction in Fig. 7.12-*Bottom*.

In order to compare the AKP method with other navigation methods, we have carried out the same setting of experiments for two additional methods. The first one is the *Reactive* approach that we introduced in Chapter 5 and we compared to the AKP in the simulations section. This method makes use of the social force (ESFM) but is not able to plan in advance, which will be demonstrated later to be a great disadvantage in challenging scene configurations. The second one is the Dynamic Window Approach [Fox et al., 1997] implemented in the ROS navigation

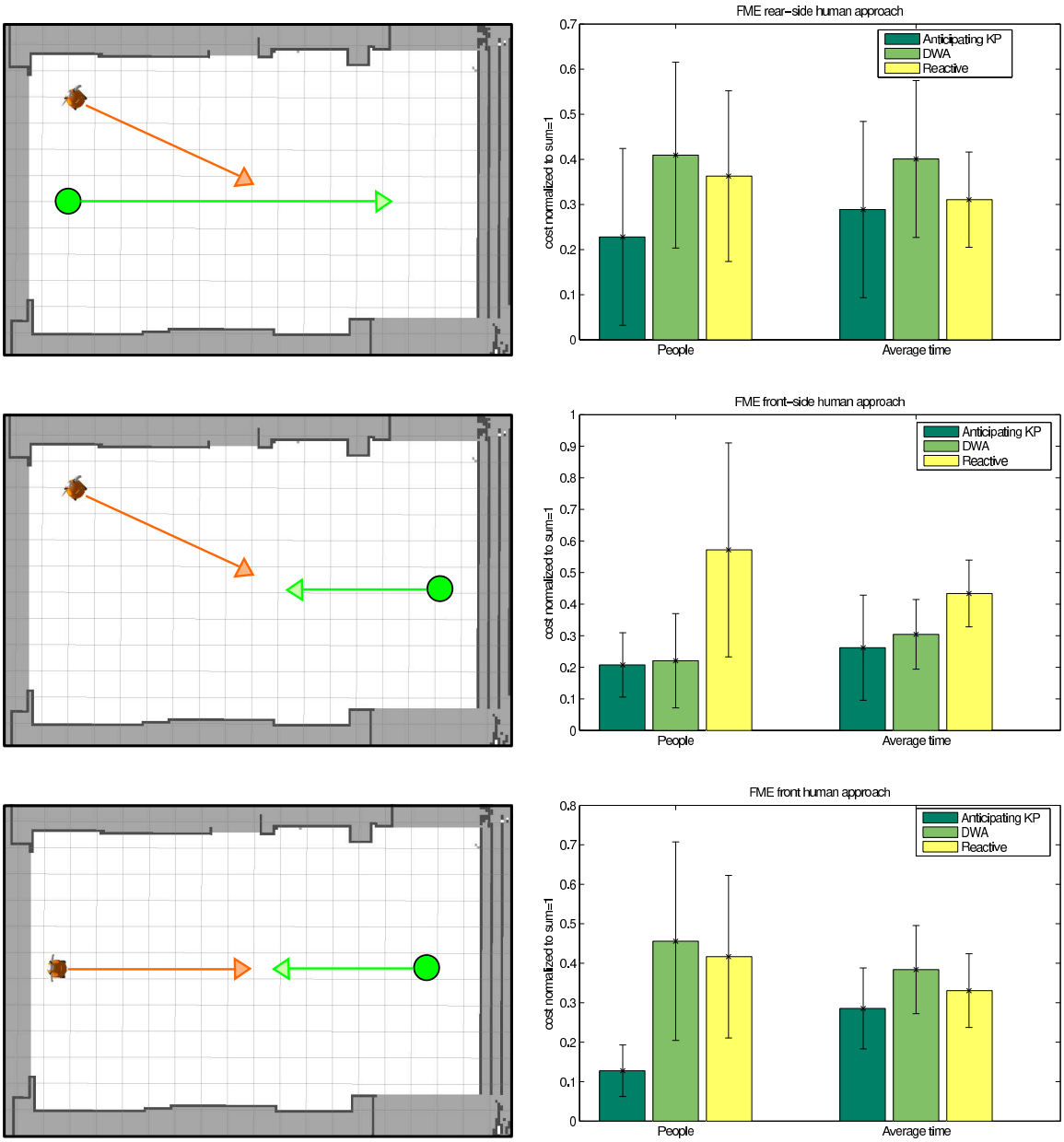

Figure 7.12: **Navigation results for different scenarios in the FME environment.** On the *Right* column is depicted the bar diagram for the people's cost and the average time of execution. Their corresponding standard deviation is drawn on each bar of the diagram. On the *Left* column appears the configuration for each of the experiments.

stack. We have configured it to consider as local obstacles a region centered at the robot of $10m \times 10m$, to be a fair comparison to the area considered by the AKP which is a circle of radius $6m$.

In Fig. 7.12-*Right* column are depicted the results of the experiments. We have chosen to show two variables: the accumulated trajectory cost of people due to the interaction with the robot, that is, the direct impact of the robot towards its environment. The second one is the average time for the robot to reach the goal. Since all methods are compared under the same conditions, and that entails the same distance to goal, with this measure we can compare objectively the different approaches in terms of efficiency of execution. All the bar diagrams appearing in Fig. 7.12 are normalized to sum the unity in order to correctly compare the overall results.

In the first scenario, in Fig. 7.12-*Top* the side-rear interaction, the results considering the people's costs show a better performance for the AKP approach than for the rest of the approaches. Considering time of execution, the AKP presents a slightly better performance. In the second scenario, the side-frontal interaction in Fig. 7.12-*Center*, the DWA is able to avoid people successfully since it can re-plan on time and their results obtained are on par with the AKP and much better than the reactive approach, that fails to avoid interaction with people. The time of execution, is better for the AKP, since it can avoid collision more efficiently than the other two approaches. In the third scenario, in Fig. 7.12-*Bottom*, we observe a clear winner: the AKP. When considering the people's cost, the AKP is able to reduce its impact towards the scene and execute its task successfully. The average time of execution is not considerably better for the AKP than the other approaches, but the fact is that our approach is really avoiding a possible collision while the other two approaches fail to re-plan on time and follow a too straight trajectory.

We can observe that the results are dependent on the configuration, the more complex the configuration is, the better relative results are obtained by our approach. We already demonstrated this statement in simulations, however it had to be verified in a real scenario.

We highly recommend to watch the videos at the project web-page for a more detailed idea of the outcome of the experiments, since movement is difficult to be captured in images or words.

7.7.2 Uncontrolled environment

In order to further validate our approach, we have tested it in a more complex scenario, where the robot receives *go-to* queries in a urban environment and more interactions take place. The testing is done under uncontrolled conditions, that is, no instructions are given to people in the scene while the robot tries to navigate. Two environments are tested, the FME where we carried out the comparison explained before, and the *Barcelona Robot Lab.* (BRL), which is a urban area in the university campus, when many students were there. The experiment's main purpose

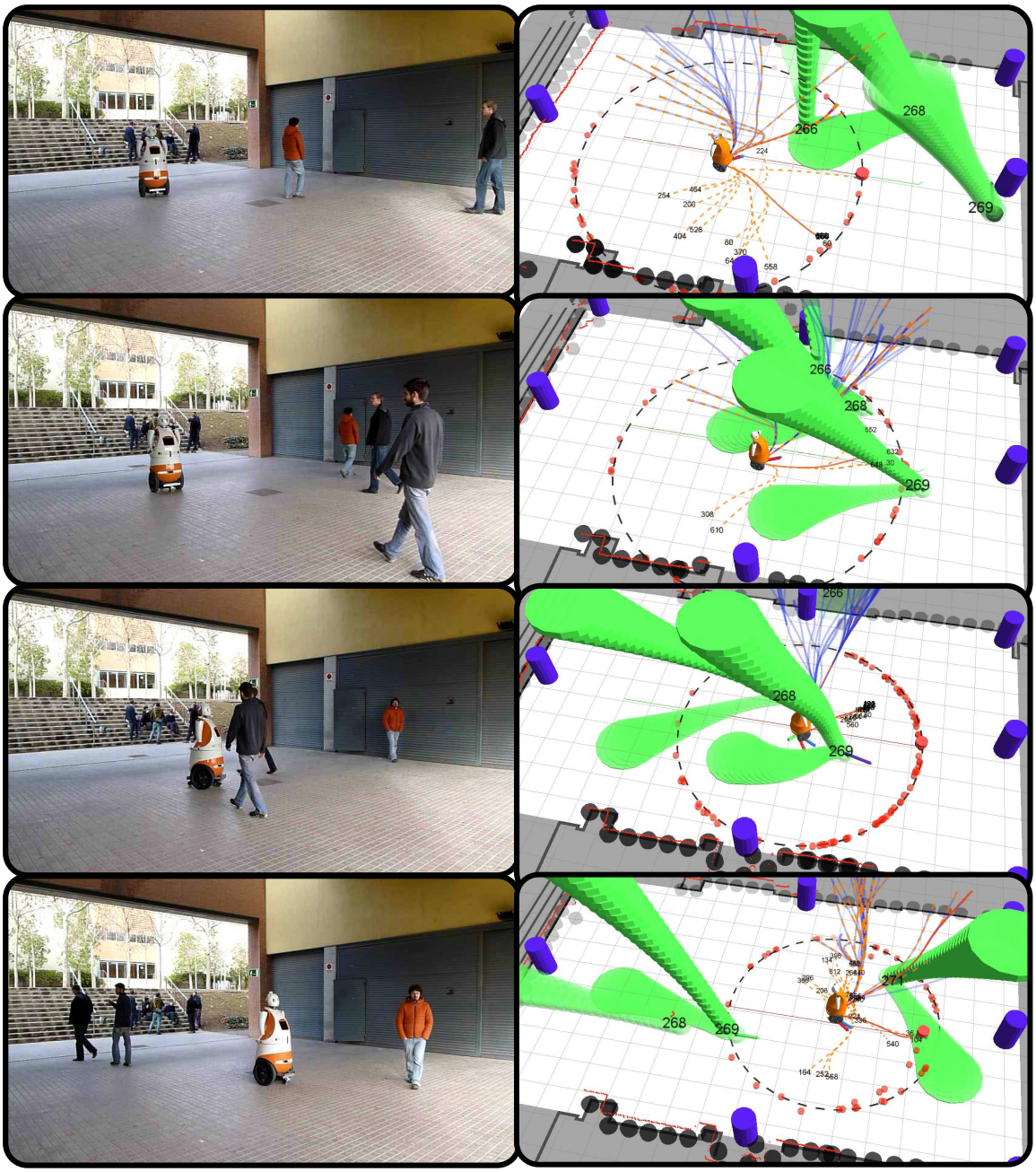

Figure 7.13: **Example of the AKP.** Sequence of a navigation experiment interacting with multiple pedestrians in the BRL environment.

is to demonstrate the success of navigation queries in a real and uncontrolled environment. To this end, we performed and recorded the experience on a video. As stated before, simple configurations with few interactions do not represent a challenge for most navigation algorithms, however the scene can increase in complexity and more challenging configurations may appear. Is in these situations when the AKP approach might helps us avoid possible collisions or abnormal robot behaviors, and deal with these situations more successfully and minimizing its impact towards the pedestrians in the scene.

A sequence of one navigation experiment is depicted in Fig. 7.13, where we observe the interaction of several people with the robot at different instants of time and how the robot is able to avoid them successfully.

7.8 Summary

The main motivation of the present chapter, as stated in the introduction, is to minimize the robot impact towards all those nearby pedestrians, while navigating and executing tasks. Throughout this chapter we have proposed an approach that is able to consider multiple objectives for robot navigation and demonstrated to be effective in real situations. In addition, the anticipative approach has proven to foresee people's trajectories and their corresponding reactions to each of the planned actions and act accordingly in advance of that information.

In this chapter we have presented an anticipative kinodynamic planner for urban environments that calculates in real time a local path that minimizes the disturbances to other pedestrians, as well as multiple objectives into the same algorithm. The solution trajectories, calculated in an RRT fashion, take into account kinodynamic and nonholonomic restrictions which are mandatory considerations for a realistic navigation in such highly time-variant scenarios like urban environments.

We have presented a seamlessly integrated prediction algorithm that builds predictions simultaneously with plans. We have demonstrated that is not necessarily true that the complexity associated to a joint approach has to dramatically increase and we have obtained multiple benefits by integrating prediction and planning.

The cost of "anticipating" is a more intensive processing since we must propagate the state of moving pedestrians accordingly to the robot propagation. The overhead generated by this trait has been demonstrated to be justified, since challenging and complex scenarios are more successfully solved by the AKP than other state of the art navigation methods. However, in more simple situations it is not necessary to consider so many factors, and a more simple approach could perform on par with the AKP.

The multi-objective approach studied in this paper has shed light into the construction, in general, of cost functions. If there are few parameters and costs involved, a direct scalarization

of the costs may be fine, however we have demonstrated that it might not hold when considering several costs. After following a multi-objective approach, we have obtained a practically invariant set of navigation parameters that can be used in many situations.

The theoretical approach presented is well supported by plenty of experiments and simulations, which the authors believe to be essential in robot navigation. There are in addition plenty of multimedia material and all the code available at the web-page http://www.iri.upc.edu/groups/lrobots/akp/ which better illustrates the results that have been discussed in this thesis.

Part III

Closing remarks

8

Closing remarks

In this final section we discuss the conclusions derived on each chapter of this thesis, and we gather them into a joint reflection to illustrate the more important ideas. Next, we present a summary of the contributions of this dissertation, and at last, we propose some future research lines that steam out from this work.

8.1 Conclusions

In Chapter 3 we have presented a method to infer human intentions into the context of a urban setting. Human intentions have been traditionally studied in other scientific fields of knowledge such as Computer Vision or Machine Learning. In the context of this thesis, we have demonstrated that they can improve motion prediction and robot navigation. Inferring intentions has demonstrated to give very useful information of the environment since we are able to describe a scene by providing a set of goals or destinations, as shown in the navigation Part II. Throughout this work we have made use of the intentionality predictor BHMIP in order to calculate the goals in the environment where people are aiming to and to improve the prediction of trajectories.

The proposed intentionality prediction BHMIP and the Social Force Model (SFM) serve as the basic elements to build a complete framework of human motion predictions in social environments, as presented in Chapter 4. In addition, we have extended the SFM model into the ESFM, in order to consider person-robot interactions and we provide a better trajectory prediction through the behavior estimation. The results of the prediction have shown that considering the BHMIP and motion behavior can greatly improve the accuracy of the human motion prediction. However, the interacting forces provided by the ESFM as well as the estimated future pedestrians' trajectories provided by the prediction framework, are inaccurate and diverge over time. For this reason, we have realized the limitations of the prediction approach. Accordingly, we should take into consideration this model as a useful but inaccurate tool for providing motion information, instead of a model describing completely and realistically trajectories for each

individual person. We have alleviated this limitation by providing the behavior estimation, but at the end, the set of parameters describing motion is different for each one of us, even it is not clear to be invariant in time to a single person, nonetheless, they provide an excellent initial idea of the future state of a scene with pedestrians, that is exactly what is required in the context of this dissertation. After studying the ESFM, we believe that it can be substituted in our approach by any equivalent potential field that models attractive and repulsive elements. The interesting part of the ESFM is that it has been used in other works and is a well known method, bridging the gap between neuroscience and robotics. The study of prediction algorithms well deserved the time we spent, since it has provided the backbone to solve and formulate most of the navigation problems appearing in this thesis.

In our first approach to the robot navigation topic, presented in Chapter 5, our initial hypothesis is to make the robot navigate according to a human model, the ESFM, and thus, it will be more accepted by humans. We threw the following questions at the introductory Chapter 1: should robots behave as a person to be considered as equals by people? or should robots take care of humans' trajectories on their own way? After this work, we conclude that our initial hypothesis is only valid in simple situations (few obstacles and moving people). In more complex situations, the robot is not able to behave like a person, due to the fact that the robotic platform studied in this thesis has wheels, and their propagation model is different than a pedestrian. In addition, we realized that the embodiment of the robot would never be perceived as a person, and hence, it is wrong to make it move as it is a person if none would treat the robot as such. Chapter 5 has motivated a change in the methodology to study robot navigation from trying to implement a completely characterized human navigation embodied in a robot into implementing a robot navigation that considers people in the scene developing its own specific strategies to success in social environments.

In our second iteration to the robot navigation topic, as presented in Chapter 7, we develop a robot navigation approach that diverges from the strategy to imitate human navigation features. Aiming to build a robot-centered approach, we propose a robot navigation approach that considers multiple objectives, such as, robot's cost, nearby people's cost, distance to goal, etc. We show that the multi-objective approach studied in this chapter has shed light into the construction, in general, of well-posed cost functions, since we have shown that when considering many different costs, classical approaches fail. After following a multi-objective approach, we have obtained a practically invariant set of navigation parameters that can be used in many situations, which is a very important conclusion and it can motivate future research lines, as we will discuss below.

We have presented in Chapter 7 a seamlessly integrated prediction algorithm that builds predictions simultaneously with plans. We have demonstrated that is not necessarily true that the complexity associated to a joint approach has to dramatically increase, and we have obtained multiple benefits by integrating prediction and planning. The authors believe that integrating initiatives, as the one proposed in this thesis, are interesting for a further development of robot

navigation, since they allow to increase the difficulty of the problems treated, and at the same time, the navigation algorithms maintain their complexity, if correctly applied.

In Chapter 7 we also showed the importance of taking into account kinodynamic and non-holonomic restrictions of the robotic platform, which are mandatory considerations for a realistic navigation in highly time-variant scenarios, like urban environments.

We have formulated a joint state of the system including the augmented robot state and the complete scene including people (dynamic obstacles). A a result, our proposed navigation algorithm, the AKP, not only considers predicted trajectories, but anticipates and foresees people's trajectories and their corresponding reactions to each of the planned actions and acts accordingly in advance of that information. This provided benefits on complex scenes, but on more simple situations, like few obstacles, it is not necessary such a demanding computation of the algorithm. It would be interesting to use this approach when needed and free computational resources on more common situations.

Nevertheless, heavy computations are alleviated by using steering heuristics for a fast calculation, in our case we map from a goal in the workspace to the action space. Without this technique, it would not be possible to implement our proposed algorithm and execute it in real time. In general, any other method could benefit from steering functions if correctly handled.

8.2 Summary of contributions

This thesis contributes with multiple developments to the human motion prediction and the robot navigation field and their intersection into a common field of knowledge. We have highlighted above the main conclusions derived from this work; related to these conclusions are the contributions produced in the present dissertation. A summary of our contributions obtained in this thesis is listed as follows:

1. **The intentionality predictor BHMIP** (Chapter 3). The method allows us to describe any social environment in terms of human motion intentionality and to build a prediction or a navigation system.

2. **The ESFM** (Chapter 4). We propose an extension to the Social Force Model that takes into account the micro-interactions between pedestrians and robots and we obtain the robot-person interaction specifically suited for Tibi&Dabo robots. This model constitutes the backbone to develop the navigation approach presented in this thesis.

3. **Generation of humans' trajectories** (Chapter 4). The integration of the intentionality predictor BHMIP and the proposed behavior estimator to formulate a reliable prediction framework of humans' trajectories under the influence of dynamic crowds, robots and any

moving obstacle. This framework is not only limited to robot navigation and it can be used in many other applications.

4. **Socially aware robot navigation** (Chapter 5). Our proposed navigation algorithm takes into account its environment and it is aware on the motion of nearby people to the robot. This idea has been refined as this thesis has evolved, nonetheless the contribution is to consider the corresponding navigation impact in addition to navigate successfully in a urban settings.

5. **Multi-objective navigation** (Chapters 5, 7). As a second iteration, we propose a set of objectives, including the impact towards the scene and many others, in a well-posed cost function, that can be applied to the robot navigation problem if we want to consider multiple criteria.

6. **Robot navigation integrated with prediction** (Chapters 6, 7). As opposed to our initial thoughts, integrating these systems does not necessarily increment the overall complexity of the algorithm, but improves the results.

7. **Anticipative planning** (Chapters 7). We obtain an anticipative behavior of the navigation algorithm by increasing the state of the system, now considering jointly the robot system as well as the states of the pedestrians. This approach is very useful only in complex scenes.

The objectives presented in Sec. 1.2 have been completely fulfilled. We have analyzed urban settings and human motion in Part I and we have studied navigation algorithms through Part II. In addition, we have integrated navigation and prediction, considered the robot navigation impact towards the environment, and validated our approach in simulations and real conditions. Moreover, have surpassed the initial objectives by providing a second iteration to many of the initial objectives, in Chapter 7.

8.2.1 Publications

The following is a list of the publications derived from this thesis:

Journals

[J4] G. Ferrer and A. Sanfeliu (2015). Anticipative Kinodynamic Planning: Robot Navigation in Urban and Dynamic Environments. To be submitted.

[J3] G. Ferrer, A. Garrell, F. Herrero, and A. Sanfeliu (2015). Robot Social-Aware Navigation Framework to Accompany People walking Side-by-Side. *Autonomous Robots*, submitted.

[J2] G. Ferrer, and A. Sanfeliu (2014). Bayesian human motion intentionality prediction in urban environments. *Pattern Recognition Letters* 44:134-140.

[J1] E. Trulls, A. Corominas Murtra, J. Pérez-Ibarz, G. Ferrer, D. Vasquez, J.M. Mirats Tur and A. Sanfeliu (2011). Autonomous navigation for mobile service robots in urban pedestrian environments. *Journal of Field Robotics* 28(3): 329-354.

Conferences

[C7] G. Ferrer and A. Sanfeliu (2015). Multi-Objective Cost-to-Go Functions on Robot Navigation in Dynamic Environments. In *Proceedings of the IEEE/RSJ International Conference on Intelligent Robots and Systems (IROS)*, accepted.

[C6] I. Huerta, G. Ferrer, F. Herrero, A. Prati and A. Sanfeliu (2014). Multimodal feedback fusion of laser, image and temporal information. In *International Conference on Distributed Smart Cameras*, pp. 25:1-25:6, Venice, Italy.

[C5] G. Ferrer and A. Sanfeliu (2014). Proactive Kinodynamic Planning using the Extended Social Force Model and Human Motion Prediction in Urban Environments. In *Proceedings of the IEEE/RSJ International Conference on Intelligent Robots and Systems (IROS)*, pp. 1730-1735, Chicago, USA.

[C4]G. Ferrer and A. Sanfeliu (2014). Behavior Estimation for a Complete Framework for Human Motion Prediction in Crowded Environments. In *Proceedings of the IEEE International Conference on Robotics and Automation (ICRA)*, pp. 5940-5945. Hong Kong, China.

[C3] G. Ferrer, A. Garrell, and A. Sanfeliu (2013). Robot companion: A social-force based approach with human awareness-navigation in crowded environments. In *Proceedings of the IEEE/RSJ International Conference on Intelligent Robots and Systems (IROS)*, pp. 1688-1694. Tokyo, Japan.

[C2] G. Ferrer, A. Garrell, and A. Sanfeliu (2013). Social-Awareness Robot Navigation in Urban Environments. In *European Conference on Mobile Robotics, (ECMR)*, pp. 331-336, Barcelona, Spain.

[C1] G. Ferrer, and A. Sanfeliu (2011). Comparative analysis of human motion trajectory prediction using minimum variance curvature. In *6th ACM/IEEE International Conference on Human-Robot Interaction (HRI)*, pp. 135-136, Lausanne, Switzerland.

Book Chapters

[B1] G. Ferrer, A. Garrell, M. Villamizar, I. Huerta, and A. Sanfeliu (2013). Robot interactive learning through human assistance. In *Multimodal Interaction in Image and Video Applications*, pp. 185-203, Springer.

8.3 Future research directions

Finally, we discuss some of the future research lines that steam out from the research and contributions presented during this thesis.

Extend the planning algorithm to a fully dynamic model: a straightforward implementation of the AKP can be reformulated considering dynamic constraints. This improvement is specially useful for higher velocities, where components currently neglected in the kinodynamic model, such as moments or inertia, might become more important for the correct calculation of motions.

Extend the behavior estimation tool: the behavior estimation can be studied in other motion tasks and formulated as new theories. Some examples are when sensing an extreme *aware* behavior from a person in the environment as an abnormal behavior, detecting threatening pedestrians which may potentially collide with the robot or detecting possible HRI interactions between a pedestrian and the robot.

Estimation of meaningful motion features: the calculation of the behavior estimation has demonstrated to increase the performance of the motion prediction algorithm. Aiming to describe a more complete social scene, we believe that the identification of other meaningful features for the prediction and navigation problems, will improve those systems.

Using virtual forces to re-formulate HRI problems: the HRI can be studied from the point of view of attractive and repulsive forces, looking for a similar approach that we have experienced during the study of human motion in this thesis. In the context of interaction, there would be no physical meaning of those forces, however they can describe well more complex interactions between people and robots.

Study of the uncertainties of the ESFM: we have presented in this thesis uncertainties associated in the social force values and their corresponding propagation errors when calculating the trajectories describing human motion. A better characterization of those uncertainties, and how they are related to nearby interactions, should improve the prediction outcome. However, it is important to note that the ESFM is only a useful method to grasp an idea of future human motion, and thus, a correct characterization of the associated error is important.

Social navigation transferred into robotic products: we have not witnessed yet the explosion of robotics as science fiction has been announcing during the last half century. Slowly, robotics are increasing their presence in specific and simple tasks such as cleaning or sweeping, aiming to execute simple tasks, and not trying to achieve a *fully autonomous* navigation system. In the years to come we will see an increment of robots carrying out tasks more and more complex. To achieve this, it is necessary to transfer novel techniques into robotics platforms. We propose to adapt the social-aware approaches developed in this thesis into the production of a new generation of robots, still far from the *fully autonomous* milestone, but more intelligently than the previous generation.

Learning in the robot navigation: apply learning techniques into the AKP approach proposed in this thesis. Multiple cost parameters could be calculated and processed using state of the art techniques in machine learning. The interesting point, similar as we have done to build a well-posed function, would be to define the learning algorithm problem in a well-posed manner.

A People detection and tracking

In this appendix we present the detection and tracking implementations carried out at the institute, which has been an essential part of the work to develop the prediction and navigation algorithms presented previously in this thesis. Although their relevance, this work remains out of the scope of the general scheme of the dissertation, and thus, we have included this appendix discussing our approach.

Either the prediction as well as the navigation methods require the perception of people in urban environments in order to calculate the necessary orientations, velocities and accelerations for our proposed algorithms, which are entirely based on spacial observations of people in the scene. Throughout this thesis, we have omitted the acquisition of this information for the clarity of the presentation. However, in this appendix we present the implementation of the perception system aiming to obtain people's trajectories and their correct association with the corresponding pedestrians describing them.

A.1 People detection

As explained in Sec. 2.1 when describing the robotic platform hardware, the hole perception system is based on range information. The perception of people is mandatory in order to study urban environments and to propose a successfully robot navigation algorithm among human beings. Thus, we propose to solve the information acquisition problem by only using range sensors. There exist many sensors, such as laser, sonar, cameras, etc., that are able to provide us all this information, however, we have chosen to use laser due to its accuracy when estimating the distance to an obstacle and the 360° field of view thanks to deploying two horizontal lasers.

Our implementation of the laser detector is fundamentally based on [Arras et al., 2007, 2008], which defines a set of geometric features related to a cluster of laser points and uses a boosting method to classify if that set of laser points corresponds to a human being. An accurate strong classifier is built by combining a set of weak classifiers based on those geometric features that determine if the laser points correspond to a leg and consequently a human being.

The implementation by Herrero [2012] developed at the IRI as a result of a final-year degree project, is shown in Fig. A.1-*Left*, where we can observe multiple detections in the Barcelona Robot Lab. represented as lilac cylinders. There are multiple detections, however, it is preferable to increase the number of detections by decreasing the classification threshold, and get more false positives, rather than being too selective and suffer a false negative, which is a very undesirable result for the next concatenated subsystem, the people tracking.

As it can be seen in Fig. A.1-*Left*, there are numerous detections, specially near the static obstacles which constitute a systematic error produced by the geometry of the scene, *i.e.* a circular trash can. Accordingly, we filter all those detections that lie inside the environment map

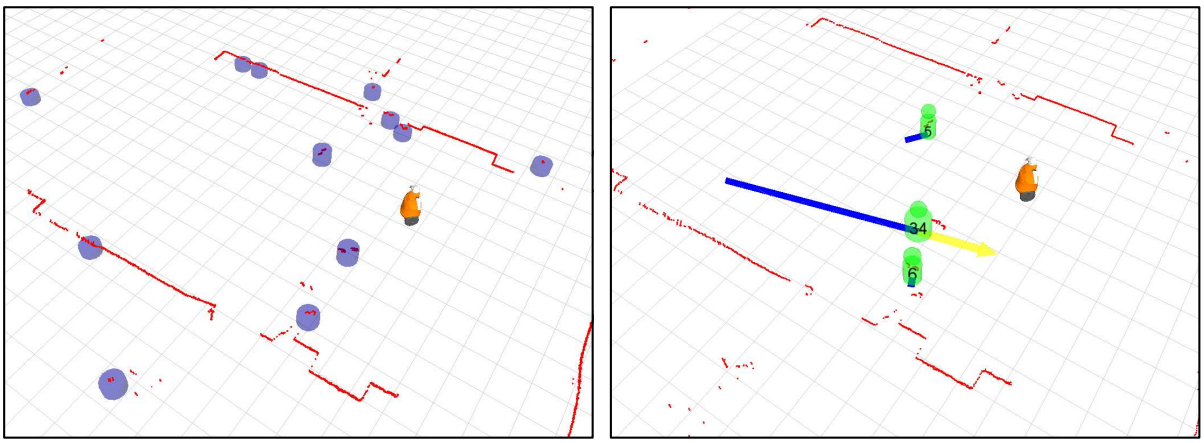

Figure A.1: **Urban scene showing multiple detections and their corresponding tracks.** Different captures of the perception system in a real environment. On the *L*eft image, we can observe multiple people's detections before filtering as lilac cylinder. On the *R*ight image is depicted the tracking output as green cylinders and their corresponding *id*s.

in order to reduce the number of false positives, while at the same time we maintain all those detections that very likely correspond to people.

A.2 People tracking

The people tracking system is necessary in order associate multiple detections in different instants of time to the same target identification or *id*. In addition to maintain the same *id* for a person, we are able to calculate velocities and accelerations since we have stored the pedestrian's trajectory, which is extremely important for the prediction and navigation algorithms as discussed previously in this thesis.

The people tracking implementation follows a similar approach of the work presented in [Reid, 1979] and some of the contributions presented in [Luber et al., 2011]. Our implementation, by Repiso [2013] is the result of a final-year degree project, which was co-tutored by Prof. Sanfeliu this thesis' author, in response to the necessity to provide a complete solution to the perception problem.

As a result, our people tracker uses a Kalman filter to propagate the pedestrians' trajectories and it combines the different detections with the existing track *id*s to calculate the most likely association hypothesis. Only time-consistent detections that are repeated multiple times become confirmed tracks, and hence, starting the tracking procedure. The algorithm can handle occlusions, crossings and loss of targets, at a relative low error.

According to our experience, the most critical source of error in the perception system occurs when the current track is lost due to long occlusions, lack of detections for geometrical reasons or other causes; then a new *id* is assigned to the target. In the current state of the tracker is not possible to completely remove these issues, although we have considered this problem and reduced the error considerably. However, a discussion of the perception system is out of the scope of the present appendix and it is important to note that any other system (vision detection, RF, etc.) would also be subject to limitations under realistic conditions.

In Fig. A.1-*Right* is depicted the people tracker GUI in a real environment. We can observe

that the number of tracks is reduced compared with the number of detections. As we have discussed, it is necessary a certain time consistency in the detections in order to confirm a track, moreover the map filter helps to reduce the number of false positives due to the geometry of the static obstacles. In result, we are able to track the pedestrians in the scene robustly and provide a good input for the prediction and navigation algorithms described in this dissertation.

Nonetheless, the detection and tracking systems are not exempt of limitations. For the experimentation that we have presented in this thesis, the system has performed well. Occasionally we provide wrong or missing information, however, our proposed navigation and prediction algorithms can handle these errors since the calculations are done iteratively at each instant of time, so they the present a great adaptability and robustness, as discussed in Sec. 3.5.

References

Alami, R., Albu-Schaeffer, A., Bicchi, A., Bischoff, R., Chatila, R., De Luca, A., De Santis, A., Giralt, G., Guiochet, J., and Hirzinger, G. (2006). Safe and dependable physical human-robot interaction in anthropic domains: State of the art and challenges. In *Workshop on pHRI - Physical Human-Robot Interaction in Anthropic Domains, IEEE/RSJ International Conference on Intelligent Robots and Systems*. Citeseer.

Althaus, P., Ishiguro, H., Kanda, T., Miyashita, T., and Christensen, H. (2004). Navigation for human-robot interaction tasks. In *Proceedings of the IEEE International Conference on Robotics and Automation*, volume 2, pages 1894–1900.

Andrieu, C., De Freitas, N., Doucet, A., and Jordan, M. I. (2003). An introduction to mcmc for machine learning. *Machine learning*, 50(1-2):5–43.

Antonini, G., Bierlaire, M., and Weber, M. (2006). Discrete choice models of pedestrian walking behavior. *Transportation Research Part B: Methodological*, 40(8):667–687.

Arechavaleta, G., Laumond, J.-p., Hicheur, H., and Berthoz, A. (2006a). Optimizing principles underlying the shape of trajectories in goal oriented locomotion for humans. In *IEEE-RAS International Conference on Humanoid Robots*, pages 131–136. IEEE.

Arechavaleta, G., Laumond, J.-P., Hicheur, H., and Berthoz, a. (2006b). The nonholonomic nature of human locomotion: a modeling study. In *The First IEEE/RAS-EMBS International Conference on Biomedical Robotics and Biomechatronics*, pages 158–163.

Arechavaleta, G., Laumond, J.-P., Hicheur, H., and Berthoz, A. (2008). An optimality principle governing human walking. *IEEE Transactions on Robotics*, 24(1):5–14.

Arras, K., Grzonka, S., Luber, M., and Burgard, W. (2008). Efficient people tracking in laser range data using a multi-hypothesis leg-tracker with adaptive occlusion probabilities. *Proceedings of the IEEE International Conference on Robotics and Automation*, pages 1710–1715.

Arras, K., Mozos, O., and Burgard, W. (2007). Using boosted features for the detection of people in 2d range data. In *Proceedings of the IEEE International Conference on Robotics and Automation*, number April, pages 3402–3407. IEEE.

Arras, K. O., Philippsen, R., Tomatis, N., De Battista, M., Schilt, M., and Siegwart, R. (2003). A navigation framework for multiple mobile robots and its application at the expo. 02 exhibition. In *Proceedings of the IEEE International Conference on Robotics and Automation*, volume 2, pages 1992–1999. IEEE.

Barraquand, J. and Latombe, J.-C. (1991). Robot motion planning: A distributed representation approach. *The International Journal of Robotics Research*, 10(6):628–649.

Bennewitz, M., Burgard, W., Cielniak, G., and Thrun, S. (2005). Learning motion patterns of people for compliant robot motion. *The International Journal of Robotics Research*, 24(1):31–48.

Bennewitz, M., Burgard, W., and Thrun, S. (2002). Learning motion patterns of persons for mobile service robots. In *Proceedings of the IEEE International Conference on Robotics and Automation*, volume 4, pages 3601–3606. IEEE.

Bergstrom, N., Kanda, T., Miyashita, T., Ishiguro, H., and Hagita, N. (2008). Modeling of natural human-robot encounters. In *Proceedings of the IEEE/RSJ International Conference on Intelligent Robots and Systems*, pages 2623–2629.

Bishop, C. et al. (2006). *Pattern recognition and machine learning*, volume 4. Springer New York.

Borenstein, J. and Koren, Y. (1991). The vector field histogram-fast obstacle avoidance for mobile robots. *IEEE Transactions on Robotics and Automation*, 7(3):278–288.

Brock, O. and Khatib, O. (1999). High-speed navigation using the global dynamic window approach. In *Proceedings of the IEEE International Conference on Robotics and Automation*, volume 1, pages 341–346.

Bruce, A. and Gordon, G. (2004). Better motion prediction for people-tracking. In *Proceedings of the IEEE International Conference on Robotics and Automation*.

Burgard, W., Cremers, A. B., Fox, D., Hähnel, D., Lakemeyer, G., Schulz, D., Steiner, W., and Thrun, S. (1999). Experiences with an interactive museum tour-guide robot. *Artificial intelligence*, 114(1):3–55.

Castro-González, A., Shiomi, M., Kanda, T., Salichs, M., Ishiguro, H., and Hagita, N. (2010). Position Prediction in Crossing Behaviors. In *IEEE/RSJ International Conference on Intelligent Robots and Systems*, pages 5430–5437, Taipei, Taiwan.

Chen, Z., Wang, L., and Yung, N. (2011). Adaptive Human Motion Analysis and Prediction. *Pattern Recognition*, 44(12):2902–2914.

Chung, S. Y. and Huang, H.-p. (2010). A Mobile Robot That Understands Pedestrian Spatial Behaviors. In *Proceedings of the IEEE/RSJ International Conference on Intelligent Robots and Systems*, pages 5861–5866.

Corominas Murtra, A., Trulls, E., Sandoval-Torres, O., Pérez-Ibarz, J., Vasquez, D., Mirats-Tur, J. M., Ferrer, M., and Sanfeliu, A. (2010). Autonomous navigation for urban service mobile robots. In *Proceedings of the IEEE/RSJ International Conference on Intelligent Robots and Systems*, pages 4141–4146.

Dautenhahn, K., Walters, M., Woods, S., Koay, K., Nehaniv, C., Sisbot, A., Alami, R., and Siméon, T. (2006). How may i serve you?: a robot companion approaching a seated person in a helping context. In *Proceedings of the 1st ACM SIGCHI/SIGART conference on Human-robot interaction*, pages 172–179. ACM.

Dautenhahn, K., Woods, S., Kaouri, C., Walters, M., Koay, K., and Werry, I. (2005). What is a robot companion-friend, assistant or butler? In *Proceedings of the IEEE/RSJ International Conference on Intelligent Robots and Systems*, pages 1192–1197.

Deb, K. (2014). Multi-objective optimization. In *Search methodologies*, pages 403–449. Springer.

Dee, H. and Hogg, D. (2004). Detecting inexplicable behaviour. *British Machine Vision Conference*, 477:486.

Demiris, Y. and Khadhouri, B. (2006). Hierarchical attentive multiple models for execution and recognition of actions. *Robotics and Autonomous Systems*, 54(5):361–369.

Dietterich, T. (2002). Machine learning for sequential data: A review. In *Structural, syntactic, and statistical pattern recognition*, pages 15–30. Springer.

Escobedo, J. A., Spalanzani, A., and Laugier, C. (2014). Using social cues to estimate possible destinations when driving a robotic wheelchair. In *Proceedings of the IEEE/RSJ International Conference on Intelligent Robots and Systems*, pages 3299–3304.

Ferrer, G., Garrell, A., and Sanfeliu, A. (2013a). Robot companion: A social-force based approach with human awareness-navigation in crowded environments. In *Proceedings of the IEEE/RSJ International Conference on Intelligent Robots and Systems*, pages 1688–1694.

Ferrer, G., Garrell, A., and Sanfeliu, A. (2013b). Social-aware robot navigation in urban environments. In *European Conference on Mobile Robotics*, pages 331–336.

Ferrer, G., Garrell, A., Villamizar, M., Huerta, I., and Sanfeliu, A. (2013c). Robot interactive learning through human assistance. In *Multimodal Interaction in Image and Video Applications*, pages 185–203. Springer.

Ferrer, G. and Sanfeliu, A. (2011). Comparative analysis of human motion trajectory prediction using minimum variance curvature. In *Proceedings of the 6th international conference on Human-robot interaction*, pages 135–136, Lausanne, Switzerland. ACM.

Ferrer, G. and Sanfeliu, A. (2014a). Bayesian human motion intentionality prediction in urban environments. *Pattern Recognition Letters*, 44:134–140.

Ferrer, G. and Sanfeliu, A. (2014b). Behavior estimation for a complete framework of human motion prediction in crowded environments. In *Proceedings of the IEEE International Conference on Robotics and Automation*, pages 5940–5945.

Ferrer, G. and Sanfeliu, A. (2014c). Proactive kinodynamic planning using the extended social force model and human motion prediction in urban environments. In *Proceedings of the IEEE/RSJ International Conference on Intelligent Robots and Systems*, pages 1730–1735.

Foka, A. and Trahanias, P. (2003). Predictive control of robot velocity to avoid obstacles in dynamic environments. In *Proceedings of the IEEE/RSJ International Conference on Intelligent Robots and Systems*, volume 1, pages 370–375.

Foka, A. and Trahanias, P. (2007). Real-time hierarchical POMDPs for autonomous robot navigation. *Robotics and Autonomous Systems*, 55(7):561–571.

Foka, A. and Trahanias, P. (2010). Probabilistic Autonomous Robot Navigation in Dynamic Environments with Human Motion Prediction. *International Journal of Social Robotics*, 2(1):79–94.

Fong, T., Nourbakhsh, I., and Dautenhahn, K. (2003). A survey of socially interactive robots. *Robotics and Autonomous Systems*, 42:143–166.

Fox, D., Burgard, W., and Thrun, S. (1997). The dynamic window approach to collision avoidance. *Robotics & Automation Magazine*, 4(1):23–33.

Fulgenzi, C., Spalanzani, A., and Laugier, C. (2009). Probabilistic motion planning among moving obstacles following typical motion patterns. In *Proceedings of the IEEE/RSJ International Conference on Intelligent Robots and Systems*, pages 4027–4033. IEEE.

Garrell, A. (2013). *Cooperative social robots: Accompanying, guiding and interacting with people*. Phd thesis, UPC.

Garrell, A. and A. Sanfeliu (2010). Model validation: robot behavior in people guidance mission using dtm model and estimation of human motion behavior. *IEEE/RSJ International Conference on Intelligent Robots and Systems*, pages 5836–5841.

Garrell, A. and Sanfeliu, A. (2012). Cooperative Social Robots to Accompany Groups of People. *The International Journal of Robotics Research*, 31(13):1675–1701.

Garrell, A., Sanfeliu, A., and Moreno-Noguer, F. (2009). Discrete Time Motion Model for Guiding People in Urban Areas using Multiple Robots. In *Proceedings of the IEEE/RSJ International Conference on Intelligent Robots and Systems*, volume 5, pages 486–491.

Glassman, E. and Tedrake, R. (2010). A quadratic regulator-based heuristic for rapidly exploring state space. In *Proceedings of the IEEE International Conference on Robotics and Automation (ICRA)*, pages 5021–5028. IEEE.

Goldberg, D. (1988). *Genetic Algorithms in Search, Optimization & Machine Learning*. Addison-Wesley.

Goldhoorn, A., Garrell, A., Alquézar, R., and Sanfeliu, A. (2014). Continuous real time pomcp to find-and-follow people by a humanoid service robot. In *IEEE-RAS International Conference on Humanoid Robots*, pages 741–747.

Haasch, A., Hohenner, S., Hüwel, S., Kleinehagenbrock, M., Lang, S., Toptsis, I., Fink, G., Fritsch, J., Wrede, B., and Sagerer, G. (2004). Biron–the bielefeld robot companion. In *Proc. Int. Workshop on Advances in Service Robotics*, pages 27–32. Stuttgart, Germany: Fraunhofer IRB Verlag.

Hall, E. T. and Hall, E. T. (1969). *The hidden dimension*. Anchor Books New York.

Havlak, F. and Campbell, M. (2014). Discrete and continuous, probabilistic anticipation for autonomous robots in urban environments. *IEEE Transactions on Robotics*, 30(2):461–474.

Helbing, D. and Molnar, P. (1995). Social force model for pedestrian dynamics. *Physical review E*, 51(5):4282–4286.

Henry, P., Vollmer, C., Ferris, B., and Fox, D. (2010). Learning to navigate through crowded environments. In *Proceedings of the IEEE International Conference on Robotics and Automation*, pages 981–986. IEEE.

Herrero, F. (2012). *Detección automática de personas mediante láser 2D y su aplicación a la robótica de servicios*. Final-year degree project, Universitat Politècnica de Catalunya.

Hsu, D., Kindel, R., Latombe, J.-C., and Rock, S. (2002). Randomized kinodynamic motion planning with moving obstacles. *The International Journal of Robotics Research*, 21(3):233–255.

Huang, W. H., Fajen, B. R., Fink, J. R., and Warren, W. H. (2006). Visual navigation and obstacle avoidance using a steering potential function. *Robotics and Autonomous Systems*, 54(4):288–299.

Ikeda, T., Chigodo, Y., Rea, D., Zanlungo, F., Shiomi, M., and Kanda, T. (2012). Modeling and prediction of pedestrian behavior based on the sub-goal concept. In *Robotics: Science and Systems*, pages 137–144.

Ishiguro, H., Ono, T., Imai, M., Maeda, T., Kanda, T., and Nakatsu, R. (2001). Robovie: an interactive humanoid robot. *Industrial robot: An international journal*, 28(6):498–504.

Jaillet, L., Cortés, J., and Siméon, T. (2010). Sampling-based path planning on configuration-space costmaps. *IEEE Transactions on Robotics*, 26(4):635–646.

Kanda, T., Shiomi, M., Miyashita, Z., Ishiguro, H., and Hagita, N. (2009). An affective guide robot in a shopping mall. In *Proceedings of the 4th ACM/IEEE international conference on Human robot interaction*, pages 173–180. ACM.

Katagami, D. and Yamada, S. (2003). Active teaching for an interactive learning robot. In *The 12th IEEE International Workshop on Robot and Human Interactive Communication*, pages 181–186. IEEE.

Khalid, S. (2010). Activity classification and anomaly detection using m-mediods based modelling of motion patterns. *Pattern Recognition*, 43(10):3636–3647.

Khatib, O. (1986). Real-time obstacle avoidance for manipulators and mobile robots. *The international journal of robotics research*, 5(1):90–98.

Kim, S., Guy, S. J., Liu, W., Wilkie, D., Lau, R. W., Lin, M. C., and Manocha, D. (2015). Brvo: Predicting pedestrian trajectories using velocity-space reasoning. *The International Journal of Robotics Research*, 34(2):201–217.

Kluge, B. (2003). Recursive agent modeling with probabilistic velocity obstacles for mobile robot navigation among humans. In *Proceedings of the IEEE/RSJ International Conference on Intelligent Robots and Systems*, volume 1, pages 376–380.

Koay, K., Sisbot, E., Syrdal, D., Walters, M., Dautenhahn, K., and Alami, R. (2007). Exploratory studies of a robot approaching a person in the context of handing over an object. *Proc. of AAAI-SS on Multi-disciplinary Collaboration for Socially Assistive Robotics*, pages 18–24.

Koren, Y. and Borenstein, J. (1991). Potential field methods and their inherent limitations for mobile robot navigation. In *Proceedings IEEE International Conference on Robotics and Automation*, pages 1398–1404. IEEE.

Kruse, T., Pandey, A. K., Alami, R., and Kirsch, A. (2013). Human-aware robot navigation: A survey. *Robotics and Autonomous Systems*, 61(12):1726–1743.

Kuderer, M., Kretzschmar, H., Sprunk, C., and Burgard, W. (2012). Feature-based prediction of trajectories for socially compliant navigation. In *Proceedings of Robotics: Science and Systems*.

Kuderer, M., Sprunk, C., Kretzschmar, H., and Burgard, W. (2014). Online generation of homotopically distinct navigation paths. In *Proceedings of the IEEE International Conference on Robotics and Automation*, pages 6462–6467.

Kümmerle, R., Ruhnke, M., Steder, B., Stachniss, C., and Burgard, W. (2014). Autonomous robot navigation in highly populated pedestrian zones. *Journal of Field Robotics*, pages 565–589.

Kunz, B. and Stilman, M. (2014). Probabilistically complete kinodynamic planning for robot manipulators with acceleration limits. In *Proceedings of the IEEE/RSJ International Conference on Intelligent Robots and Systems*, pages 3713–3719.

LaValle, S. M. and Kuffner, J. J. (2001a). Randomized kinodynamic planning. *The International Journal of Robotics Research*, 20(5):378–400.

LaValle, S. M. and Kuffner, J. J. (2001b). Rapidly-exploring random trees: Progress and prospects. In *Algorithmic and Computational Robotics: New Directions: the Fourth Workshop on the Algorithmic Foundations of Robotics*, page 293. AK Peters, Ltd.

Levitt, T. S. and Lawton, D. T. (1990). Qualitative navigation for mobile robots. *Artificial intelligence*, 44(3):305–360.

Liu, X. and Karimi, H. (2006). Location awareness through trajectory prediction. *Computers, Environment and Urban Systems*, 30(6):741–756.

Luber, M., Spinello, L., Silva, J., and Arras, K. O. (2012). Socially-aware robot navigation: A learning approach. In *Proceedings of the IEEE/RSJ International Conference on Intelligent Robots and Systems*, pages 902–907.

Luber, M., Stork, J. A., Tipaldi, G. D., and Arras, K. O. (2010). People tracking with human motion predictions from social forces. In *Proceedings of the IEEE International Conference on Robotics and Automation*, pages 464–469. IEEE.

Luber, M., Tipaldi, G. D., and Arras, K. (2011). Place-dependent people tracking. *The International Journal of Robotics Research*, 30(3):280–293.

Madhava Krishna, K., Alami, R., and Simeon, T. (2006). Safe proactive plans and their execution. *Robotics and Autonomous Systems*, 54(3):244–255.

Majecka, B. (2009). *Statistical Models of Pedestrian Behaviour in the Forum*. Msc. dissertation, School of Informatics, University of Edinburgh.

Marler, R. T. and Arora, J. S. (2004). Survey of multi-objective optimization methods for engineering. *Structural and multidisciplinary optimization*, 26(6):369–395.

Matveev, A., Wang, C., and Savkin, A. (2012). Real-time navigation of mobile robots in problems of border patrolling and avoiding collisions with moving and deforming obstacles. *Robotics and Autonomous Systems*, pages 769–788.

Michalowski, M., Sabanovic, S., and Simmons, R. (2006). A spatial model of engagement for a social robot. In *9th IEEE International Workshop on Advanced Motion Control*, pages 762–767.

Morris, B. T. and Trivedi, M. M. (2011). Trajectory learning for activity understanding: Unsupervised, multilevel, and long-term adaptive approach. *IEEE Transactions on Pattern Analysis and Machine Intelligence*, 33(11):2287–2301.

Moussaïd, M., Helbing, D., and Theraulaz, G. (2011). How simple rules determine pedestrian behavior and crowd disasters. *Proceedings of the National Academy of Sciences*, 108(17):6884–6888.

Nakauchi, Y. and Simmons, R. (2002). A social robot that stands in line. *Autonomous Robots*, 12(3):313–324.

Nourbakhsh, I., Kunz, C., and Willeke, T. (2003). The mobot museum robot installations: A five year experiment. In *Proceedings of the IEEE/RSJ International Conference on Intelligent Robots and Systems*, volume 4, pages 3636–3641.

Olivera, V. M. and Simmons, R. (2002). Implementing human-acceptable navigational behavior and a fuzzy controller for an autonomous robot. In *Proceedings WAF: 3rd Workshop on Physical Agents, Murcia, Spain*, pages 113–120.

Owen, E. and Montano, L. (2005). Motion planning in dynamic environments using the velocity space. In *Proceedings of the IEEE/RSJ International Conference on Intelligent Robots and Systems*, pages 2833–2838.

Pacchierotti, E., Christensen, H. I., and Jensfelt, P. (2006). Embodied social interaction for service robots in hallway environments. In *Field and Service Robotics*, pages 293–304. Springer.

Palmieri, L. and Arras, K. O. (2014). A novel rrt extend function fo efficient and smooth mobile robot motion planning. In *Proceedings of the IEEE/RSJ International Conference on Intelligent Robots and Systems*, pages 205–211.

Panangadan, A., Matarić, M., and Sukhatme, G. (2004). Tracking and Modeling of Human Activity Using Laser Rangefinders. *International Journal of Social Robotics*, pages 1–13.

Papadopoulos, A. V., Bascetta, L., and Ferretti, G. (2013). Generation of human walking paths. In *Proceedings of the IEEE/RSJ International Conference on Intelligent Robots and Systems*, pages 1676–1681. IEEE.

Pellegrini, S., Ess, A., Schindler, K., and Van Gool, L. (2009). You'll never walk alone: Modeling social behavior for multi-target tracking. In *IEEE 12th International Conference on Computer Vision*, pages 261–268.

Perez, A., Platt, R., Konidaris, G., Kaelbling, L., and Lozano-Perez, T. (2012). Lqr-rrt*: Optimal sampling-based motion planning with automatically derived extension heuristics. In *Proceedings of the IEEE International Conference on Robotics and Automation*, pages 2537–2542. IEEE.

Pérez Hurtado, I., Capitán, J., Caballero, F., and Merino, L. (2015). An extension of ghmms for environments with occlusions and automatic goal discovery for person trajectory prediction. In *European Conference on Mobile Robotics*, pages 331–336.

Pransky, J. (2004). Social adjustments to a robotic future. *Wolf and Mallett*, pages 137–59.

Prassler, E., Bank, D., and Kluge, B. (2002). Key technologies in robot assistants: Motion coordination between a human and a mobile robot. *Transactions on Control, Automation and Systems Engineering*, 4(1):56–61.

Quigley, M., Gerkey, B., Conley, K., Faust, J., Foote, T., Leibs, J., Berger, E., Wheeler, R., and Ng, A. (2009). ROS: an open-source Robot Operating System. In *ICRA Workshop on Open Source Software*.

Reid, D. B. (1979). An algorithm for tracking multiple targets. *IEEE Transactions on Automatic Control*, 24(6):843–854.

Repiso, E. (2013). *Multi-hypothesis person tracker for urban environments*. Final-year degree project, Universitat Politècnica de Catalunya.

Retamino Carrión, E. and Sanfeliu, A. (2014). Human-robot collaborative scene mapping from relational descriptions. In *ROBOT2013: First Iberian Robotics Conference*, pages 331–346. Springer.

Sanfeliu, A., Andrade-Cetto, J., Barbosa, M., Bowden, R., Capitán, J., Corominas, A., Gilbert, A., Illingworth, J., Merino, L., Mirats, J. M., Moreno, P., Ollero, A., Sequeira, J., and Spaan, M. T. (2010). Decentralized sensor fusion for ubiquitous networking robotics in urban areas. *Sensors*, 10(3):2274–2314.

Satake, S., Kanda, T., Glas, D., Imai, M., Ishiguro, H., and Hagita, N. (2009). How to approach humans?: strategies for social robots to initiate interaction. In *4th ACM/IEEE International Conference on Human-Robot Interaction*, pages 109–116.

Sehestedt, S., Kodagoda, S., Alempijevic, A., and Dissanayake, G. (2009). Efficient learning of motion patterns for robots. In *Australasian Conference on Robotics and Automation*.

Shatkay, H. and Kaelbling, L. P. (2002). Learning geometrically-constrained hidden markov models for robot navigation: Bridging the topological-geometrical gap. *Journal of Artificial Intelligence Research*, 16(1):167–207.

Shi, D., Collins, E., Donate, A., Liu, X., Goldiez, B., and Dunlap, D. (2008). Human-aware robot motion planning with velocity constraints. In *International Symposium on Collaborative Technologies and Systems*, pages 490–497. IEEE.

Shin, D., Singh, S., and Whittaker, W. (1993). Path generation for robot vehicles using composite clothoid segments. In *IFAC symposia series*, pages 443–453. Pergamon press.

Silverman, B. (1986). *Density estimation for statistics and data analysis*, volume 26. Chapman & Hall/CRC.

Simmons, R. (1996). The curvature-velocity method for local obstacle avoidance. In *Proceedings of the IEEE International Conference on Robotics and Automation*, volume 4, pages 3375–3382.

Sisbot, E. A., Marin-Urias, L. F., Alami, R., and Simeon, T. (2007). A human aware mobile robot motion planner. *IEEE Transactions on Robotics*, 23(5):874–883.

Stachniss, C. and Burgard, W. (2002). An integrated approach to goal-directed obstacle avoidance under dynamic constraints for dynamic environments. In *Proceedings of the IEEE/RSJ International Conference on Intelligent Robots and Systems*, pages 508–513.

Svenstrup, M., Bak, T., and Andersen, H. J. (2010). Trajectory planning for robots in dynamic human environments. In *Proceedings of the IEEE/RSJ International Conference on Intelligent Robots and Systems*, pages 4293–4298.

Sviestins, E., Mitsunaga, N., Kanda, T., Ishiguro, H., and Hagita, N. (2007). Speed adaptation for a robot walking with a human. In *Proceedings of the 2nd ACM/IEEE international conference on Human-robot interaction*, pages 349–356.

Tasaki, T., Matsumoto, S., Ohba, H., Toda, M., Komatani, K., Ogata, T., and Okuno, H. (2004). Dynamic communication of humanoid robot with multiple people based on interaction distance. In *IEEE International Workshop on Robot and Human Interactive Communication*, pages 71–76.

Thrun, S., Bennewitz, M., Burgard, W., Cremers, A., Dellaert, F., Fox, D., Hahnel, D., Rosenberg, C., Roy, N., Schulte, J., et al. (1999). Minerva: A second-generation museum tour-guide robot. In *Proceedings of the IEEE International Conference on Robotics and Automation*, volume 3, pages 1999–2005.

Trahanias, P., Burgard, W., Argyros, A., Hahnel, D., Baltzakis, H., Pfaff, P., and Stachniss, C. (2005). Tourbot and webfair: Web-operated mobile robots for tele-presence in populated exhibitions. *IEEE Robotics & Automation Magazine*, 12(2):77–89.

Trautman, P. and Krause, A. (2010). Unfreezing the robot: Navigation in dense, interacting crowds. In *Proceedings of the IEEE/RSJ International Conference on Intelligent Robots and Systems*, pages 797–803.

Trautman, P., Ma, J., Murray, R. M., and Krause, A. (2013). Robot navigation in dense human crowds: the case for cooperation. In *Proceedings of the IEEE International Conference on Robotics and Automation*, pages 2145–2152.

Trautman, P., Ma, J., Murray, R. M., and Krause, A. (2015). Robot navigation in dense human crowds: Statistical models and experimental studies of human–robot cooperation. *The International Journal of Robotics Research*, 34(3):335–356.

Trulls, E., Corominas Murtra, A., Pérez-Ibarz, J., Ferrer, G., Vasquez, D., Mirats-Tur, J., and Sanfeliu, A. (2011). Autonomous navigation for mobile service robots in urban pedestrian environments. *Journal of Field Robotics*, 28(3):329–354.

van den Berg, J., Guy, S. J., Lin, M., and Manocha, D. (2011). Reciprocal n-body collision avoidance. *Robotics Research, Springer Tracts in Advanced Robotics*, 70:3–19.

van den Berg, J., Lin, M., and Manocha, D. (2008). Reciprocal velocity obstacles for real-time multi-agent navigation. In *Proceedings of IEEE International Conference on Robotics and Automation*, pages 1928–1935. IEEE.

Vasquez, D. (2007). *Incremental learning for motion prediction of pedestrians and vehicles*. PhD thesis, Grenoble, INPG.

Vasquez, D., Fraichard, T., and Laugier, C. (2009). Markov Models: An Incremental Tool for Learning and Predicting Human and Vehicle. *The International Journal of Robotics Research*, 28(11):1486–1506.

Vasquez, D., Okal, B., and Arras, K. O. (2014). Inverse reinforcement learning algorithms and features for robot navigation in crowds: An experimental comparison. In *Proceedings of the IEEE/RSJ International Conference on Intelligent Robots and Systems*, pages 1341–1346. IEEE.

Vieilledent, S., Kerlirzin, Y., Dalbera, S., and Berthoz, a. (2001). Relationship between velocity and curvature of a human locomotor trajectory. *Neuroscience letters*, 305(1):65–9.

Villamizar, M., Garrell, A., Sanfeliu, A., and Moreno-Noguer, F. (2012). Online human-assisted learning using random ferns. In *International Conference on Pattern Recognition*, pages 2821–2824. IEEE.

Walters, M., Dautenhahn, K., Woods, S., and Koay, K. (2007). Robotic etiquette: results from user studies involving a fetch and carry task. In *2nd ACM/IEEE International Conference on Human-Robot Interaction*, pages 317–324.

Wang, Z., Mülling, K., Deisenroth, M. P., Amor, H. B., Vogt, D., Schölkopf, B., and Peters, J. (2013). Probabilistic movement modeling for intention inference in human–robot interaction. *The International Journal of Robotics Research*, 32(7):841–858.

Wilkes, D., Pack, R., Alford, A., and Kawamura, K. (1997). Hudl, a design philosophy for socially intelligent service robots. *Socially Intelligent Agents*, pages 140–145.

Wolpert, D. M. and Ghahramani, Z. (2000). Computational principles of movement neuroscience. *Nature neuroscience*, 3 Suppl(november):1212–7.

Zanlungo, F., Ikeda, T., and Kanda, T. (2011). Social force model with explicit collision prediction. *EPL (Europhysics Letters)*, 93(6):68005.

Ziebart, B. D., Maas, A., Bagnell, J. A., and Dey, A. K. (2008). Maximum Entropy Inverse Reinforcement Learning. In *Proceedings of the AAAI Conference on Artificial Intelligence*, pages 1433–1438.

Ziebart, B. D., Ratliff, N., Gallagher, G., Mertz, C., Peterson, K., Bagnell, J. A., Hebert, M., Dey, A. K., and Srinivasa, S. (2009). Planning-based prediction for pedestrians. In *Proceedings of the IEEE/RSJ International Conference on Intelligent Robots and Systems*, pages 3931–3936.

Zinn, M., Khatib, O., Roth, B., and Salisbury, J. (2004). Playing it safe [human-friendly robots]. *IEEE Robotics & Automation Magazine*, 11(2):12–21.